AFWAL-TR-87-3068

EVALUATION OF RST STRUCTURAL DURABILITY AND LIFE CYCLE COSTS

W. R. GARVER, D. Y. LEE, AND D. E. GORDON
GENERAL DYNAMICS FORT WORTH DIVISION
P. O. Box 748
Fort Worth, Texas 76101

19 October 1987

FINAL REPORT FOR PERIOD October 1983 - September 1987

APPROVED FOR PUBLIC RELEASE; DISTRIBUTION UNLIMITED.

FLIGHT DYNAMICS LABORATORY
AIR FORCE WRIGHT AERONAUTICAL LABORATORIES
AIR FORCE SYSTEMS COMMAND
WRIGHT-PATTERSON AIR FORCE BASE, OHIO 45433

NOTICE

When Government drawings, specifications, or other data are used for any purpose other than in connection with a definitely related Government procurement operation, the United States Government thereby incurs no responsibility nor any obligation whatsoever; and the fact that the government may have formulated, furnished, or in any way supplied the said drawings, specifications, or other data, is not to be regarded by implication or otherwise as in any manner licensing the holder or any other person or corporation, or conveying any rights or permission to manufacture use, or sell any patented invention that may in any way be related thereto.

This report has been reviewed by the Office of Public Affairs (ASD/PA) and is releasable to the National Technical Information Service (NTIS). At NTIS, it will be available to the general public, including foreign nations.

This technical report has been reviewed and is approved for publication.

Margery E. Artley
MARGERY E. ARTLEY
Project Engineer

Frank D. Adams
FRANK D. ADAMS, Chief
Structural Integrity Branch
Structures Division

FOR THE COMMANDER

Henry A Bondaruk
HENRY A. BONDARUK, Jr., Colonel, USAF
Chief, Structures Division

"If your address has changed, if you wish to be removed from our mailing list, or if the addressee is no longer employed by your organization please notify AFWAL/FIBEC *W-PAFB, OH 45433 to help us maintain a current mailing list".*

Copies of this report should not be returned unless return is required by security considerations, contractual obligations, or notice on a specific document.

Unclassified

SECURITY CLASSIFICATION OF THIS PAGE

REPORT DOCUMENTATION PAGE

1a. REPORT SECURITY CLASSIFICATION
Unclassified

1b. RESTRICTIVE MARKINGS

2a. SECURITY CLASSIFICATION AUTHORITY

2b. DECLASSIFICATION/DOWNGRADING SCHEDULE

3. DISTRIBUTION/AVAILABILITY OF REPORT
Approved for public release; distribution unlimited

4. PERFORMING ORGANIZATION REPORT NUMBER(S)

5. MONITORING ORGANIZATION REPORT NUMBER(S)
AFWAL-TR-87-3068

6a. NAME OF PERFORMING ORGANIZATION
General Dynamics/
Fort Worth Division

6b. OFFICE SYMBOL *(If applicable)*

7a. NAME OF MONITORING ORGANIZATION
Air Force Wright Aeronautical Laboratories
(AFWAL/FIBEC)

6c. ADDRESS *(City, State and ZIP Code)*
P.O. Box 748
Fort Worth, TX 76101

7b. ADDRESS *(City, State and ZIP Code)*
Wright-Patterson Air Force Base
Ohio 45433

8a. NAME OF FUNDING/SPONSORING ORGANIZATION
AFWAL/FIBEC

8b. OFFICE SYMBOL *(If applicable)*

9. PROCUREMENT INSTRUMENT IDENTIFICATION NUMBER
F33615-83-C-3227

8c. ADDRESS *(City, State and ZIP Code)*
Wright-Patterson Air Force Base
Ohio 45433

10. SOURCE OF FUNDING NOS.

PROGRAM ELEMENT NO.	PROJECT NO.	TASK NO.	WORK UNIT NO.
62201F	2401	01	69

11. TITLE *(Include Security Classification)* Evaluation of RST Structural Durability and Life Cycle Costs

12. PERSONAL AUTHOR(S)
Garver, W.R., Lee, D.Y., and Gordon, D.E.

13a. TYPE OF REPORT	13b. TIME COVERED	14. DATE OF REPORT (Yr., Mo., Day)	15. PAGE COUNT
Final Report	FROM Oct. 83 TO Sept 87	1987, October 19	161

16. SUPPLEMENTARY NOTATION
[redacted]

17. COSATI CODES

FIELD	GROUP	SUB. GR.
0103	1403	1107

18. SUBJECT TERMS *(Continue on reverse if necessary and identify by block number)*
Equivalent Initial Flaw Size, RST Structures, P/M Aluminum Alloys, Spectrum Loading, Fatigue, Time-to-Crack-Initiation, Crack Growth, Initial Fatigue Quality, Reliability,

19. ABSTRACT *(Continue on reverse if necessary and identify by block number)*
The main objective of this study is to characterize the structural durability of high-strength powder metallurgy (P/M) aluminum alloys. The selected materials were CW67 extrusions, 7091-extrusions and 7091-forgings for P/M alloys and 2124-plate and 7475-plate for baseline materials. An F-16 aft fuselage bulkhead (FS446) was chosen as a prime configuration since a preliminary trade study predicted good weight savings from P/M alloys for this application. This also provides a good opportunity to study and compare two manufacturing technologies, machined plate vs. net shape forging. Therefore, test specimens were designed to model a critical location in the F-16 FS446 bulkhead. Spectrum fatigue tests were conducted under two types of spectrum load histories, HUD34 and NOR1. HUD 34 is a tension-compression type spectrum representing the 500-hour block spectrum for the F-16 FS446 bulkhead, while NOR1 is a tension-dominated type spectrum representing the B-1 wing carry-through box spectrum. Test results obtained from spectrum fatigue tests were analyzed based upon the equivalent initial flaw size (EIFS) concept. The data analysis shows that the EIFS concept is a powerful tool to characterize and evaluate the

20. DISTRIBUTION/AVAILABILITY OF ABSTRACT
UNCLASSIFIED/UNLIMITED ☒ SAME AS RPT. ☐ DTIC USERS ☐

21. ABSTRACT SECURITY CLASSIFICATION
Unclassified

22a. NAME OF RESPONSIBLE INDIVIDUAL	22b. TELEPHONE NUMBER (Include Area Code)	22c. OFFICE SYMBOL
Margery Artley	(513)255-6104	AFWAL/FIBEC

DD FORM 1473, 83 APR EDITION OF 1 JAN 73 IS OBSOLETE.

Unclassified

SECURITY CLASSIFICATION OF THIS PAGE

19. (Continued)

structural durability of P/M alloys. The EIFS distribution is common to all spectra and stress levels for a given material and can be conveniently used to quantify structural performance of P/M alloys. The analyzed data demonstrated that initial fatigue quality and spectrum fatigue crack growth resistance of P/M alloys are better compared with baseline materials. From the fatigue quality model parameters obtained in this study, reliability was determined as a function of maximum stress level in spectrum loading. Results showed that reliability of P/M alloys is superior to that of baseline materials for a given stress level.

Delete the <u>Export</u> <u>Restrictions</u> <u>Apply</u> statement in Block 16 of the DD Form 1473.
Per Ms. Evelyn Foster, AFWAL/IST

SUMMARY

This report summarizes a research program aimed at achieving the following goals:

1. To quantify the failure processes in rapidly solidified technology (RST) structures in order to characterize their damage tolerance and durability.

2. To develop a "figure of merit" within the framework of fracture-based design which will reflect the relative merit of RST material versus conventional construction.

A preliminary trade study had established an F-16 aft fuselage bulkhead (FS446) as a prime configuration for weight savings of Powder Metallurgy alloys over conventional ingot metallurgy aluminum alloys. Spectrum fatigue tests were conducted on approximately 150 test coupons designed to model a critical location in the F-16 FS446 bulkhead. Tests were conducted on two different P/M alloys, CW67 and 7091, and compared to two ingot metallurgy aluminum alloys, 7475-T7351 and 2124-T851. Also, 7071 material produced under two manufacturing technologies, machined plate and net shape forging were compared.

Spectrum fatigue tests were conducted under two types of spectrum load histories, HUD34 and NOR1. HUD34 is a tension-compression type spectrum representing the 500-hour block spectrum for the F-16 FS446 bulkhead, while NOR1 is a tension-dominated type soectrum representing the B-1 wing carry-through box spectrum. Test results obtained from spectrum fatigue tests were analyzed based upon the equivalent initial flaw size (EIFS) concept. Methodology used in comparing RST structures with conventional I/M structures is presented and discussed. Techniques which can be used in design studies are proposed.

FOREWORD

This report was prepared by General Dynamics/Fort Worth Division, Fort Worth, Texas, for the Structural Integrity Branch, Structures Division, Air Force Wright Aeronautical Laboratories, Wright-Patterson Air Force Base, Ohio under Contract F33615-83-C-3227. Ms. Margery Artley of AFWAL/FIBEC, was the Project Engineer.

General Dynamics/Fort Worth Division was the contractor for this program. Dr. W. R. Garver served as Program Manager. Dr. D. Y. Lee and Mr. D. E. Gordon were Principal Investigators.

Many individuals at General Dynamics contributed to this program. All tests were performed in General Dynamics' Materials and Processes Laboratory by R. O. Nay under the direction of R. L. Jones. Fractographic readings were made by K. M. Koepsel and S. B. Kirschner. R. W. Haile, R. S. Prowant, and M. A. Osterkamp developed computer software for the program. B. S. Head and P. L. Carper performed all nondestructive examinations of the test specimens. J. H. Chung conducted crack growth predictions. S. R. Fisk typed the report.

This report is the Final Technical Report for this program, covering all work during the period October, 1983 through September, 1987.

TABLE OF CONTENTS

TABLE OF CONTENTS (Continues)

TABLE OF CONTENTS (Concluded)

LIST OF FIGURES

LIST OF FIGURES (Continues)

LIST OF FIGURES (Continues)

LIST OF FIGURES (Continues)

LIST OF FIGURES (Concluded)

FIGURE PAGE

LIST OF TABLES

SECTION I

INTRODUCTION

The current Air Force structural integrity [MIL-A-87221, Ref. 1] design specifications require that an aircraft be designed to meet both damage tolerance [MIL-A-83444, Ref. 2] and durability [MIL-A-8866B, Ref. 3, and MIL-A-8867B, Ref. 4] requirements. Using a fracture mechanics approach, these design criteria assume that initial quality of aircraft primary structures must be such that there is no catastrophic failure nor widespread damage accumulation within one design service life.

The selection of the initial flaw size and geometry to be used for design is one of the most important tasks in implementing the damage tolerance and durability requirements. The flaw sizes and geometries currently specified in MIL-A-83444 and MIL-A-8866B have been developed primarily for conventional ingot metallurgy (I/M) aerospace alloys. With the advent of rapid solidification processing (RSP), the data base for establishing initial flaw sizes must be expanded for RSP Powder Metallurgy alloys. The main objective of this study is to provide data for two types of RSP structural concepts that can be used to base assumptions of initial flaw size and geometry for direct use within the current Air Force specifications.

A second goal of this program is to provide the designer with a realistic way to assess design trade-offs for using high strength P/M alloys over conventional I/M alloys. A methodology similar to that used in assessing advanced joining concepts was used [5]. Based on this methodology, the reliability of high strength P/M alloys can be compared to conventional I/M alloys.

SECTION II

BACKGROUND OF RSP ALUMINUM ALLOYS

During recent years, improvements in mechanical properties of aluminum alloys have been achieved by rapid solidification processing (RSP). Extending control of microstructure via higher solidification rates has led to the development of unique alloy systems [6].

Fine grains, small constituents and dispersoids, as well as a homogeneous distribution of alloy elements, have been developed as a direct consequence of Rapid Solidification (RS) processes, including Powder Metallurgy (P/M). The uniformity in microstructures achieved in RS alloys created superior combinations of mechanical properties and resulted in an improved balance between strength, toughness, fatigue properties and corrosion resistance.

Unfortunately, the cost of RST structural aluminum alloys remains higher than those produced from standard ingot metallurgy. Therefore, their applications are limited to components where superior performance requirements must justify their use. The growth of P/M alloys has also been constrained by the size of billets available for processing into wrought products. Quality and end-product consistency have also hindered acceptance of aluminum wrought P/M products, particularly in aerospace applications. Even though P/M alloys exhibit significantly greater combinations of strength and fracture toughness compared to conventional ingot alloys, inclusions which can be introduced during processing must be controlled in order for these materials to be reliable in critical applications. It has been recognized that one of the most important factors controlling the fatigue performance of RST materials is the cleanliness of the RST material [6]. For example, it has been revealed that recent failures of Boeing's 7090 landing gear forgings for the 757 were associated with large inclusions of size about 0.060 inch [7].

Table 1 lists the compositions of I/M and several P/M alloys which have been developed by Alcoa. These alloys contain Zn, Mg, and Cu and utilize various types and amounts of dispersoid forming elements such as Cr, Zr, Co, or Ni to control recrystallization.

Table I Nominal Compositions* of 7XXX Aluminum P/M Alloy

Alloy	Zn	Mg	Cu	Co	Cr	Zr	Ni	O	Al	Ref.
7075 I/M	5.6	2.5	1.6	---	0.23	---	---	---	Bal.	
7050 I/M	6.2	2.2	2.3	---	---	0.12	---	---	Bal.	
7090	8.0	2.5	1.0	1.5	---	---	---	0.35	Bal.	a
7091	6.5	2.5	1.0	0.4	---	---	---	0.35	Bal.	a
CW67	9.0	2.5	1.5	---	---	0.14	0.1	0.35	Bal.	b

(a) Aluminum Company of America, Tech Brief, March, 1985
(b) Alcoa IRAD, April, 1983
* Elements in Weight %

The advantage that P/M alloys have over slowly cooled I/M alloys is the ability to utilize rapid solidification to refine the dispersoid size and spacing as well as dendrite arm spacing.

The refined microstructural features in the atomized powder ultimately results in a fine grain size in the wrought alloy with improved combinations of properties as demonstrated in Figure 1. In die forgings, P/M alloys 7090 and 7091 in a T7 temper have better strength and toughness than I/M 7075 [8]. Continued development of 7XXX P/M alloys [9] has led to the second generation alloy designated by Alcoa as CW67. As shown in Figure 1, this alloy which has twice the fracture toughness as 7090 with equivalent strength, is expected to play a major role in the continued commercialization of 7000 series P/M alloys for aerospace applications.

P/M alloys also exhibit superior corrosion resistance compared to I/M alloys. Figure 2 shows that P/M alloys offer between 10 to 20 percent greater strength compared to 7075-T73 and had no failures [10] in short-transverse tensile bars stressed at 45 ksi (310 MPa).

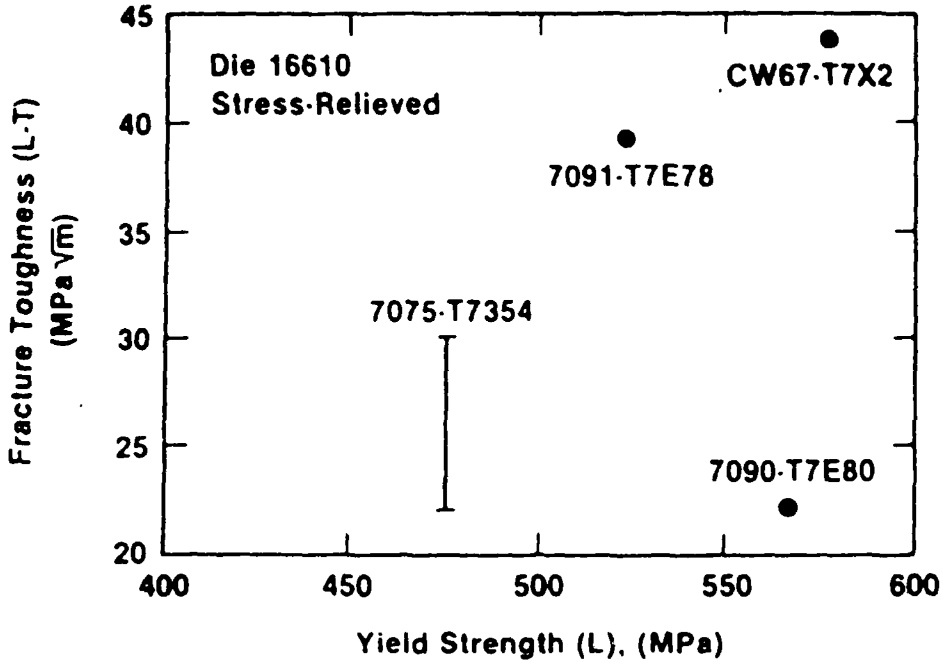

Figure 1. Fracture Toughness and Yield Strength for 7XXX P/M Versus 7075 1/M Forgings

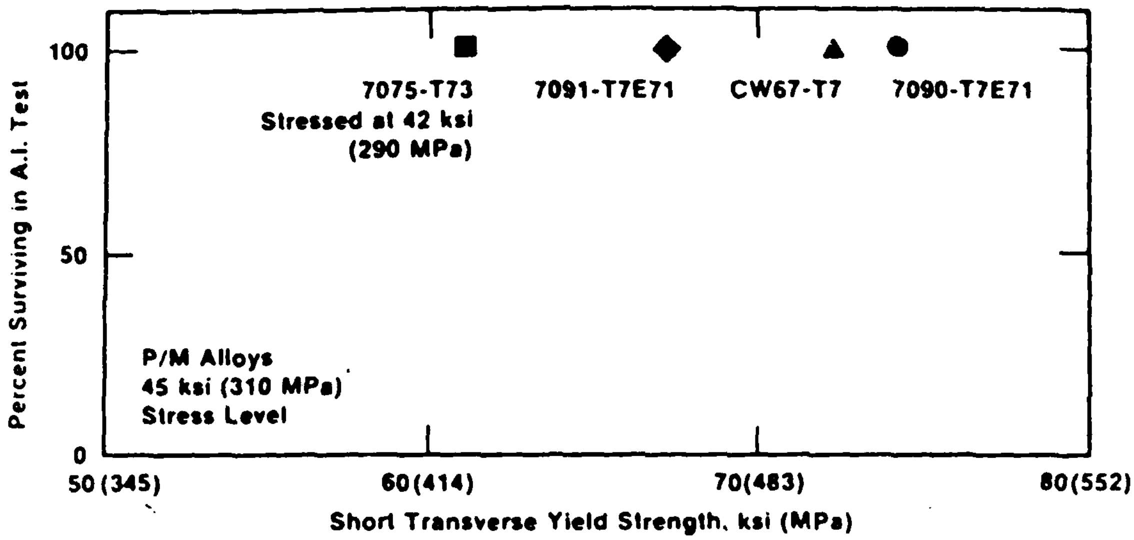

Figure 2. Results of ASTM G44-75 SCC Tests for T7 Type Tempers

SECTION III

EXPERIMENTAL PROCEDURES

3.1 SELECTION OF RST TEST ELEMENT

A list of 48 fracture critical parts were obtained from the F-16C/D aircraft as potential parts to be replaced by P/M alloys. An F-16 aft fuselage bulkhead (FS446) was chosen for this study as a prime configuration since a preliminary trade study predicted good weight savings from P/M alloys for this application (Figure 3). Potential cracking problems were known to exist in this bulkhead, also. This also provided a good opportunity to compare two manufacturing technologies, machined plate vs. net shape forging. Therefore, spectrum fatigue test specimens were designed to model a critical location in the F-16 FS446 bulkhead as shown in Figure 4. The test element geometry is shown in Figure 5.

Load transfer between 1/4" fastener holes was accomplished with a composite strap. Mylar tape between the strap and the specimen minimizes fretting that would promote crack initiation at locations away from the fastener holes. Specimens were tested in the as-machined condition with no additional surface treatment. No intentional pre-flaws were introduced.

3.2 SELECTION OF MATERIALS

The high strength P/M aluminum alloys selected for this program were CW67-extrusions, 7091-extrusions, and 7091-forgings. Both the Alcoa second generation alloy, CW67, and first generation alloy, 7091, were discussed in Section II. The CW67 and 7091 extrusions were obtained in the form of bars (1.5 inch thick and 4.5 inch wide). The CW67 material was obtained in the T7E91 heat treat. This heat treat consisted of:

(a) Solution treatment at 910°F for 2 hrs,
(b) cold water quench,
(c) artificially aging at 250°F for 24 hrs. followed by
(d) artificially aging at 325°F for 1 hr.

The 7091 material was obtained in the T7E69 heat treat. This heat treatment is shown in Table 2. The 7091-forgings were

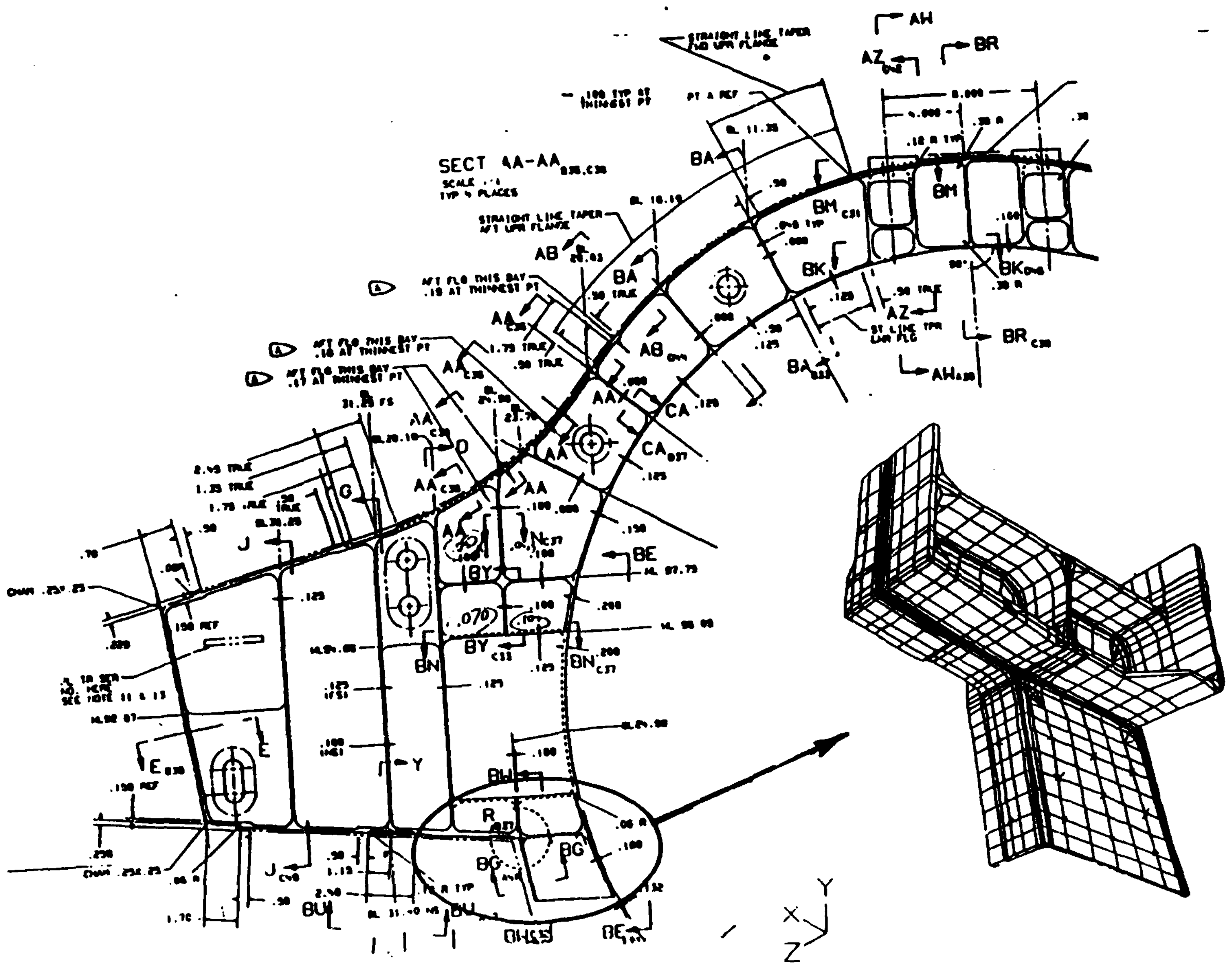

Figure 3. Drawing of FS 446 Bulkhead On F-16 Aircraft

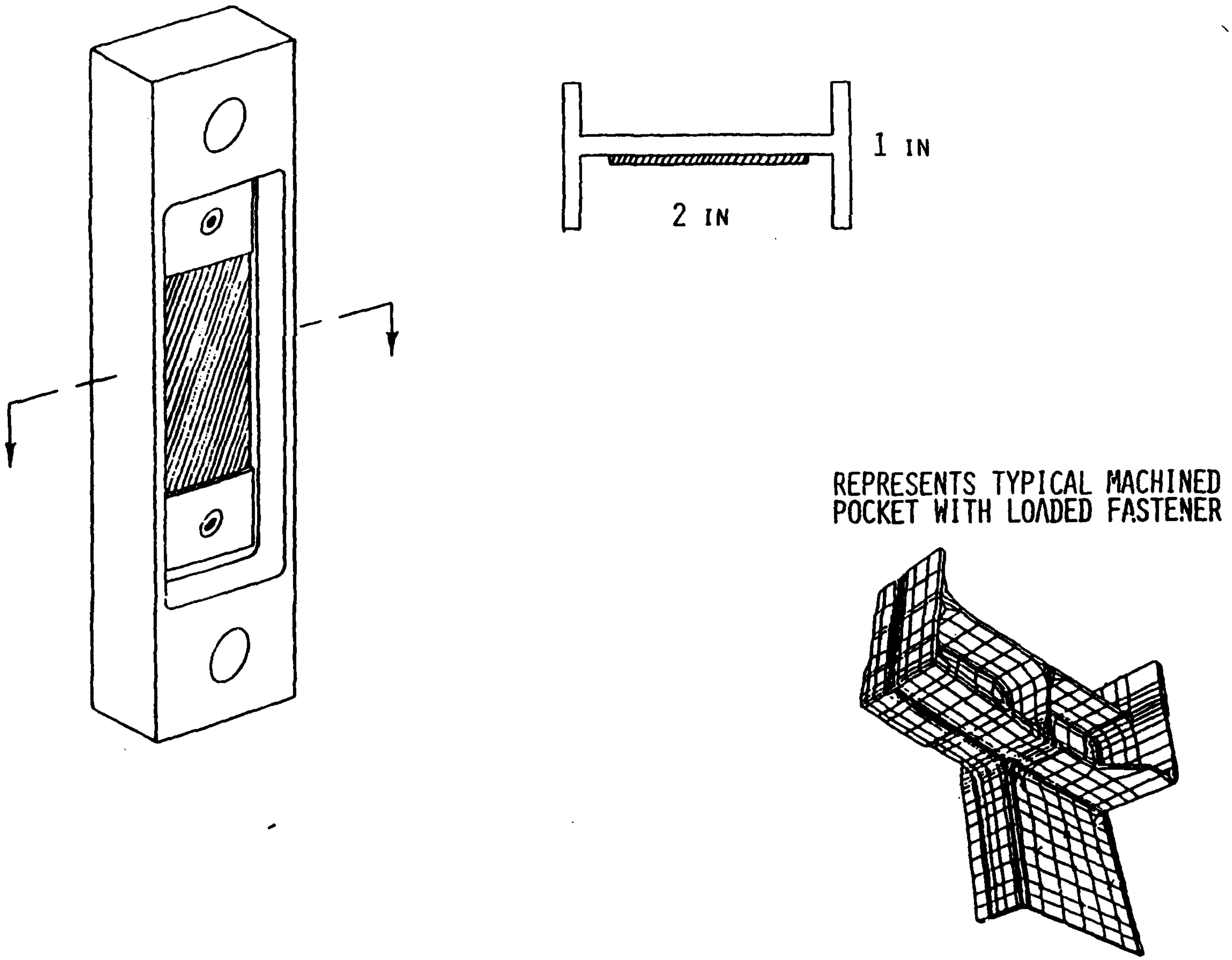

Figure 4. Test Element Design

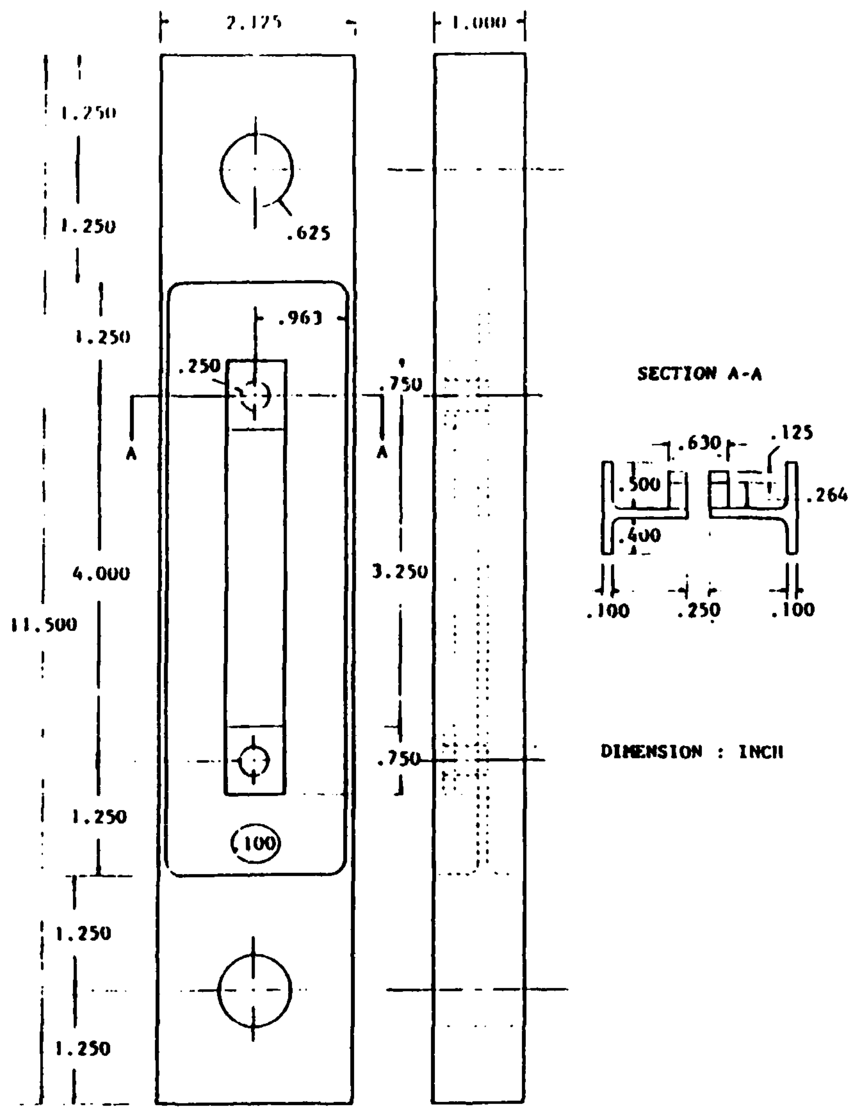

Figure 5. Test Element Geometry

TABLE 2. PROCEDURE USED IN HEAT TREATING 7091 P/M ALUMINUM ALLOY

	7091-EXTRUSIONS	7091-FORGINGS
SOLUTION TREATMENT	920°F, 2 HRS	920°F, 2 HRS
WATER QUENCH	R. T.	R. T.
STRESS RELIEF	3% STRETCH	NONE
NATURAL AGING	R. T., 5 DAYS	R. T., 5 DAYS
1ST STEP ARTIFICIAL AGING	250°F, 24 HRS	250°F, 24 HRS
2ND STEP ARTIFICIAL AGING	325°F, 8 HRS	325°F, 20 HRS

prepared from 7091-T7E69 extruded bars by a precision forging process at Pioneer Aluminum Forging Company, Colorado Springs, Colorado. A hydraulic press was used for forging preheated (3 hours at 800°F) blanks of 7091. During the forging process, the die temperature was also 800°F. Forged specimens were air cooled to room temperature. Post forging heat treatments are also shown in Table 2.

During the final step of artificial aging, the forged material was heated at 325°F until hardness values similar to the extruded material were obtained (Figure 6). Longer times were required for aging at 325°F (20 hrs) for the forged material as compared to the extruded material (8 hrs. at 325°F).

The baseline materials selected were 2124-plate and 7475-plate. Both materials are used on the F-16 aircraft.

The 2124-T851 aluminum plate alloy is used extensively in the F-16 fuselage in various thicknesses up to 5.5 inches. Its fracture toughness is not as high as 7475 but its crack growth resistance is very good, particularly in a corrosive media under spectrum loading [11]. The 2124-T851 aluminum alloy is currently being used in the F-16 aft fuselage bulkhead (FS446).

The 7475-T7351 aluminum plate alloy was selected because it is representative of the primary material of the F-16 aircraft for safety-of-flight structure up to 4.0-inches thick. Thin plate (0.625-inch) is used for the lower wing skin, where fracture control is a prime design requirement. Thicker plate (1.0 - 4.0 inches) is used for wing spars and certain of the thinner center fuselage lower bulkhead segments. This material is also used in the aft fuselage to a limited extent. The combination of this alloy and temper exhibits high resistance to exfoliation and stress corrosion cracking in all directions, and has extremely high fracture toughness [11].

All 2124-T851 and 7475-T7351 test coupons were obtained from plate (1.5 inch thick). All material used in the program was obtained from Aluminum Company of America.

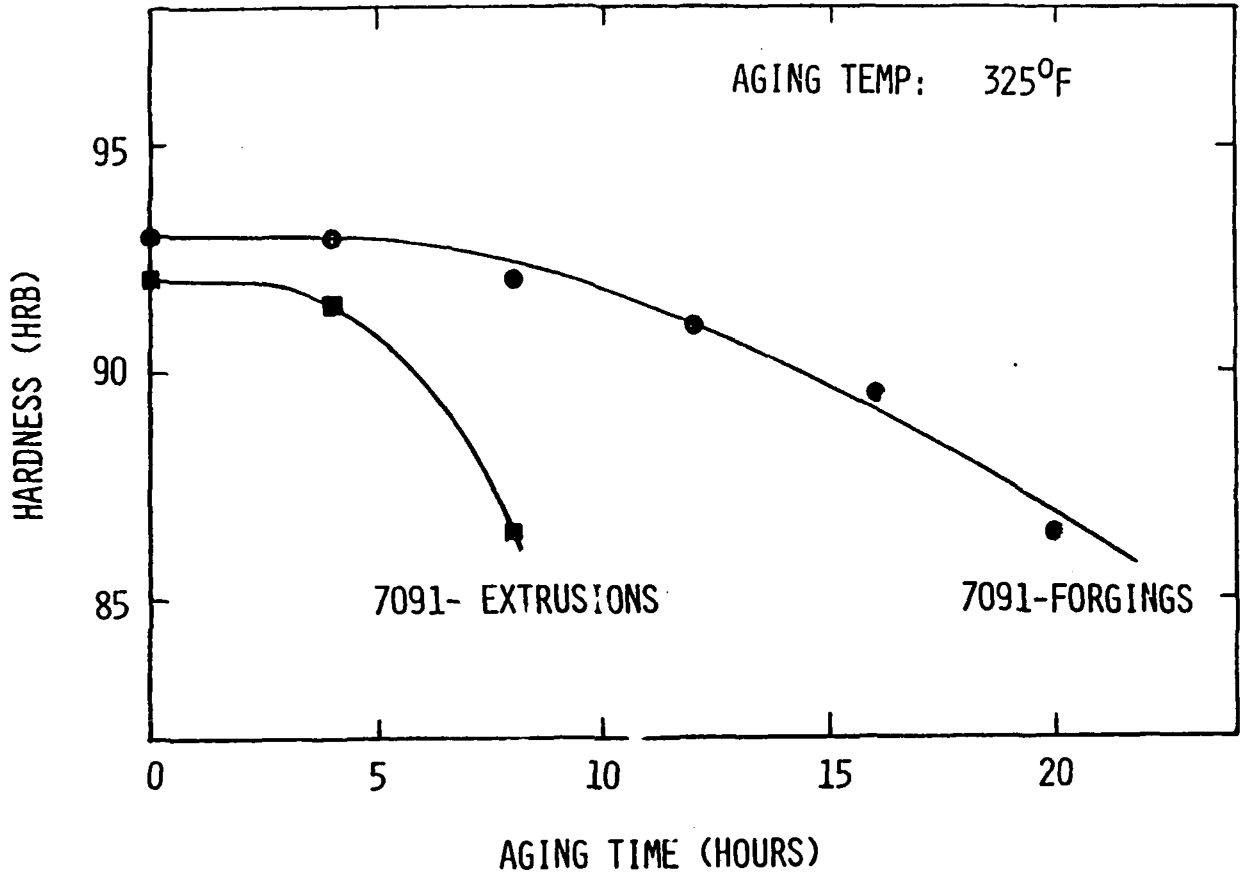

Figure 6. Aging Characteristics of 7091 Aluminum Alloy

3.3 LOAD HISTORY DEVELOPMENT AND SPECTRUM FATIGUE TESTING

Spectrum fatigue tests were conducted under two types of spectrum load histories, HUD34 and NOR1 (Figures 7 and 8). HUD34 represents the 500-hour block spectrum for the F-16 FS446 bulkhead (A tension-compression type spectrum), while NOR1 represents the B-1 wing carry-through box spectrum (a tension-dominated type spectrum). All specimens were spectrum fatigue tested for the equivalent of three design lives or until failure, whichever occurred first. One design life for HUD34 and NOR1 are 8,000 and 13,500 flight hours, respectively. Following testing, unfailed specimens were monotonically tested to failure and residual strength of each specimen was recorded. The crack growth data were determined by a fractographic method [5] using a Bausch and Lomb stereomicroscope and digital X-Y stage micrometers. The data were read continuously from the final crack length back to the origin. Both spectra produced easily distinguishable markings on the fracture surfaces (Figures 8 and 9).

For tests conducted under the HUD34 test spectrum, maximum tensile stresses of 35 ksi and 40 ksi were selected for the 2124-T851 aluminum alloy while maximum tensile stresses of 40 ksi and 45 ksi were selected for the 7091 and CW67 P/M materials (Table 3). For spectrum fatigue studies conducted under the NOR1 spectrum, maximum tensile stresses of 45 ksi and 50 ksi were used (Table 3).

Testing was conducted in computer-controlled test frames within the Materials and Processing Group Laboratory. Load cells in these facilities were periodically calibrated under Air Force supervision. Test rates were set so that program and feedback loads agreed to within two percent at all load levels. Due to the design of the test specimen, no lateral constraints were required during testing.

Table 3 summarizes the spectrum fatigue test plan. The experimental results obtained from the spectrum fatigue testing are presented in Section 5.

3.4 INSPECTION PROCEDURES

Nondestructive techniques were used to characterize all fastener holes subjected to cyclic loading. For determining initial hole quality, eddy current techniques and dial bore gauge

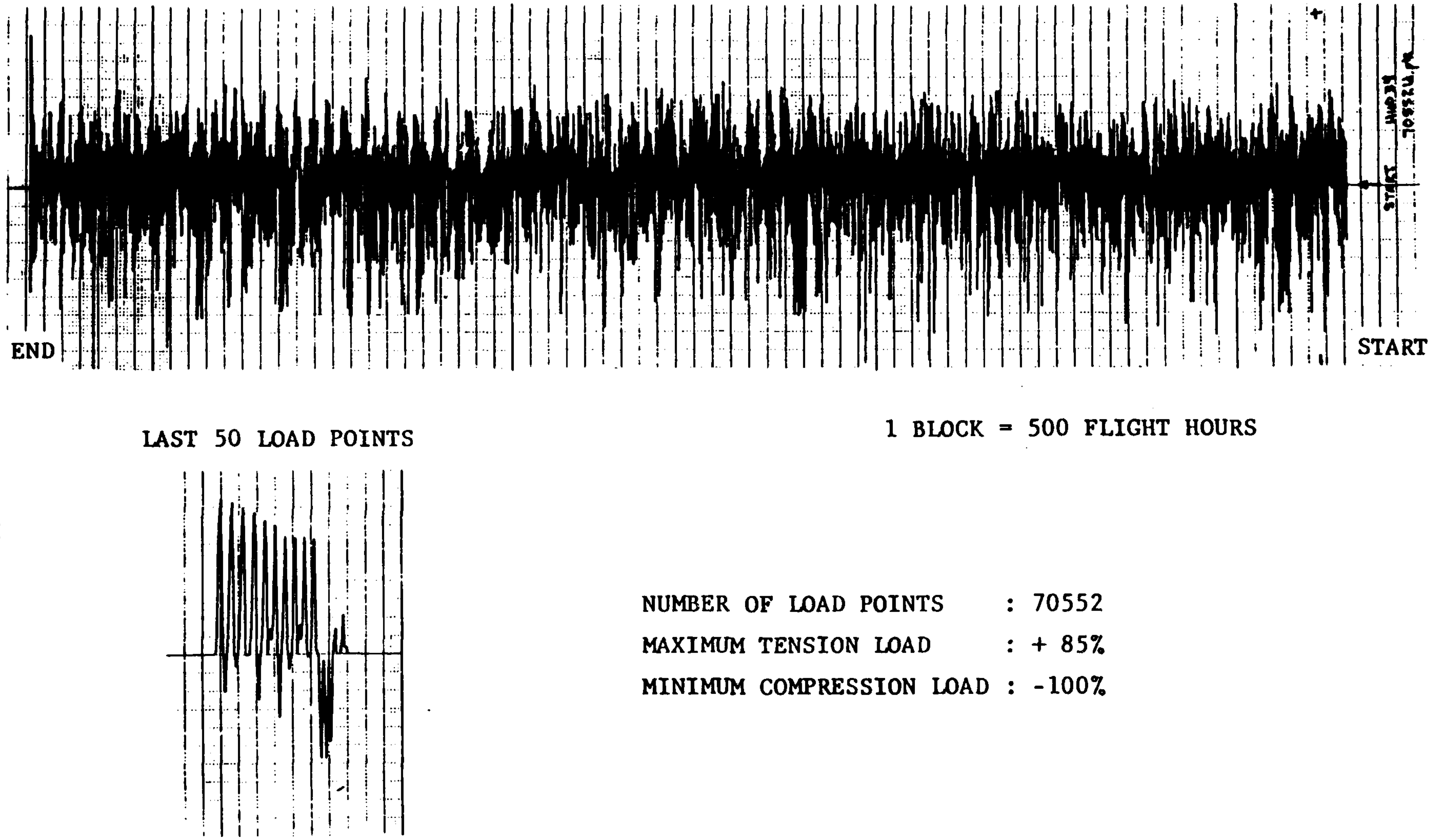

NUMBER OF LOAD POINTS : 70552
MAXIMUM TENSION LOAD : + 85%
MINIMUM COMPRESSION LOAD : -100%

Figure 7. HUD 34 Test Spectrum

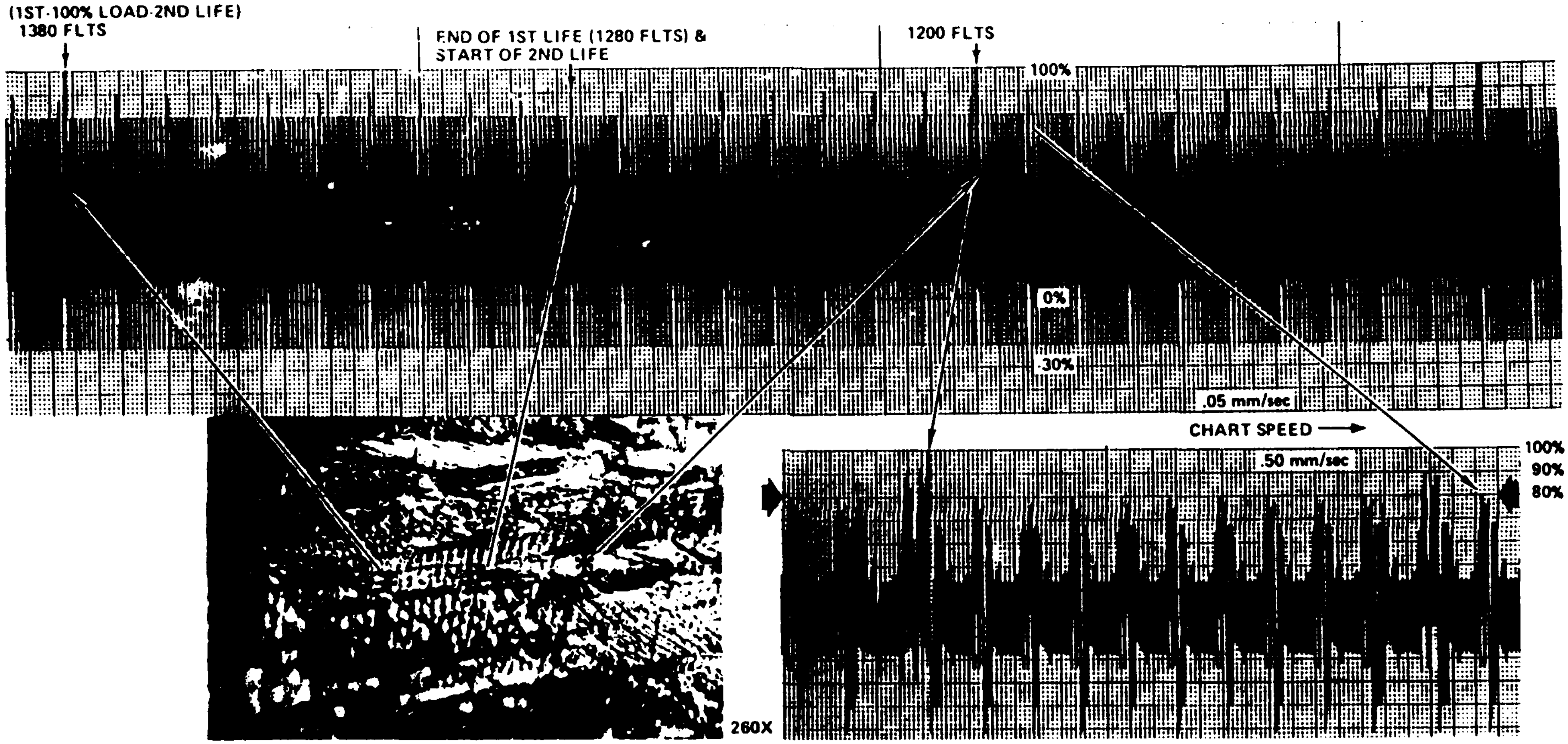

SEGMENT OF B1-BOMBER SPECTRUM SHOWING TRANSITION FROM 1ST TO 2ND LIFE

Figure 8. NOR 1 Test Spectrum

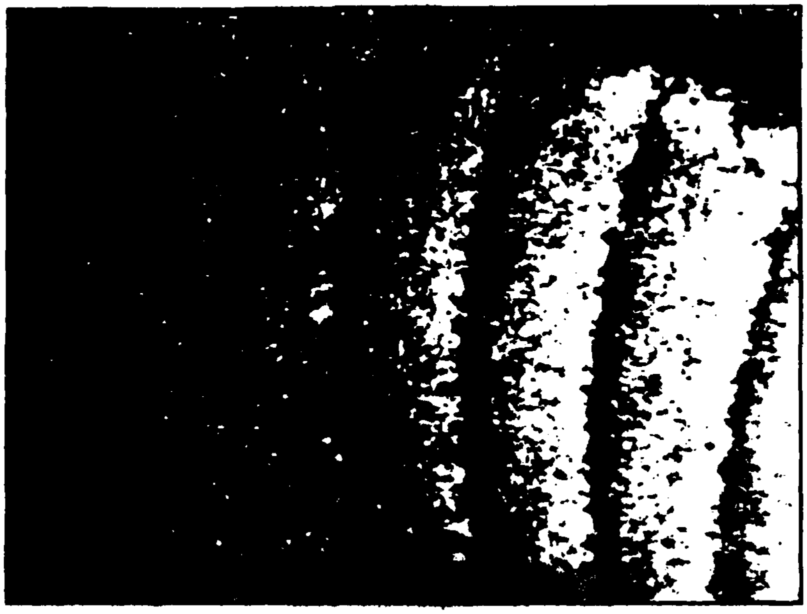

7091 Extrusion 40X

Figure 9. Fractographic Markings On A 7091 Extrusion Fracture Surface Exposed To HUD 34 Spectrum

TABLE 3 SPECTRUM FATIGUE TEST MATRIX

MATERIAL	SPECTRUM	STRESS	NO. OF SPECIMENS
2124-T851	HUD34	35	15
	HUD34	40	15
	NOR1	45	10
7475-T7351	NOR1	45	10
7091-EXTRUSION	HUD34	40	15
	HUD34	45	15
	NOR1	45	10
	NOR1	50	10
7091-FORGING	HUD34	40	9
	HUD34	45	9
CW67-EXTRUSION	HUD34	40	10
	HUD34	45	10
	NOR1	45	10

measurements were made. Comparisons were made between NDI parameters as measured by the different inspection techniques and fatigue properties. Cracks initiated at the fastener holes in all test specimens. They initiated from inclusions, defects, out of roundness of holes and axial scratches.

Since control of inclusions is a major problem in the high strength P/M aluminum alloys, ultrasonic and x-ray inspections were also made of all RST test coupons prior to cyclic loading. Both inspection techniques are known to be particularly sensitive to detecting inclusions.

In the 7091-forged specimens, surface residual stresses in the test coupons were also considered. In the forged material, the residual stress distributions are considered an additional unknown variable which could affect spectrum fatigue performance. All NDI techniques used in this program are shown in Table 4. All inspection procedures are described below.

3.4.1 Eddy Current

Eddy current procedures for inspecting fastener hole quality were similar to those described in the "Initial Quality of Advanced Joining Concepts" program [5] and "Fastener Hole Quality" program [12]. An automated eddy current inspection unit was used for inspecting fastener holes. The unit consists of an Automation Industries EM 3300 eddy current unit, a mini-scanner head and a dual channel recorder. The eddy current signal, after being filtered and amplified, is sent to a dual channel recorder, where the data is then plotted.

Considerable insight was gained during the Fastener Hole Quality program [12] into the types of initial defects that most seriously affect the fatigue behavior of fastener holes. The axial or vertical scratch in a fastener hole has been identified as an initial defect that significantly affects the fatigue behavior of fastener holes under no-load transfer conditions. Consequently, the eddy current technique has been optimized to detect axial scratches. Shown in Figure 10 are eddy current signatures of typical manufacturing induced axial scratches. A signal-to-noise ratio of about 7 has been achieved in the detection of this type of initial defect.

TABLE 4. NDI TEST MATRIX

- RST MATERIALS

ULTRASONIC	- INCLUSIONS, VOIDS, (FORGING LAPS)
X-RADIOGRAPHY	- INCLUSIONS, VOIDS, (FORGING LAPS)
EDDY CURRENT	- CRACKS, SCRATCHES IN FASTENER HOLES
DIAL BORE GAGE	- DIAMETER, ROUNDNESS OF FASTENER HOLES

- CONVENTIONAL ALLOYS

  EDDY CURRENT

  DIAL BORE GAGE

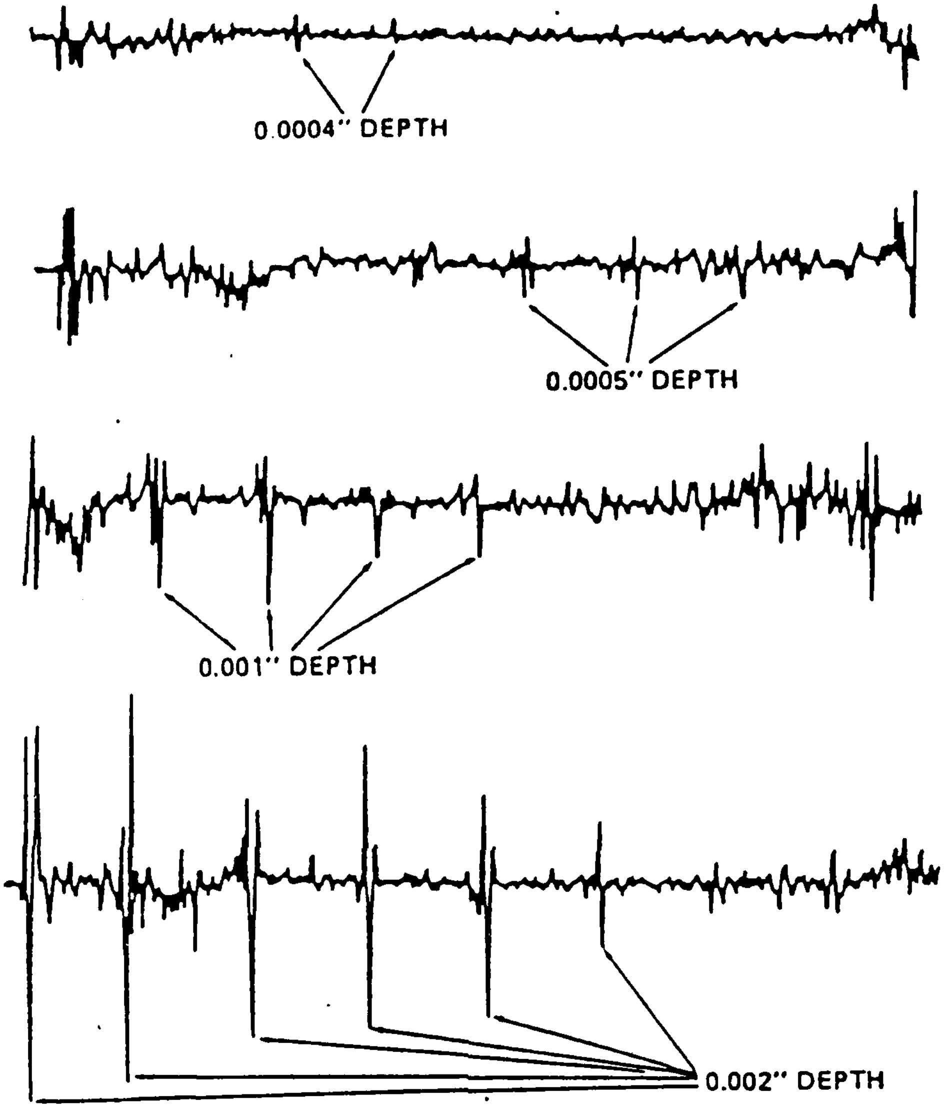

Figure 10. Sensitivity of Eddy Current To Surface Defects

Despite the sensitivity of eddy current inspection, it is difficult to detect some of the axial scratches or voids which can adversely affect fatigue performance. It is possible, however, to monitor variations in hole dimensions, such as hole out-of-roundness, with eddy current inspection. Also, surface roughness can easily be detected.

3.4.2 Dial Bore Gauge

A dial bore gauge (Boise Model No. 1) was used to measure the diameter of the fastener holes at different orientations (Figure 11), and thus, give a relative measure of out-of-roundness (OOR). Measurements were taken at different depths in the hole, also, to determine if hole tapering was present. Numbering of the holes for dial bore gauge and eddy current measurements were in accordance with Figure 11.

3.4.3 X-Radiography

In the inspection of the 7091 and CW-67 coupons, a Field Emission Corporation Faxitron, Model 805, radiographic inspection system was used. Specimens were mounted such that the center of the x-ray beam were normal to the face of the specimen. A film-to-source distance (FTSD) of 22.0 inches was used. X-ray parameters found to work best were either 35 kv, 3 ma, for 5 minutes or 35 kv 3 ma, for 6.5 minutes. The longer exposure time is slightly more effective for the detection of higher density inclusions which might be present. Kodak Type AA film was used.

3.4.4 Ultrasonic

Ultrasonic inspections were performed on all P/M specimens in the transmission mode. Ultrasonic C-scans were taken with the samples immersed in an Automation Industries research tank. Measurements were made with 5MHz transducers with a separation of 5.0 inches. A flaw level of 20 percent was used for these scans.

3.4.5 X-ray Diffraction

For surface residual stress measurements, a portable Ruud-Barrett Residual Stress System was used [13]. This system used x-ray diffraction techniques to measure residual stresses (Figure 12).

DIAMETERS

DEPTH / ANGLE	X	Y
A		
B		
C		
D		

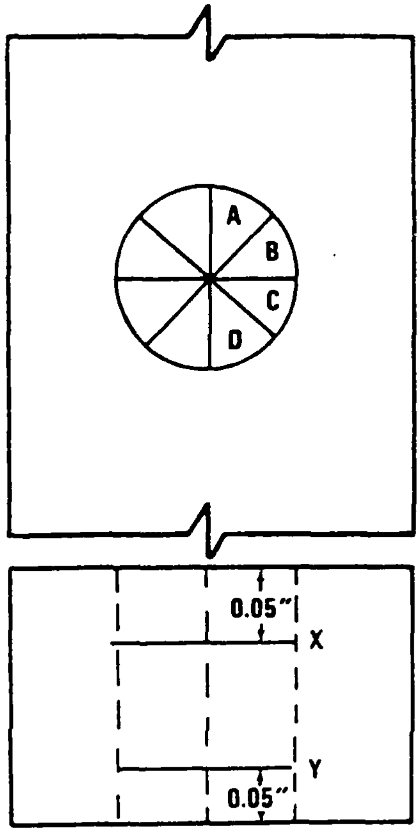

Figure 11. Dial Bore Gauge Inspection Scheme

PORTABLE RUUD-BARRETT RESIDUAL STRESS SYSTEM

Figure 12. Portable Ruud-Barrett Residual Stress System

In two specimens, residual stress depth profiles were obtained. These measurements were obtained by etching away different thicknesses of material and measuring the depth of removed material.

SECTION IV

DURABILITY AND DAMAGE TOLERANCE METHODS DEVELOPMENT

In this section, techniques used in predicting fatigue crack growth (FCG) and determining the equivalent initial flaw size (EIFS) are described. Comparisons of crack growth predictions with actual crack growth data are presented in Section V. EIFS distributions of actual test results are also shown in Section V.

4.1 CRACK GROWTH ANALYSIS

Crack growth analyses were conducted using a computer code called RXN. The RXN computer code is a production code used at General Dynamics/Fort Worth Division [14]. The RXN code is an improved version of R5N which has been used in previous programs [5].

The existing RXN program can analyze up to fifteen different crack geometries using any combination of seven different crack growth models and four retardation models. The combination of geometry type/retardation model/crack growth model is defined simply by selecting the respective values for three input variables. Table 5 lists the specific geometry types, retardation models, and crack growth laws internally available in the program.

These new features available on RXN are especially valuable. First stress intensity factors for both surface flaws [15] and corner cracks at loaded bolt holes [16] are available for the case of bending loading as well as for uniform tension stress. Second, the Rockwell/Chang retardation Model [17] helps to correct for compressive loading effects.

Finally, the tabular input options for the stress intensity factor (either corner bolt hole or through flaws) allows complex or unique stress intensity factor solutions to be incorporated into the crack growth analysis.

For the predictions used in this program, the "Modified Walker Crack Growth Equation" was used in conjunction with the "Generalized Willenborg Retardation Model." These options are listed in Table 5.

TABLE 5. RXN CRACK GROWTH PROGRAM CAPABILITIES

GEOMETRY TYPES	RETARDATION MODELS	CRACK GROWTH LAWS
PT SF TEN (CONST. MF)	WHEELER	PARIS
PT SF TEN (EQ. MF)	GENERALIZED WILLENBORG	FORMAN
PT SF TEN (NEWMAN)	MULTI-PARAMETER YIELD ZONE	MODIFIED FORMAN
PT SF BEND (NEWMAN)	ROCKWELL/CHANG	WALKER ΔK
TT SF TEN	NO RETARDATION	WALKER KMAX
CF AT HOLE TEN		VROMAN/CHANG
CF AT HOLE BER		TABULAR
CF AT HOLE TEN + BER		
TT AT HOLE TEN		
TT AT HOLE BER		
TT AT HOLE TEN + BER		
CF AT EDGE TEN		
TT AT EDGE TEN		
CF (INPUT SIF)		
TT (INPUT SIF)		

PT - PART THROUGH THICKNESS FLAW
CF - CORNER FLAW
TEN - TENSION STRESS
BER - BEARING STRESS

TT - THROUGH THICKNESS FLAW
SF - SURFACE FLAW
BEND - BENDING STRESS
SIF - STRESS INTENSITY FACTOR

All crack growth analyses were conducted for the HUD34 spectrum at a nominal stress level of 40 ksi. Analyses were performed for single and double (symmetric) cracks emanating from the critical fastener holes. Both corner and through cracks were considered. All analyses used appropriate stress intensity factor estimates for loaded bolt holes. The starting crack size was taken as 0.001 inch. Analyses were terminated upon reaching the estimated critical crack size or upon reaching two design lifetimes. Crack geometries are shown in Figure 13.

Calculations were conducted for three different materials, 2124-T851, 7475-T7351, and 7091-extrusions. Results of these calculations are shown in Figure 14-16. A comparison of materials for two corner plus a through crack is shown in Figure 17. According to the analysis, superior crack growth resistance is obtained in the 7475-T7351 material as compared to 7091-T7E69 and 2124-T851. Comparisons of predicted crack growth and actual crack growth will be discussed in Section V.

Following a methodology developed previously at GD/FWD [18,19] and using a modified secant method [20], crack growth rate ($\frac{\Delta a}{\Delta t}$) was predicted as a function of crack length, a. These calculations were conducted for crack geometries, spectra, and stress level shown in Figures 14-16.

Figures 18-20 summarize the crack growth analyses for three different materials, 2124-T851, 7475-T7351, and 7091-T7E69. A comparison of these materials for two corner and one through crack is shown in Figure 21. Predictions based on this methodology are discussed in Section V.

4.2 DETERMINATION OF EQUIVALENT INITIAL FLAW SIZE

A model for initial fatigue quality based on the equivalent initial flaw size (EIFS) concept has been established from several preceding programs [5,12,21,22]. Many details of the model which support its usage will not be presented here. Several variations in modeling crack growth to fit fractographic data have been presented [5,12,21]. However, the model followed in this program is similar to that used in the "Initial Quality of Advanced Joining Concepts" program [5].

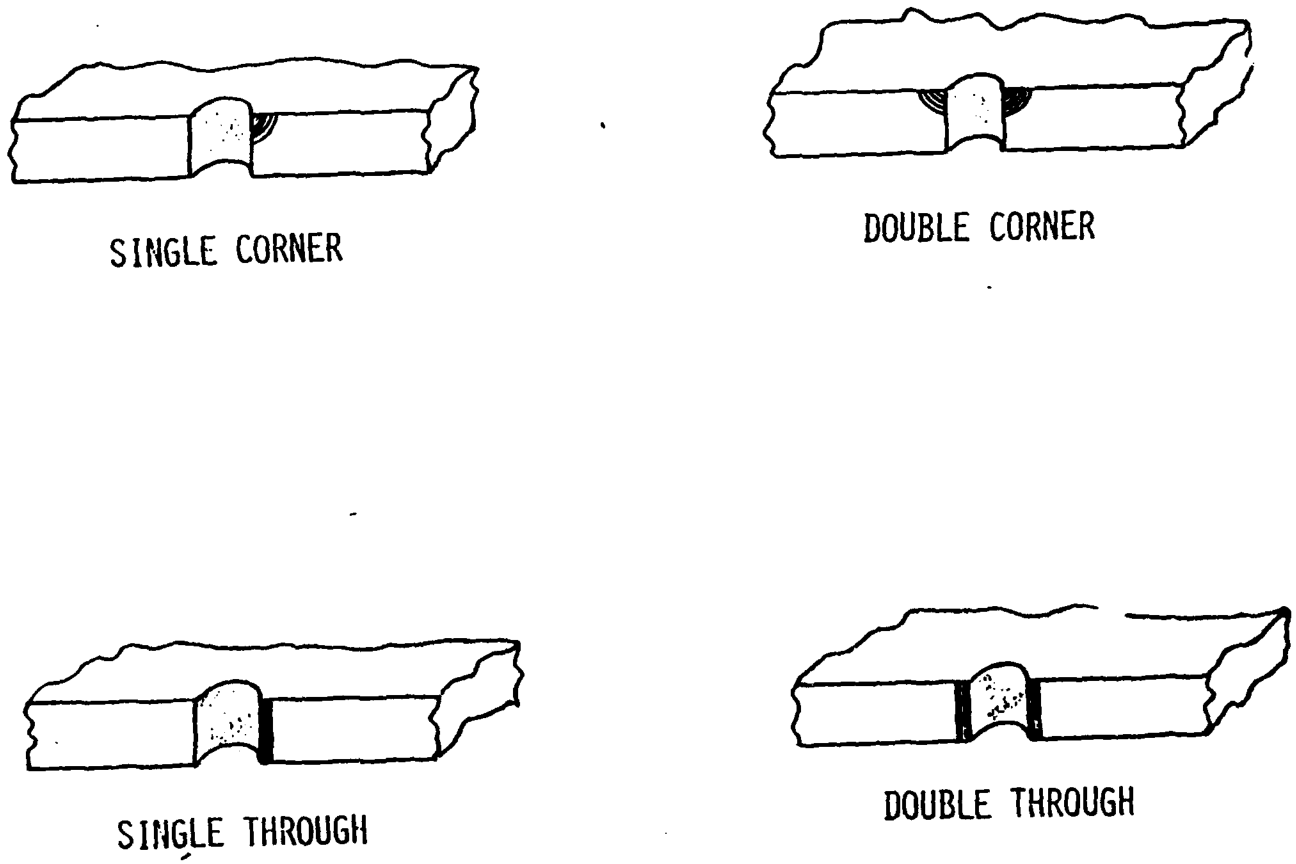

Figure 13. Initial Crack Geometries For Crack Growth Predictions

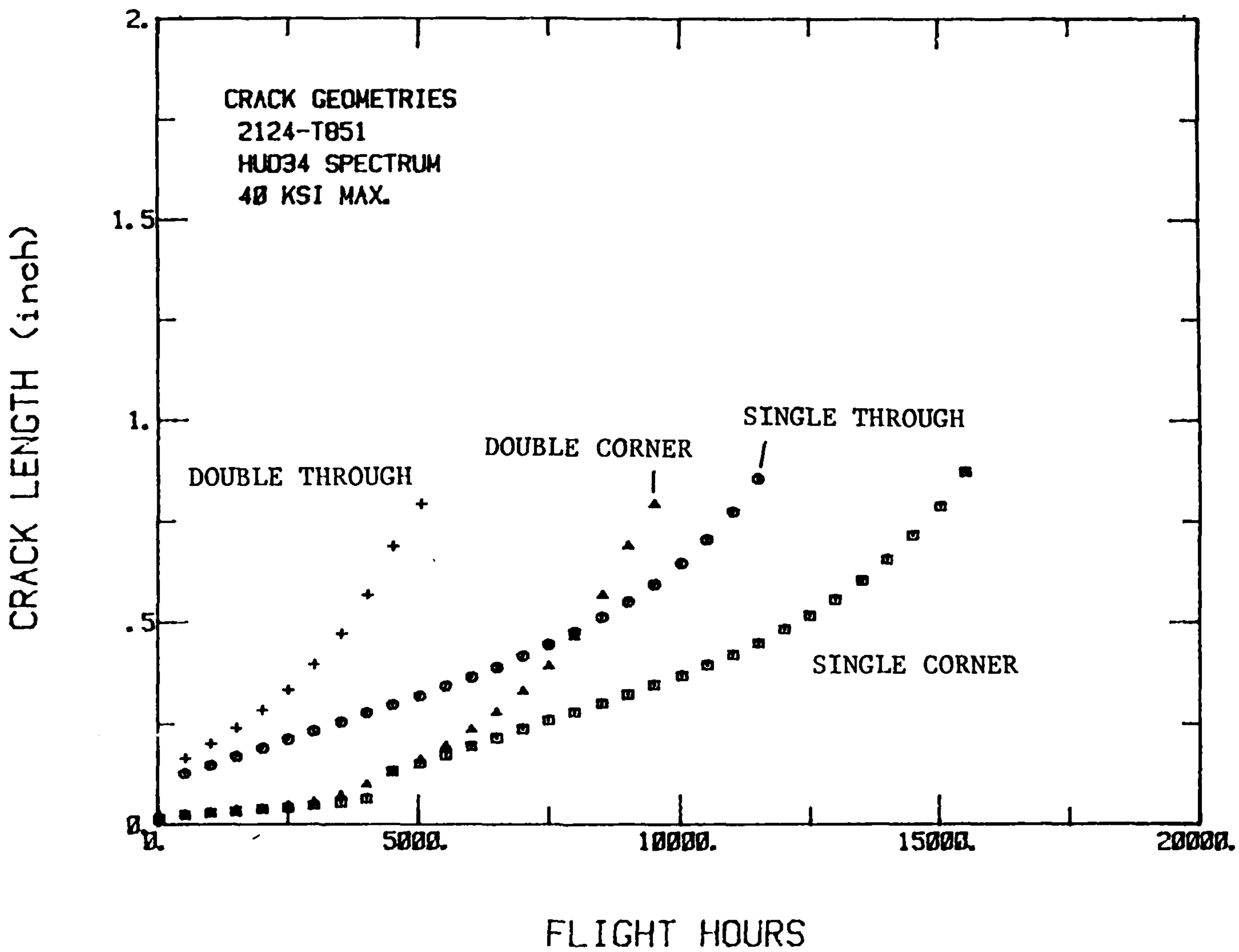

Figure 14. Crack Growth Predictions For 2124-T851 Aluminum Alloy

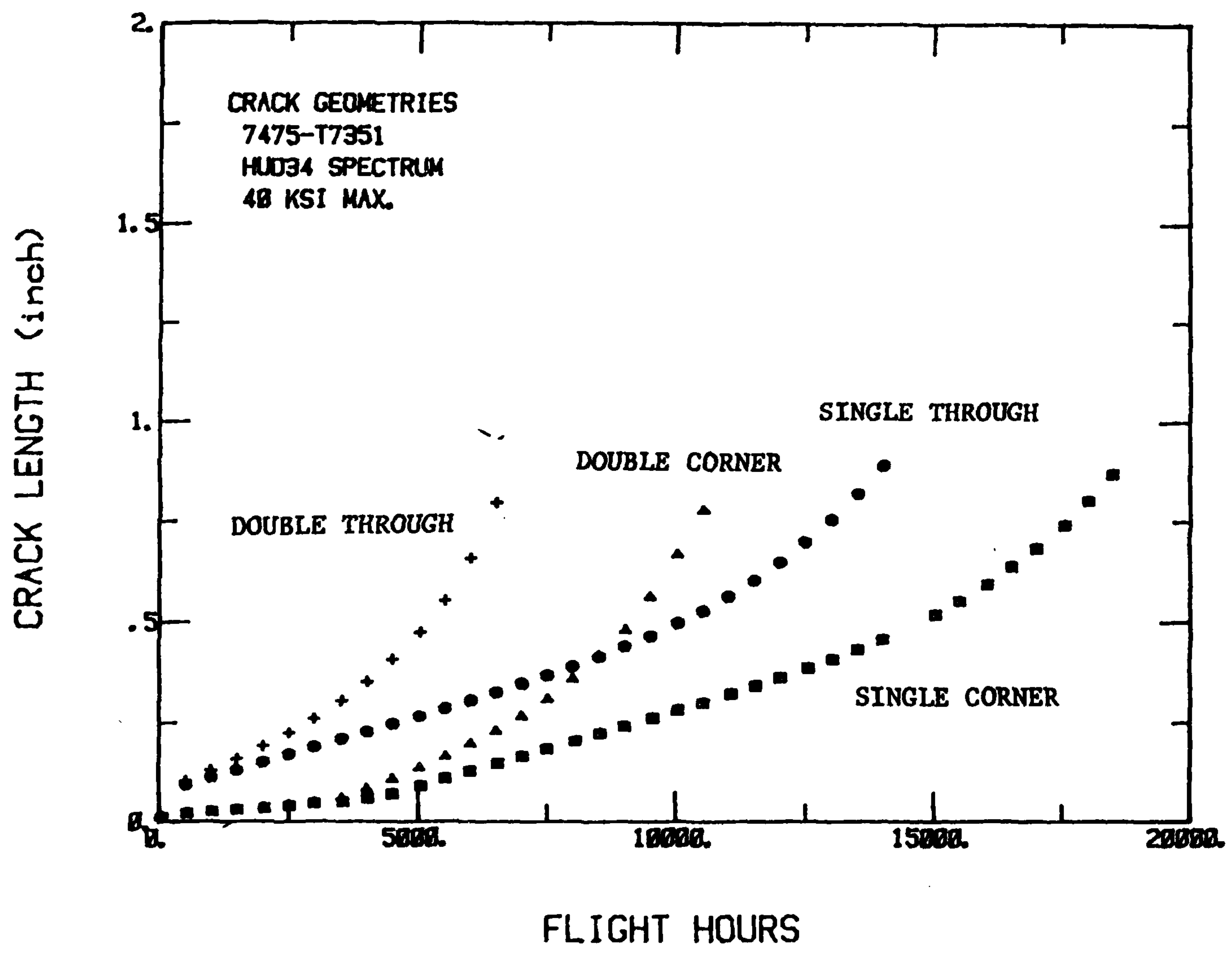

Figure 15. Crack Growth Predictions for 7475-T7351 Aluminum Alloy

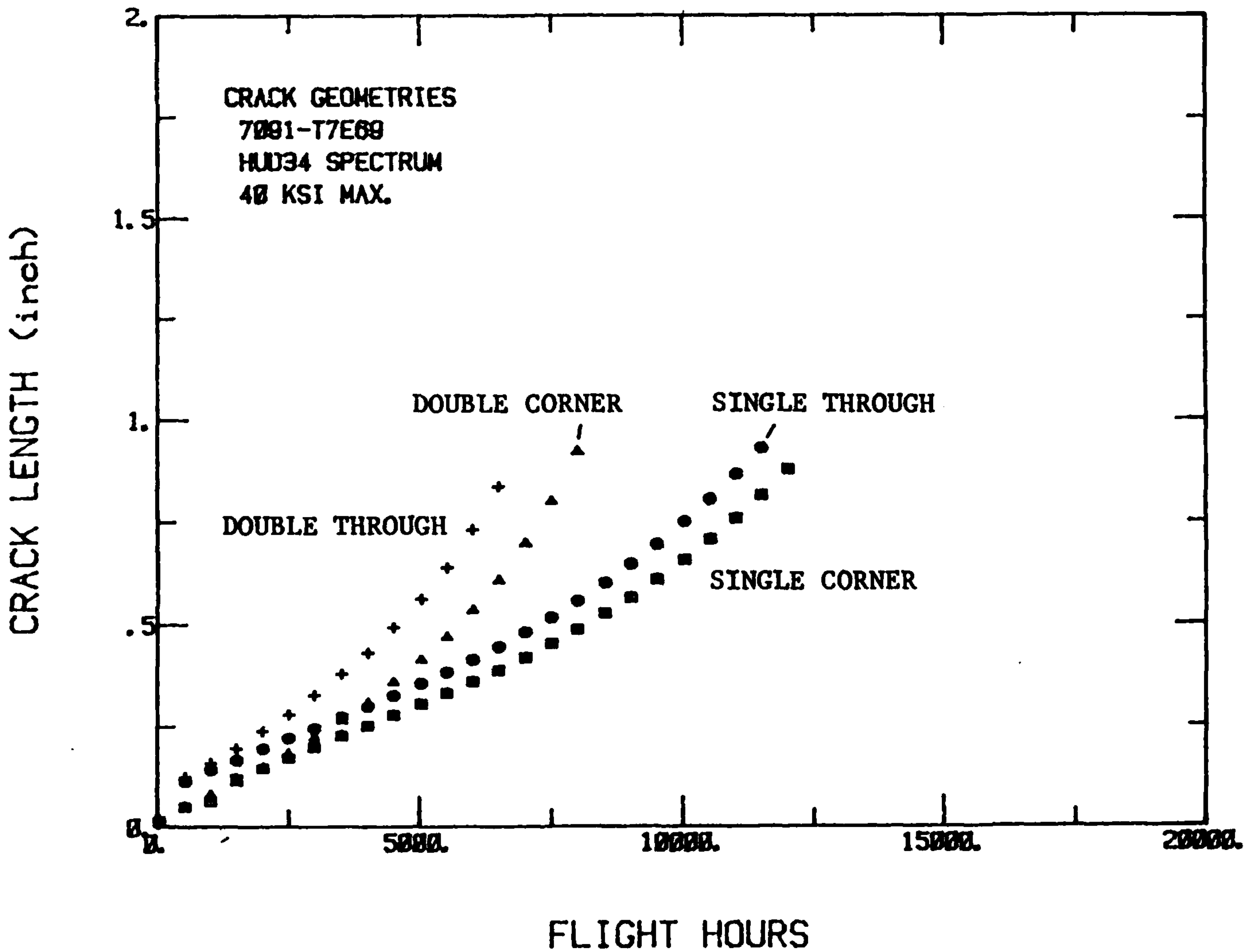

Figure 16. Crack Growth Predictions for 7091-T7E69 Aluminum Alloy

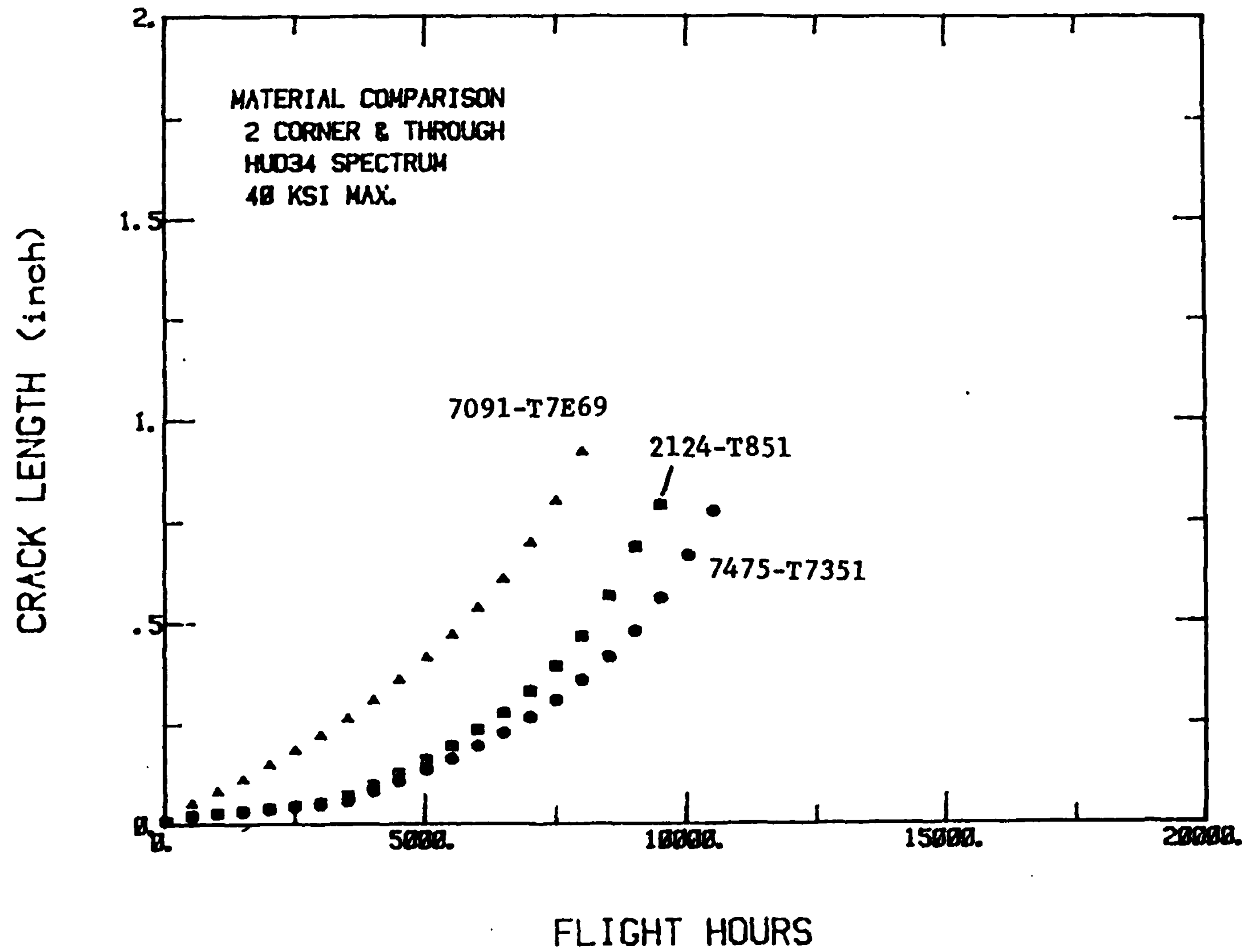

Figure 17. Crack Growth Prediction Comparisons for Three Aluminum Alloys

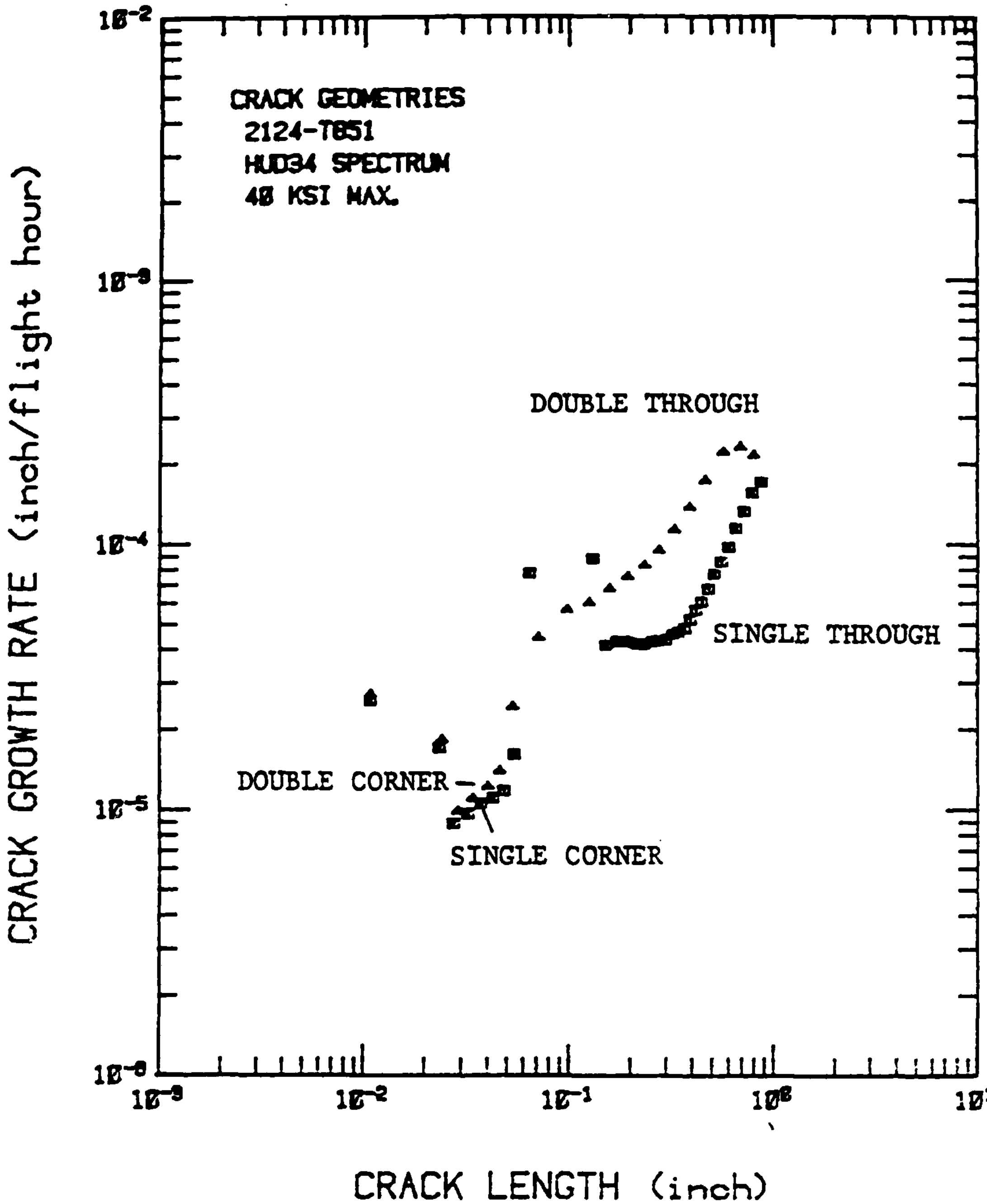

Figure 18. Crack Growth Rate Predictions for 2124-T851 Aluminum Alloy

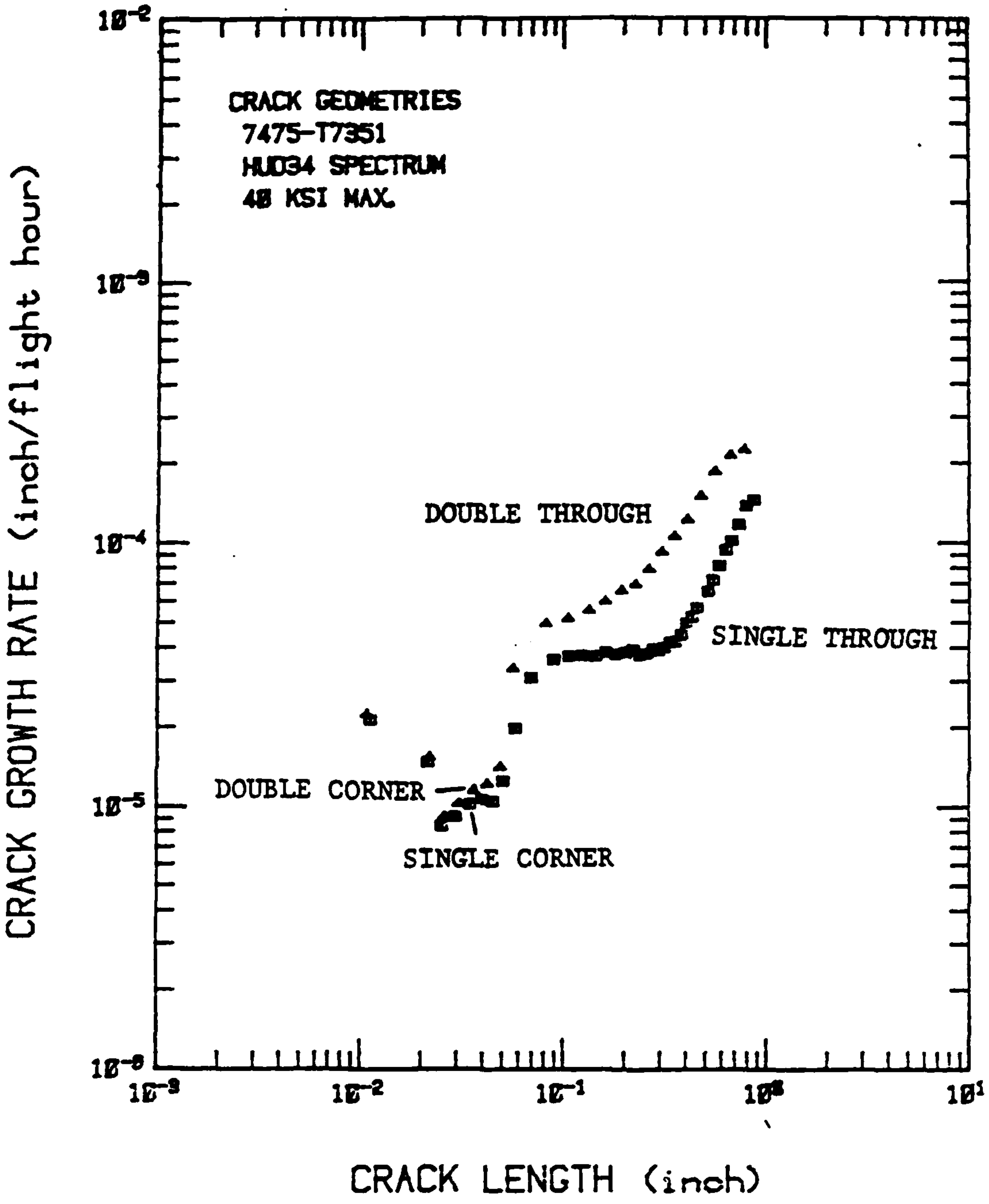

Figure 19. Crack Growth Rate Predictions for 7475-T7351 Aluminum Alloy

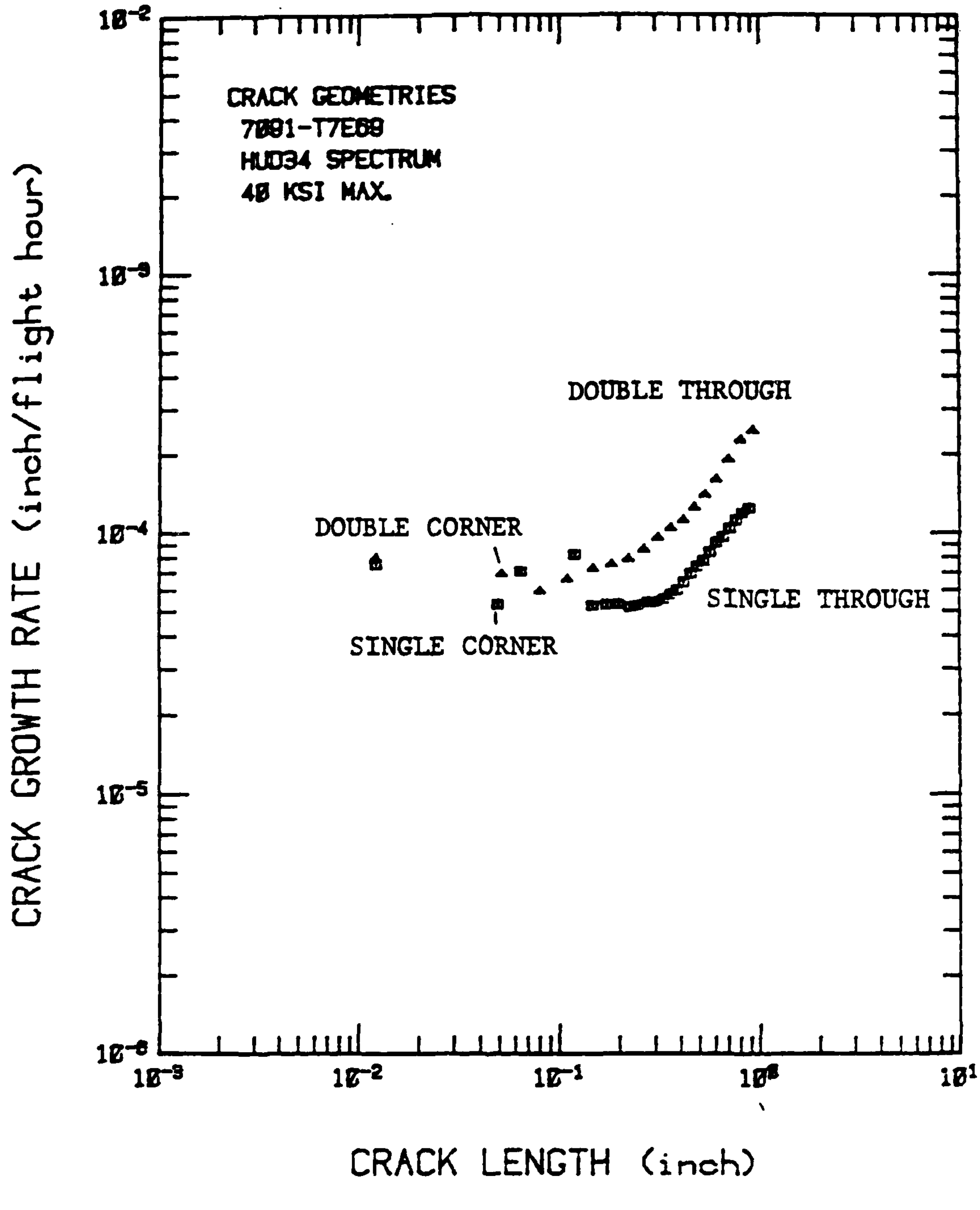

Figure 20. Crack Growth Rate Predictions for 7091-T7E69 Aluminum Alloy

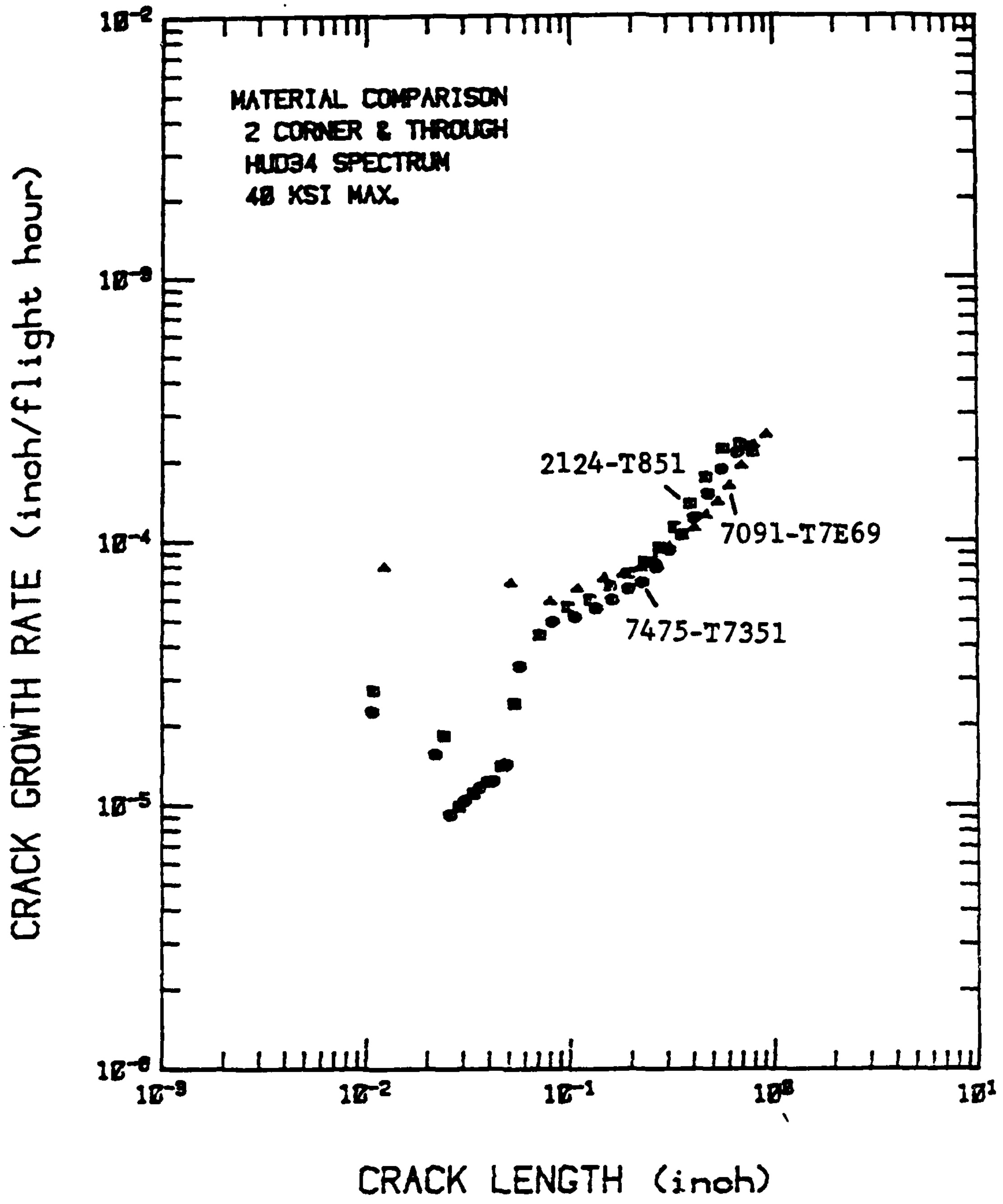

Figure 21. Crack Growth Rate Prediction Comparisons for Three Aluminum Alloys

One of the most important factors governing the structural performance of advanced structural concepts is the initial fatigue quality (IFQ). IFQ defines the initial manufactured state of a structural detail with respect to crack growth which is expected to occur in service. The IFQ for a group of replicate details can be presented by a distribution of equivalent initial flaw sizes (EIFS). Given that a crack occurs in a structure during service, the EIFS is the size of a hypothetical initial flaw which would result in the observed crack. The EIFS can be derived using fractography from fatigue test results. Crack growth observed after fatigue testing (fractography) is extrapolated backward to estimate EIFS. An EIFS distribution is obtained by fitting a statistical distribution to EIFS data sets.

An arbitrary crack size a_0 can be selected such that it can be unambiguously observed. The time required for an initial defect to become a fatigue crack of size a_0 is defined as the time-to-crack-initiation (TTCI). In general, the EIFS distribution is chosen so that the crack growth rate maps the EIFS distribution into the observed TTCI distribution. A conceptual description of the IFQ mcdel is shown in Figure 22.

It has long been noted that fatigue failure distributions can be fit by three-parameter Weibull distributions. Since failure in fracture critical structure corresponds to attainment of the critical crack size, it is reasonable to hope that this distributional form is appropriate for all crack sizes of interest. Preceding programs show [5,18,19] that observed TTCI values for small crack sizes can usually be fit very well by a three-parameter Weibull distribution.

Therefore, a fractographically observed TTCI distribution can be expressed as:

$$F_T(t) = P[T \leq t] = 1 - \exp\{-[\frac{t-\varepsilon}{\beta}]^{\alpha}\} \quad ; \quad t > \varepsilon \tag{1}$$

where T is a random variable indicating TTCI and $F_T(t)$ is just $P[TTCI \leq t]$. The Weibull parameter α , is the shape parameter, β is the scale parameter, and ϵ is the lower bound of TTCI. The parameters α , β and ϵ , are determined from a best-fit of fractography data, according to conditions discussed further below.

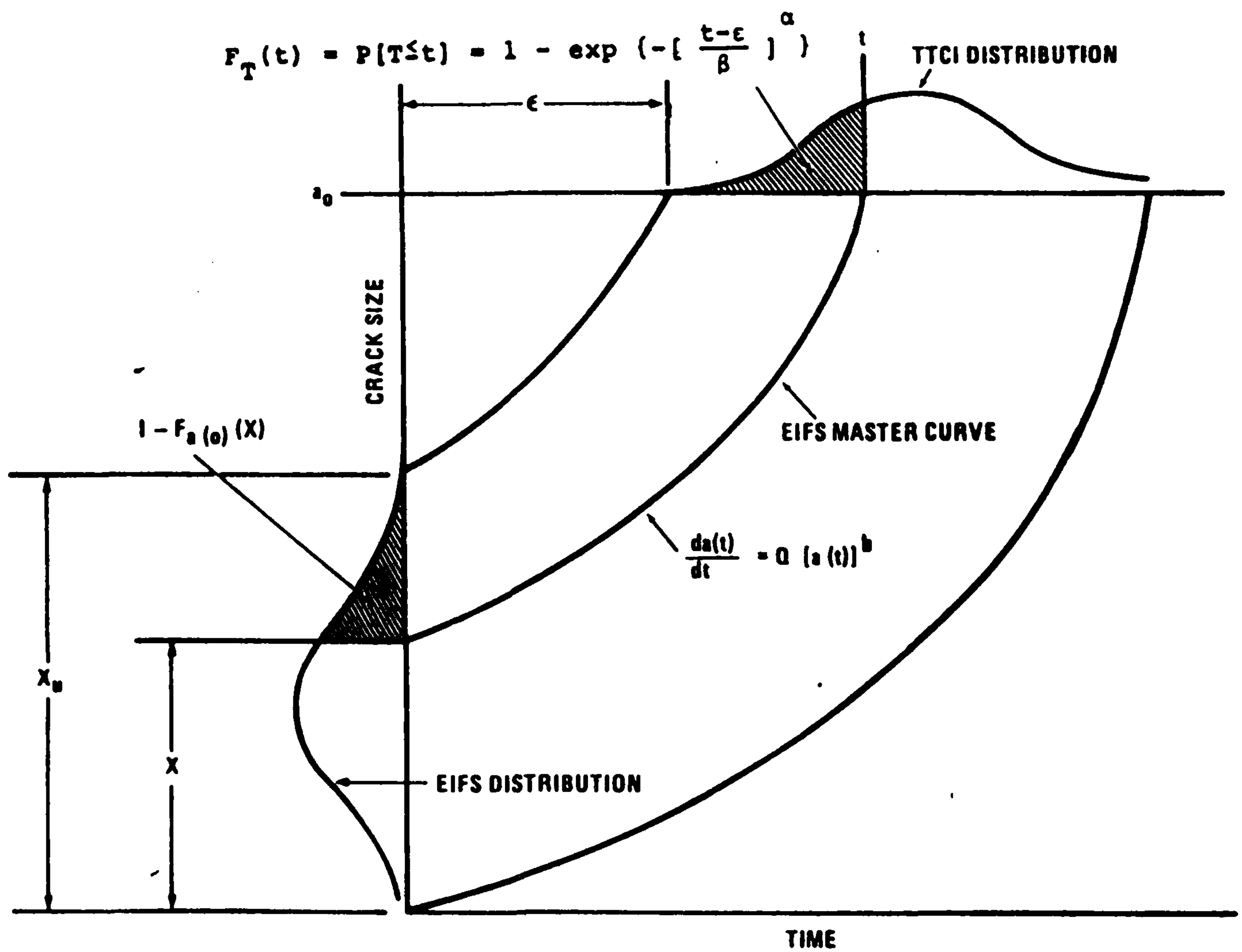

Figure 22. Conceptual Description of IFQ Model

The crack growth rate over the crack size range of interest is assumed to be expressed as:

$$\frac{da(t)}{dt} = Q[a(t)]^b \tag{2}$$

where a(t) is the crack size at time t, and Q and b are constants that are determined from the least square fit of all log da/dt vs. log a pairs of the sample.

Integrating Eq. (2) from t = 0 to t = T, the relationship between the crack size at t = 0, a(o) (i.e., EIFS), and that at t = T (i.e. a_0) is found to be:

$$\mathrm{EIFS} = a(0) = \frac{a_0}{\left(1+a_0^c\, cQT\right)^{1/c}} \tag{3}$$

where c = b -1.

Combining Eq. (1) and (3), one may obtain the EIFS distribution as:

$$F_{a(o)}(x) = \exp\left\{-\left[\frac{x^{-c} - x_u^{-c}}{cQ\ \beta}\right]^{\alpha}\right\} \quad ; \ 0 < x \le x_u \tag{4}$$

$$= 1 \quad ; \ x \ge x_u$$

where $F_{a(o)}(x)$ is just P[EIFS < x] and where x_u is the upper bound of the EIFS which is defined as:

$$x_u = [a_0^{-c} + cQ\epsilon]^{-1/c} \tag{5}$$

Therefore, the EIFS distribution can be determined from Eq. (4), if the parameters Q, c =b-1, α, β, and ϵ are properly calibrated based on the fractographic data.

As mentioned previously, EIFS is intuitively a generic property of such factors as the material, manufacturing/assembly techniques, and workmanship and should be independent of load spectrum and stress level. Eq. (4) shows that the necessary conditions to ensure that the EIFS distribution is generic among two or more data sets are:

$$\begin{gathered} b_1 = b_2 = \ldots\ldots = b_n \\ \alpha_1 = \alpha_2 = \ldots\ldots = \alpha_n \\ Q_1\beta_1 = Q_2\beta_2 = \ldots\ldots = Q_n\beta_n \end{gathered} \tag{6}$$

Accordingly, it is recommended that any sample of identically prepared test elements be randomly split into at least two groups (Figure 23). These should be tested at different stress levels. If possible, a third group tested with a different spectrum is desirable. Then all fractography is least squares fit subject to the conditions given in Eq. (6). Adequate fits to the data have been found so far using this procedure, and this procedure ensures that the EIFS is as generic as can be among the conditions tested. Testing at two stress levels also reveals the dependence of crack growth on stress level, which is useful for preforming trade studies.

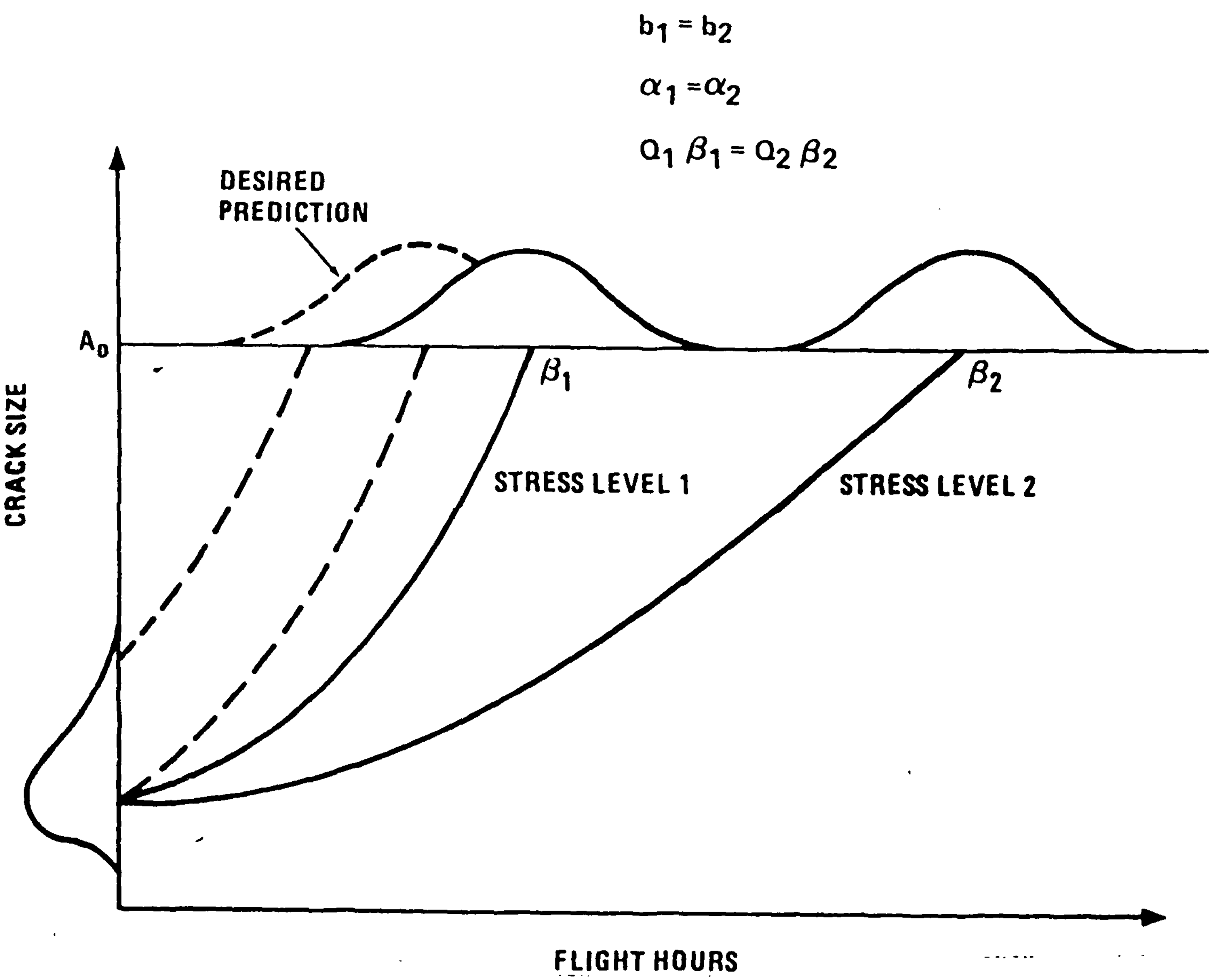

Figure 23. Generic EIFS Concept

SECTION V

RESULTS AND DISCUSSION

In this section. all experimental results are presented and analyzed. These results include: (1) basic mechanical properties, (2) NDI results, and (3) spectrum fatigue tests. Spectrum fatigue results are divided into the following categories: (a) time-to-failure (TTF), (b) fatigue crack growth rate (FCGR), (c) time-to-crack-initiation (TTCI), and (d) measurements of equivalent initial flaw size (EIFS).

Also, in this section, the durability and damage tolerance of RST structures are discussed. Methodology used in comparing RST structures with conventional I/M structures is presented and discussed. Techniques which can be used in design studies are proposed.

5.1 MECHANICAL PROPERTIES

Table 6 shows basic mechanical properties of 2124-T851, 7475-T7351, 7091-T7E69 extruded material, 7091-forgings, and CW67-T7E91 extruded material.

Improved strength is observed in the RST P/M alloys as compared to the ingot metallurgy materials. Ultimate tensile strengths as high as 90 ksi were observed in the CW67 extruded material in the (L) orientation.

Fracture toughness values of CW67-T7E91 are quite high, also. Values as high as 50 ksi $\sqrt{in.}$ (L-T orientation) were obtained from one billet of material. These toughness values are comparable to values obtained for 7475-T7351 (48 ksi $\sqrt{in.}$) and higher than those obtained in 7091-T7E69 and 2124-T851 (36 ksi $\sqrt{in.}$ and 29 ksi $\sqrt{in.}$, respectively.

By controlling the heat treat, the mechanical properties of 7091-forgings were quite similar to values obtained for 7091-extrusions (Table 6). As discussed in Section III, final aging times at 325°F were extended in the 7091-forged material in order to achieve these strength values.

TABLE 6. BASIC MECHANICAL PROPERTIES OF LONGITUDINAL ORIENTATION

MATERIAL	YIELD STRENGTH (ksi)	TENSILE STRENGTH (ksi)	PERCENT ELONGATION (%)	FRACTURE TOUGHNESS (ksi $\sqrt{in.}$)
2124-T851	64	71	9	29
7475-T7351	63	73	14	48
7091-T7E69	75	83	14	36
7091-FORG.	73	80	15	--
CW67-T7E91	86	90	12	50

Results of mechanical tests conducted on CW67 extrusions are shown in Table 7. The first batch of spectrum fatigue coupons tested were obtained from a CW67 powder billet, #514553-2. The specimens tested later were obtained from powder billets, #514570 and #514571. Higher strengths and larger fracture toughness values were obtained for material obtained from billet #514553-2. Better fatigue properties were also obtained from test coupons fabricated from this billet. Fatigue properties are discussed in Section 5.3. Slightly higher elongation and reduction of area was obtained in CW67 extrusions obtained from billets #514570 and #514571.

Some anisotropy was observed in basic mechanical properties for the CW67 extrusions. Ultimate tensile strengths are observed to decrease from 90.7 ksi in the front (L) orientation to 82.7 ksi in the rear (ST) orientation for material from the #514553-2 billet. Fracture toughness values decreased from 49.8 ksi $\sqrt{\text{in.}}$ in the (L-T) orientation to 24.1 $\sqrt{\text{ksi}}$ in. in the (S-L) orientation for the same material.

5.2 NDI RESULTS

5.2.1 Baseline Specimens

Eddy current and dial bore gauge measurements were made on all fastener holes of the spectrum fatigue test coupons. NDI parameters such as eddy current amplitude, hole out-of-roundness, and hole diameter were measured and compared to fatigue life.

Typical eddy current scans for fastener holes in two test coupons, are shown in Figure 24. Also shown is the eddy current signature from a reference hole containing a 0.022-inch-deep fatigue crack. In general, no correlation was observed between eddy current amplitude and fatigue life. Typical results where eddy current amplitude is plotted as a function of fatigue life is shown in Figure 25. These results are shown for 7475-T7351 test coupons imposed to the NOR 1 spectrum. Eddy current results indicated that the hole quality was fairly equivalent in all of the holes.

Dial bore gauge results also indicated little correlation between hole quality parameters such as out-of-roundness or oversized holes with fatigue life. Results are shown in Figures 26-

TABLE 7. RESULTS OF MECHANICAL TESTS ON CW67 EXTRUSION

Billet No.	Temper	Location of Test Specimens	Specimen Orientation	UTS (ksi)	YS (ksi)	EL (%)	RA (%)	Kic (ksi $\sqrt{in.}$)
514553-2	T7E91	Front	L (L T)	90.7	86.2	11.8	23	49.8
			LT (T-L)	85.9	81.6	10.9	23	29.8
			ST (S-L)	84.0	74.3	8.6	13	24.1
		Rear	L (L-T)	89.7	85.0	12.3	24	49.8
			LT (T-L)	84.0	79.8	10.7	26	31.0
			ST (S-L)	82.7	73.6	9.9	22	27.3
514570 and 514571		Front	L(L-T)	89.2	84.7	12.9	31.0	44.1
			LT(T-L)	84.7	78.4	12.9	25.2	24.0
			ST (S-L)	82.2	72.9	8.7	18.0	20.4
		Rear	L(L-T)	86.4	81.3	13.3	34.4	45.7
			LT(T-L)	81.0	74.1	12.0	27.9	26.1
			ST(S-L)	81.3	68.8	9.7	18.2	25.5

* Results obtained from Alcoa.

(a) 2124 Specimen 2124-6(1)

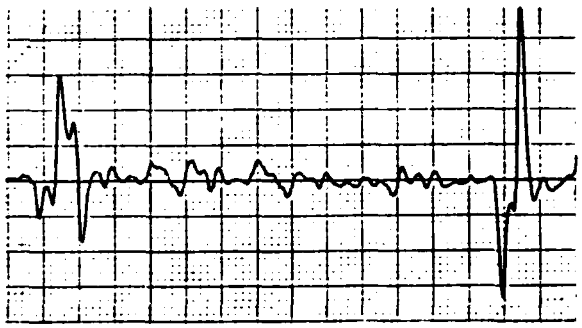

(b) Specimen 2124-41(2)

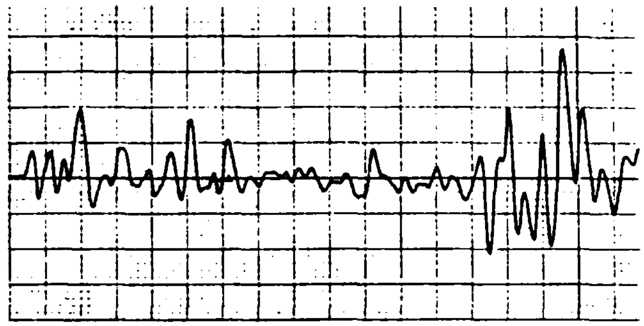

(c) Standard specimen - .022""fatigue crack

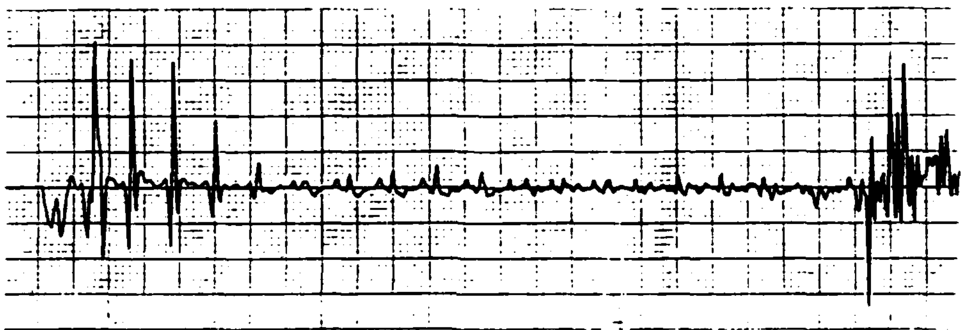

Figure 24. Typical Eddy Current Bolt Hole Scans.
(a) Specimen No. 2124-6, (b) Specimen No. 2124-41,
(c) Standard Specimen with .022 Inch Fatigue Crack

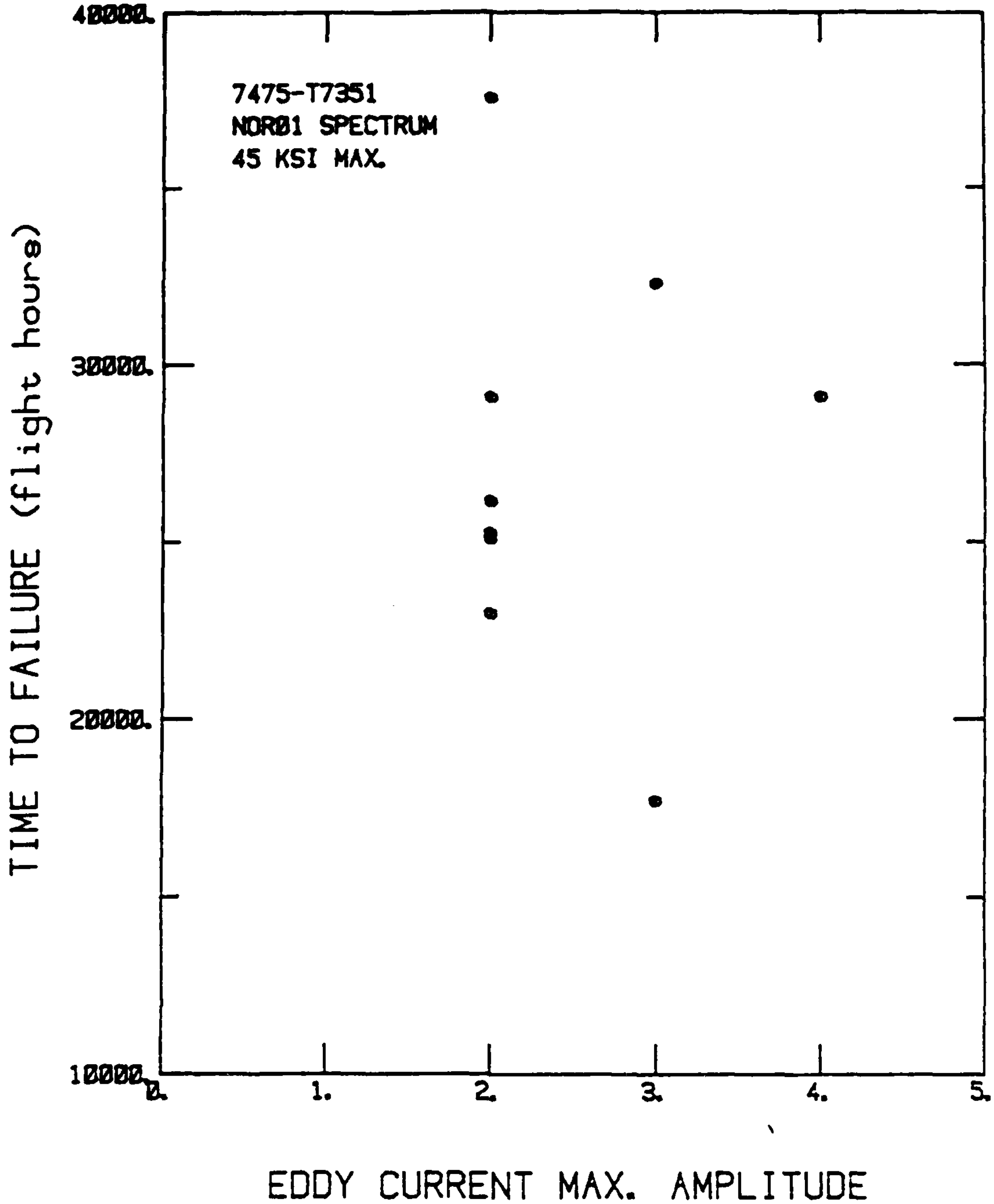

Figure 25. Eddy Current Amplitude Versus Time-To-Failure In 7475-T7351 Aluminum Alloy

27 for 7475-T7351 test coupons tested under the NOR 1 spectrum at a maximum spectrum stress of 45 ksi.

The results of little or no correlation between fatigue behavior and hole quality as measured by the two different NDE techniques are consistent with results obtained from the "Fastener Hole Quality" [12] and "Initial Quality of Advanced Joining Concept programs" [5]. In the "Fastener Hole Quality" program, flaws which degraded the cosmetic hole quality, such as rifling marks, gouges, drill tool chatter marks, etc., did not necessarily affect structural fatigue performance.

5.2.2 RST Specimens

Eddy current and dial bore gauge measurements were also made on all fastener holes in the RST test coupons. In addition, ultrasonic and x-ray inspections were made on all of the P/M specimens and residual stress measurements were made on the 7091-forged test coupons. Ultrasonic and x-ray inspections were only made on the RST test coupons since control of inclusions is considered extremely important in these materials. Both ultrasonic and x-ray inspection techniques are considered sensitive NDI techniques for detecting these inclusions.

Similar to results obtained for baseline coupons, no correlation between NDI parameters such as eddy current amplitude, hole out-of-roundness, and hole diameter and fatigue life were obtained in the RST materials.

Ultrasonic and x-ray inspections of the RST test coupons revealed no large inclusions or voids in these materials. A typical ultrasonic C-scan of the 7091 material is shown in Figure 28. Inspections of the 7091-forged test coupons did not reveal any defects due to forging such as forging laps.

Residual stress measurements taken on the surface of the 7091-forged coupons before testing indicated small compressive stresses. The depth of this compressive layer measured less than 0.010 inch deep as shown in residual stress depth profile measurements (Table 8). Little correlation between magnitude of the surface residual stresses and time-to-failure were observed in 7091-forged coupons tested under the HUD34 spectrum at a maximum stress level of 45 ksi (Figure 29).

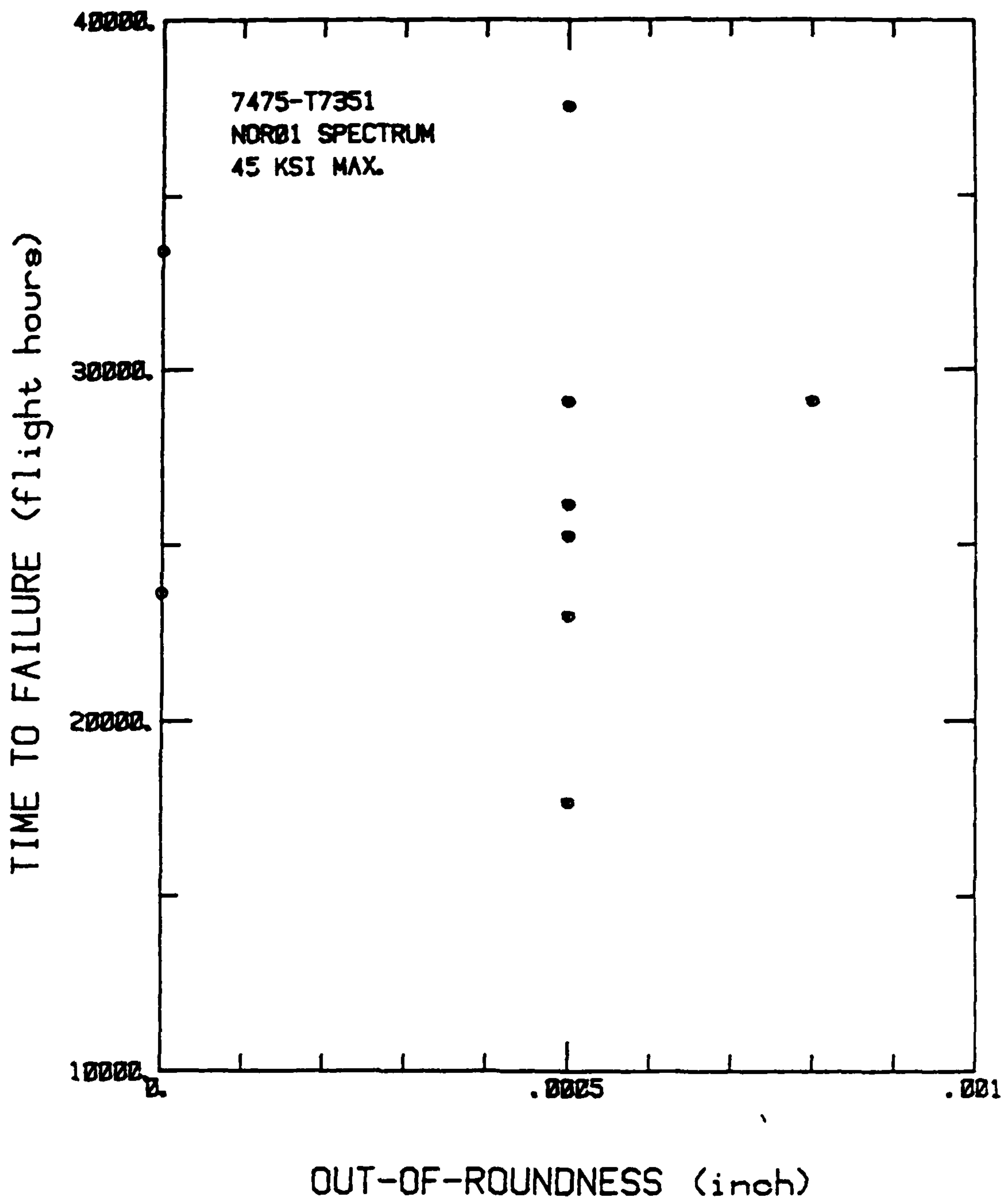

Figure 26. Hole Out-Of-Roundness Versus Time-To-Failure In 7475-T7351 Aluminum Alloy

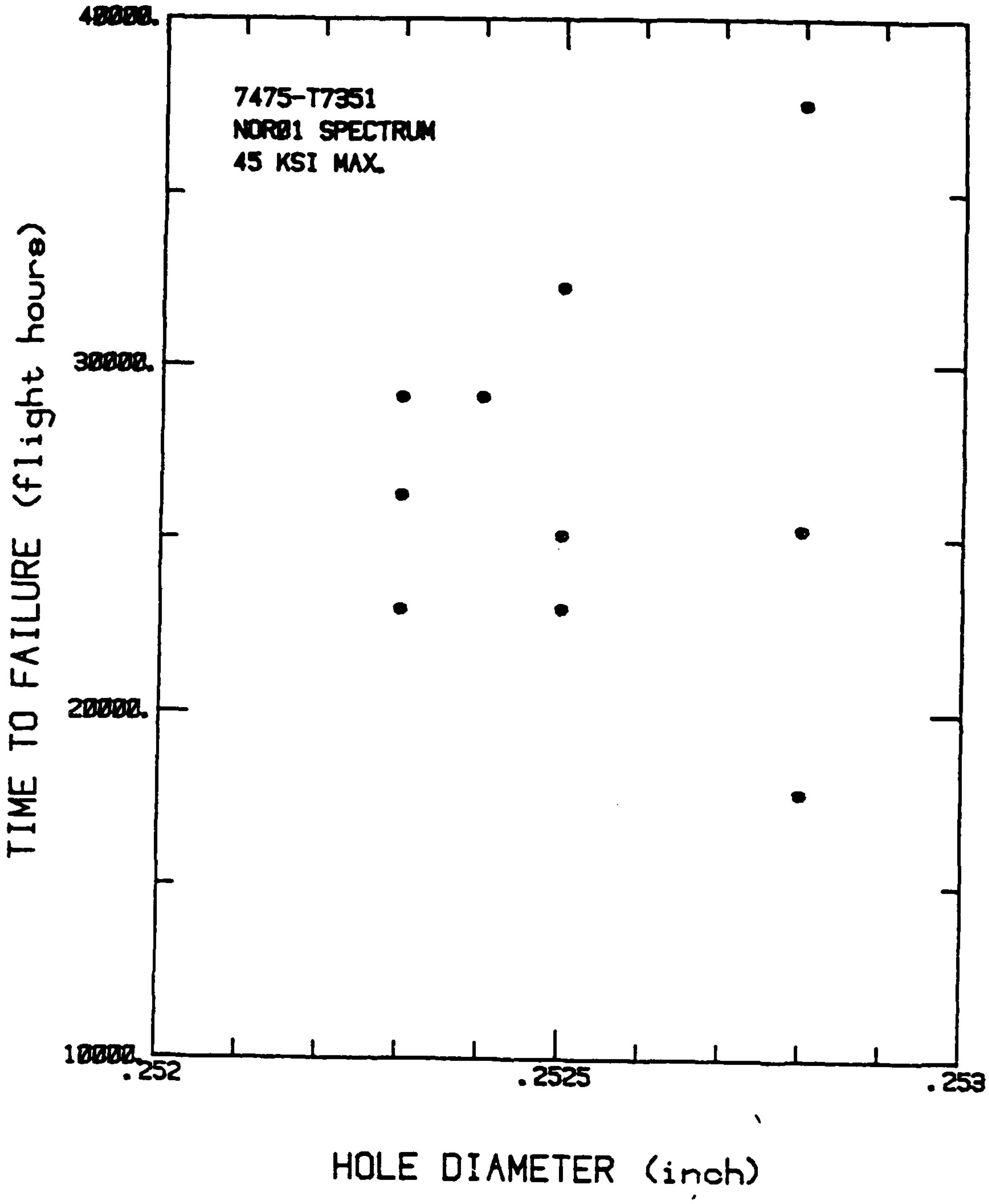

Figure 27. Hole Diameter Versus Time-To-Failure In 7475-T7351 Aluminum Alloy

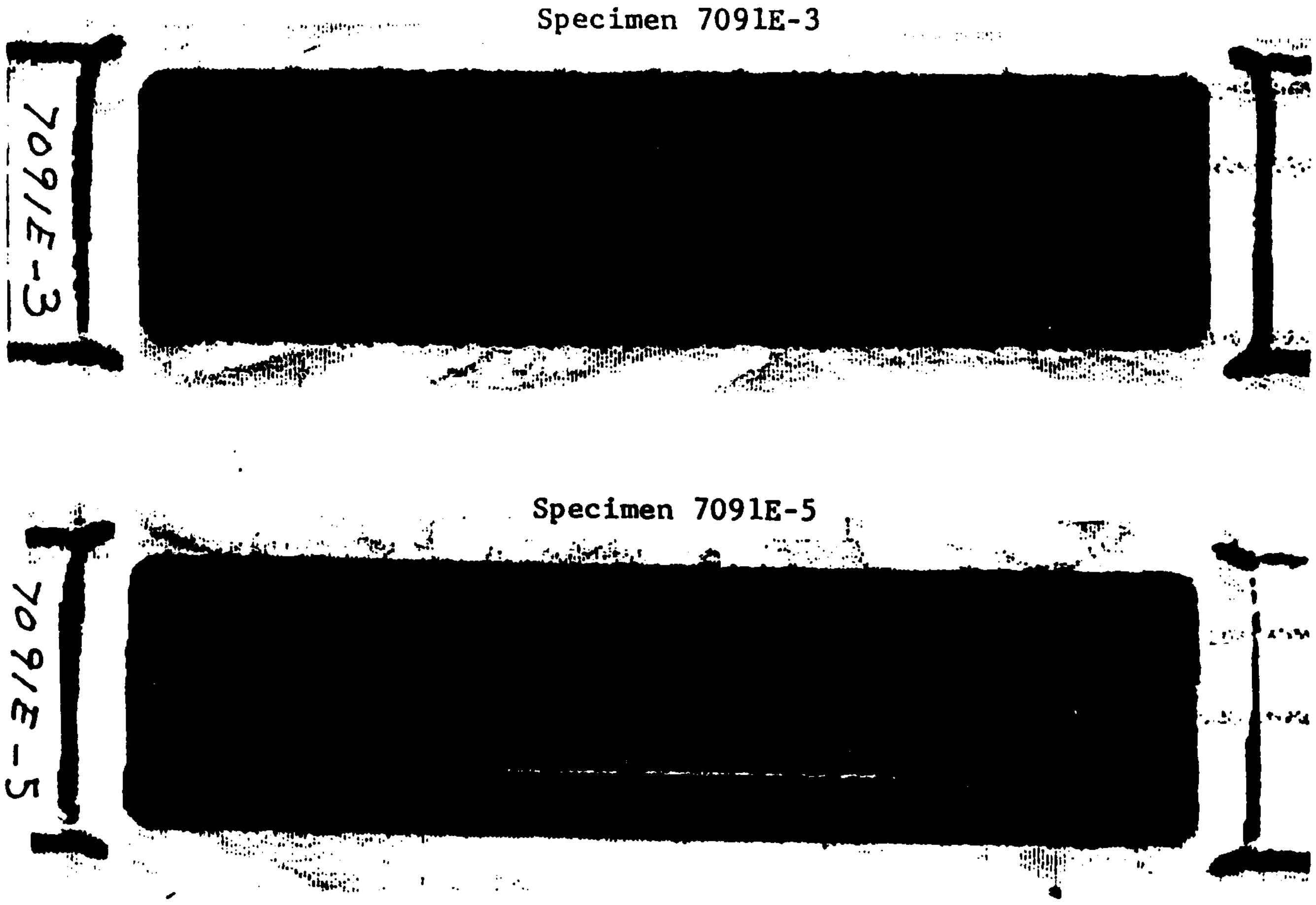

Figure 28. Typical Ultrasonic C-Scan In 7091 Aluminum Alloy

TABLE 8. RESIDUAL STRESS DEPTH PROFILE

7091F-12		7091F-17	
DEPTH (In.)	STRESS (ksi)	DEPTH (In.)	STRESS (ksi)
SURFACE	-10	SURFACE	-16
0.001	-12	0.002	-14
0.002	-13	0.004	-14
0.010	-1	0.010	-2

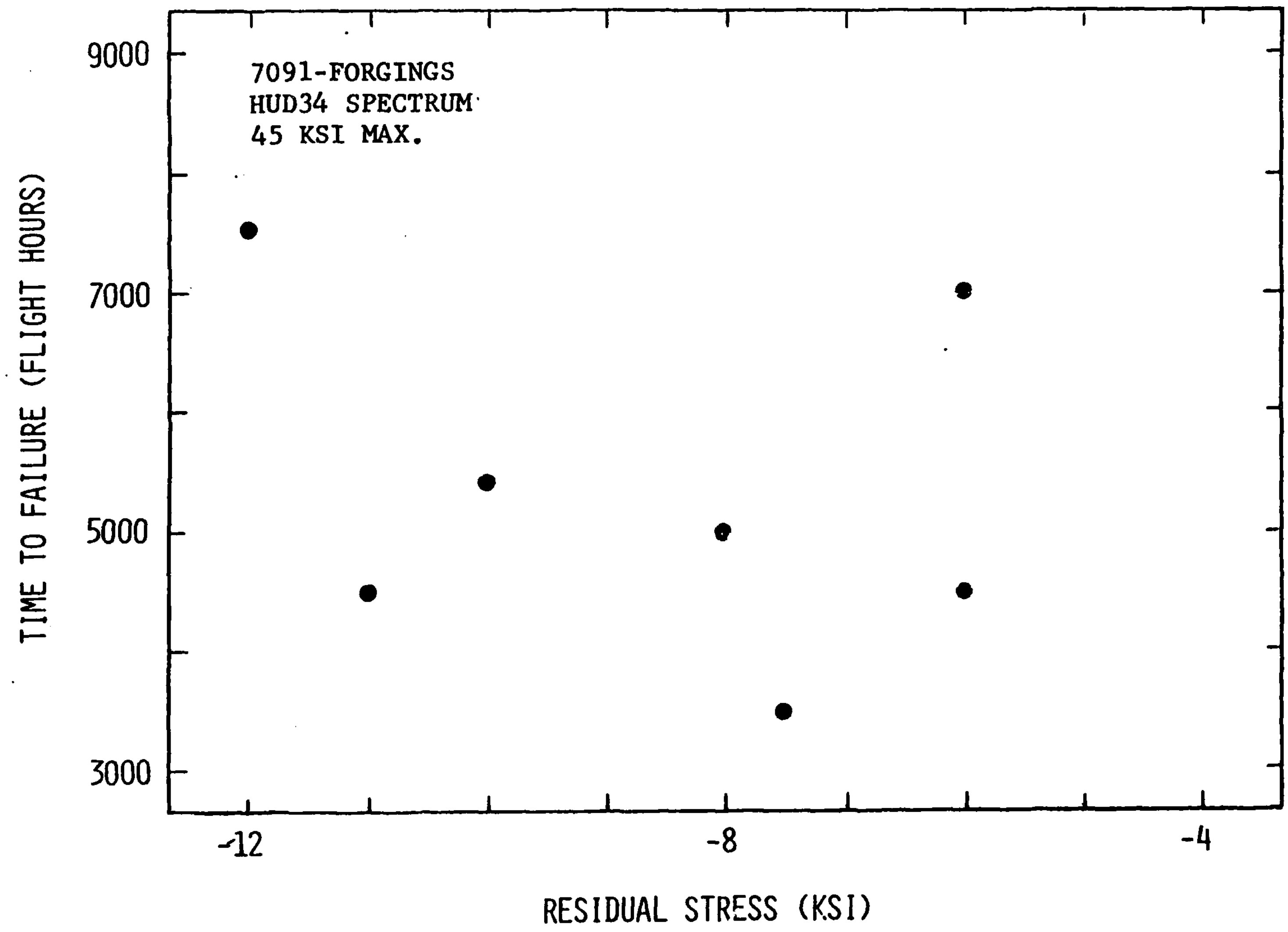

Figure 29. Residual Stress Versus Time-To-Failure In 7091-Forged Specimens

5.3 SPECTRUM FATIGUE TESTS

Results of the spectrum fatigue tests are given in this section. Results are based on approximately 150 tests. The section is divided into four areas: (a) time-to-failure (TTF), (b) fatigue crack growth rate (FCGR), (c) time-to-crack-initiation (TTCI), and (d) measurements of equivalent initial flaw size (EIFS).

All spectrum fatigue crack growth data were analyzed based upon the equivalent initial flaw size (EIFS) concept [5,12,18,21,22]. The basic elements of the initial fatigue quality (IFQ) model include a power law crack growth description containing parameters Q and b and a Weibull distribution describing the time for a fatigue crack to grow to any arbitrary size, a_0. The Weibull distribution is described by parameters α , β , and ϵ . The concepts of the IFQ model and the procedures for determining IFQ model parameters are described in detail *in Section 4.2.*

Table 9 summarizes the IFQ model parameters for this program. Table 9 shows that the values of b , α , and $Q\beta$ do not vary with the test condition. These invariance conditions must be *satisfied in order for the equivalent initial flaw size (EIFS)* distribution to be generic, that is, independent of spectrum or stress level. This property is desirable since we expect the initial fatigue quality to depend on structural concept, material, and manufactured quality rather than on subsequent service conditions.

The information in Table 9 is a complete description of the results of approximately one hundred fifty spectrum tests. It contains all the information necessary for determining the crack growth performance of each structural concept. It is the information needed for predicting crack growth behavior, as shown in Section 4. Q and b in Table 9 describe the average crack growth for each test condition, according to equation (2). The parameters α and β , describe the time to initiate a crack of arbitrary size a_0. The upper bound of the EIFS distribution, x_u, is determined by the other parameters.

TABLE 9 INITIAL FATIGUE QUALITY MODEL PARAMETERS

SPECIMEN	SPECTRUM	STRESS (KSI)	a_0 (IN.)	X_U (IN.)	Q	b	α	β	$Q\beta$	TTF (Flt Hrs)	a_{crit} (IN.)
2124-I851	HUD34	35	0.15	0.15	3.4012 X 10-4	0.8209	2.8556	11088	3.7713	14993	.74
	HUD34	40	0.15	0.15	7.8911 X 10-4	0.8209	2.8556	4779	3.7713	5886	.49
	NOR1	45	0.15	0.15	2.6592 X 10-4	0.8209	2.8556	14182	3.7713	15423	.59
7475-T7351	NOR1	45	0.15	0.15	1.5314 X 10-4	0.8343	3.5257	20749	3.1776	26465	.69
7091-EXTR.	HUD34	40	0.15	0.15	1.4106 X 10-4	0.6096	2.4417	9830	1.3866	17997	.78
	HUD34	45	0.15	0.15	3.8433 X 10-4	0.6096	2.4417	3608	1.3866	7309	.80
	NOR1	45	0.15	0.15	6.5999 X 10-5	0.6096	2.4417	21009	1.3866	36949	.74
	NOR1	50	0.15	0.15	1.3795 X 10-4	0.6096	2.4417	10051	1.3866	15238	.72
7091-FORG.	HUD34	40	0.15	0.15	1.7583 X 10-4	0.5622	2.6221	6709	1.1796	11667	.80
	HUD34	45	0.15	0.15	3.7679 X 10-4	0.5622	2.6221	3131	1.1796	5544	.80
CW67	HUD34	40	0.15	0.15	2.1798 X 15-4	0.7094	2.6717	6386	1.5818	14360	.92
	HUD34	45	0.15	0.15	4.2535 X 10-4	0.7094	2.6717	3940	1.5818	10572	.91
	NOR1	45	0.15	0.15	1.0663 X 10-4	0.7094	2.6717	15732	1.5818	21939	.89

5.3.1 Time-To-Failure (TTF)

A summary of spectrum fatigue test results are given in Table 10. Average time-to-failure (TTF) values are given along with the standard deviation. In general, stress levels were selected such that fatigue failure was achieved before three lifetimes were completed. Table 10 shows that the P/M alloys (CW67-T7E91 and 7091-T7E69) exhibit longer total time-to-failure (TTF) than the I/M alloys (2124-T851 and 7475-T7351). In general, scatter of experimental data, was observed to be no greater in the high starength P/M alloys than in the I/M alloys. Only one group of P/M specimens, (7091-T7E69 under the data set RINR45) exhibited a fairly large standard deviation in TTF.

Material comparisons in TTF were made in terms of Weibull probability plots. In Figures 30-32, comparisons are made where tests were conducted under identical spectra and stress levels. For test coupons tested under the HUD34 spectrum at a maximum stress level of 40 ksi, optimum fatigue life was obtained in the 7091-extruded test coupons survived three lifetimes (24,000 flight hours) without failing. Considerable improvement in fatigue life was observed in the 7091 P/M material as compared to the 2124-T851 I/M test coupons. Average TTF values for the 7091-extruded specimens were approximately three times as large as for 2124-T851 (17,997 flight hours as compared to 5,886 flight hours). Some degradation in fatigue life was observed in the 7091-forged material as compared to extruded specimens. However, superior TTF was still observed in the P/M forged material as compared to 2124-T851 (Figure 30).

CW67 P/M material tested under the HUD34 spectrum at a maximum stress of 40 ksi were obtained from billets, #514570 and #514571. Coupons tested from these billets had inferior spectrum fatigue properties compared to specimens obtained from billet #514553.

However, the CW67 test coupons from these billets still had considerable improvement in total fatigue life as compared to the 2124-T851 I/M test coupons (Figure 30).

For coupons tested under the HUD 34 spectrum at a maximum stress level of 45 ksi, largest TTF values were obtained in CW67-T7E91 P/M material (Figure 31). Extruded CW67 coupons used in these tests were from billet #514553 which showed superior fatigue properties. An increase in TTF of 45 percent was obtained

TABLE 10. SUMMARY OF SPECTRUM FATIGUE TESTS RESULTS

MATERIAL	SPECTRUM	STRESS LEVEL (ksi)	DATA SET NAME	NUMBER OF SPECIMENS	AVERAGE TTF (Flt. Hrs.)	STANDARD DEVIATION (Flt. Hrs.)
2124-T851	HUD34	35	C1HD35	15	14,933	5,558
	HUD34	40	C1HD40	15	5,886	1,276
	NOR1	45	C1NR45	10	15,423	5,162
7475-T7351	NOR1	45	C2NR45	11	26,465	5,104
7091-T7E69	HUD34	40	R1HD40	14	17,997	5,997
	HUD34	45	R1HD45	15	7,309	2,807
	NOR1	45	R1NR45	10	26,949	10,282
	NOR1	50	R1NR50	10	15,238	3,233
7091-FORG.	HUD34	40	R2HD40	9	11,667	2,667
	HUD34	45	R2HD45	9	5,544	1,362
CW-67-T7E91	HUD 34	40	R3HD40	10	14,360	5090
	HUD 34	45	R3HD45	8	10,572	1250
	NOR 1	45	R3NR45	10	21,939	5650

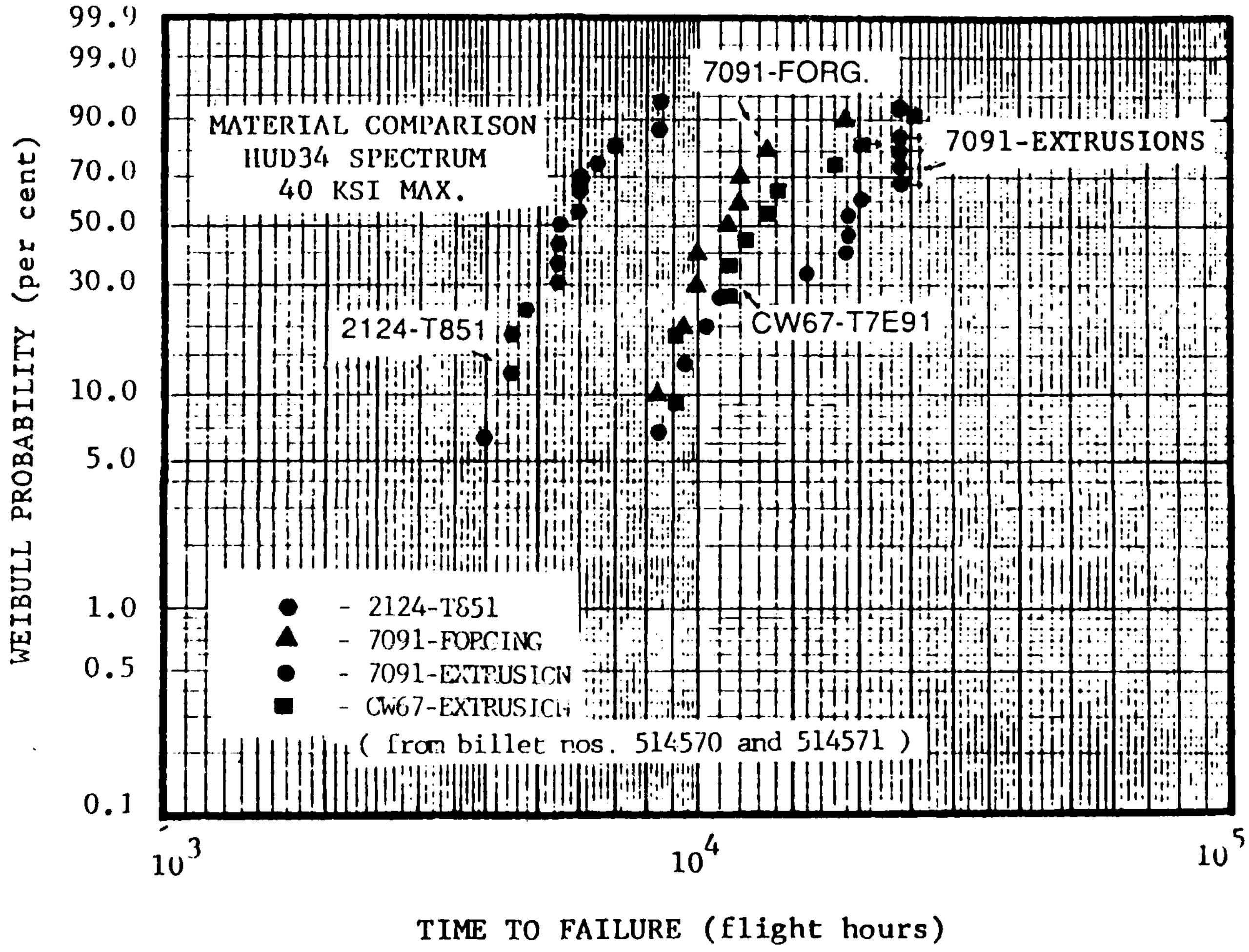

FIGURE 30. Time-To-Failure Comparisons For Materials Tested Under The HUD 34 Spectrum (Maximum Stress = 40 ksi)

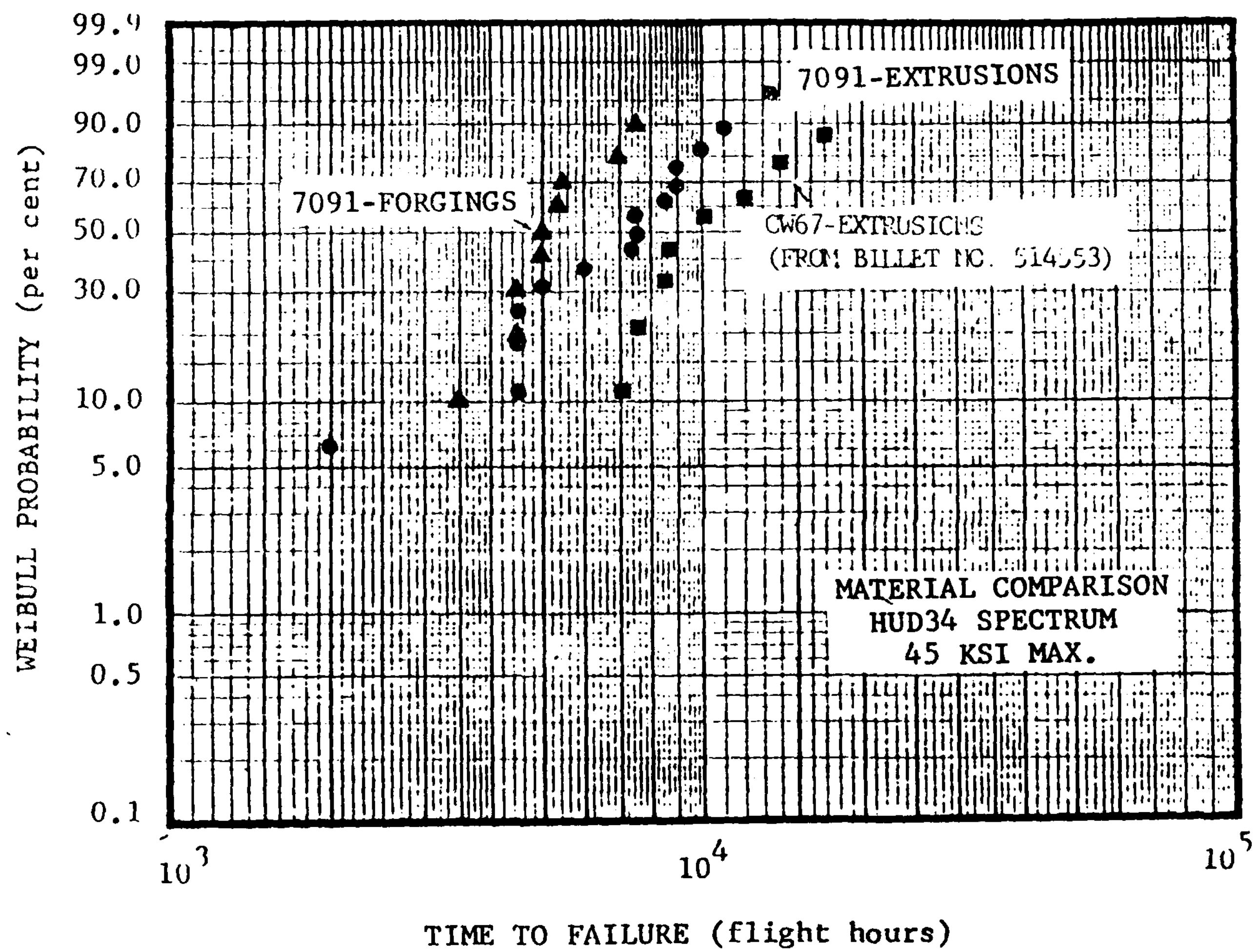

FIGURE 31. Time-To-Failure Comparisons For RST Material (HUD 34 Spectrum, Maximum Stress = 45 ksi)

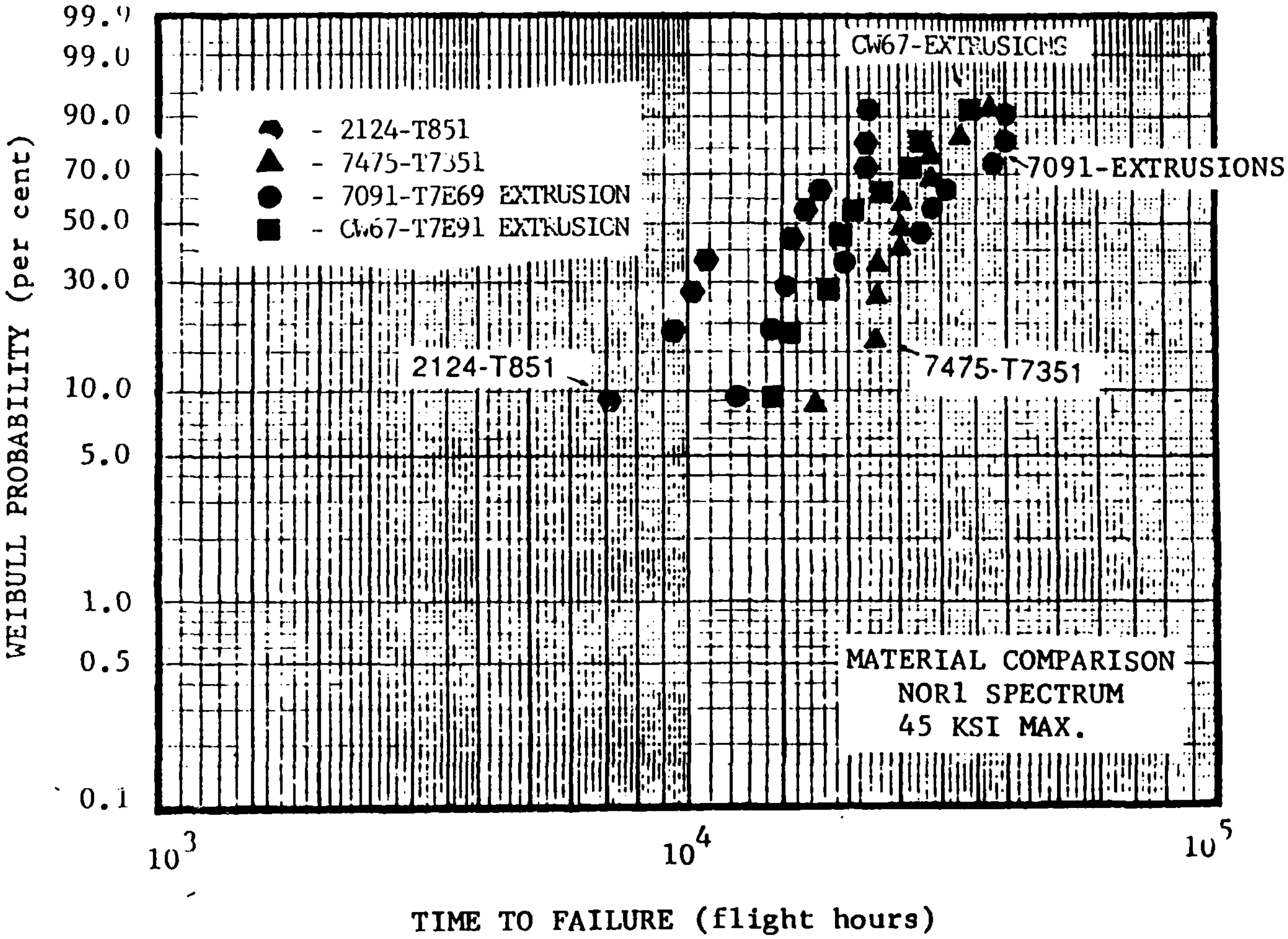

Figure 32. Time-To-Failure Comparisons for Materials Tested Under The NOR 1 Spectrum (Maximum Stress = 45 ksi)

over extruded 7091-T7E69 at this stress level. Some degradation in fatigue life was observed in the 7091-forged material as compared to extruded material at the 45 ksi stress level, also.

Results for test coupons tested under the NOR1 spectrum at a maximum stress level of 45 ksi are shown in Figure 32. For the I/M alloys, 7475-T7351 exhibited superior fatigue performance over 2124-T851. The average values of TTF for 7475-T7351 was 26,465 flight hours compared to 15,423 flight hours for 2124-T851. Experimental scatter was about the same in the two I/M materials. Considerably more scatter was observed in the P/M 7091-extruded material. The lower ranked 7091 test coupons exhibited poorer fatigue performance than 7475-T7351 test specimens whereas the higher ranked 7091 specimens exhibited better TTF than 7475-T7351. Average values of TTF were approximately the same in the two materials (26,949 flight hours for 7091-T7E69 vs. 26,465 flight hours for 7475-T7351).

Five CW67 test coupons tested under the NOR 1 spectrum were obtained from billet #514553 while the other five coupons were fabricated from billets #514570 and #514571. All of the better performing CW67 test coupons (longer TTF) were obtained from the #514553 billet. Average values of TTF for CW67 specimens from billet #514553 were 26,121 flight hours. This value is approximately the same as obtained for 7091-T7E69 and 7475-T7351 (26,949 flight hours and 26,465 flight hours, respectively). However, average values of TTF for CW67 coupons from billets #514570 and #514571 were 17,557 flight hours. Although greater than the average TTF obtained for 2124-T851 (15,423 flight hours), this value is still considerably less than obtained for 7091-T7E69, 7475-T7351, and CW67-T7E91 (from billet #514553).

Largest critical crack lengths were obtained in the CW67-T7E91 extrusions (Table 9). Crack lengths of primary cracks reached approximately 0.9 inch before failure occurred in all three data sets. Smallest critical crack lengths occurred in 2124-T851. Critical crack sizes ranged from 0.49 inches for the HUD34, 40 ksi data set to 0.74 inch for material tested under the HUD34, 35 ksi data set (Table 9). These results are consistent with fracture toughness values for these two alloys where CW67 extrusions had the largest plane strain fracture toughness values and 2124-T851 had the poorest fracture toughness of the materials tested.

Figures 30 and 32, show improvement of fatigue performance in 7091 over 2124 is much greater under the tension-compression HUD34 spectrum than under the tension-dominated NOR1 spectrum. This seems to be related to cyclic stability of materials. A recent study [23] has demonstrated that cyclic stability of materials strongly depends on the type of load histories encountered. Under strain-controlled low cycle fatigue tests with strain ratio -1, 2124-T851 exhibits cyclic softening behavior, while 7091-T7E69 is cyclically stable. However, cyclic softening behavior of 2124-T851 disappears when strain ratios are increased to 0 and 0.3 Therefore, the greater difference in fatigue performance between 2124-T851 and 7091-T7E69 under the tension-compression HUD34 spectrum can at least be partially attributed to cyclic softening behavior of 2124-T851.

The stress level dependence on fatigue life can be observed for 2124-T851 in Figure 33. A considerable decrease in average TTF is observed at 40 ksi. More scatter is observed at the lower stress level as expected. The stress level dependence on fatigue properties will be discussed in Section 5.4.2.

5.3.2 Fatigue Crack Growth Rate (FCGR)

Fracture critical structures using the "Damage Tolerance Concept" rely on slow crack growth in order to withstand two design lives before failure. Therefore, it is important to separate the crack initiation stage from propagation in analyzing fatigue data. The crack growth rates of P/M alloys compared to I/M alloys are presented and analyzed in this section.

Procedures used in crack growth analysis assuming different crack geometries were discussed in Section 4.1. Calculations were conducted for three different materials, 2124-T851, 7475-T7351, and 7090-extrusions. Comparisons between predicted data and actual data are shown in Figures 34-35 for 2124-T851 and 7091-T7E69. Actual data was compared to assumed double corner cracks and double through cracks. Results indicated comparable prediction results to test data in 2124-T851 (Figure 34). However, the crack growth analysis in 7091-T7E69 was somewhat conservative. Actual crack growth rates in this material were considerably better than the model had predicted (Figure 35).

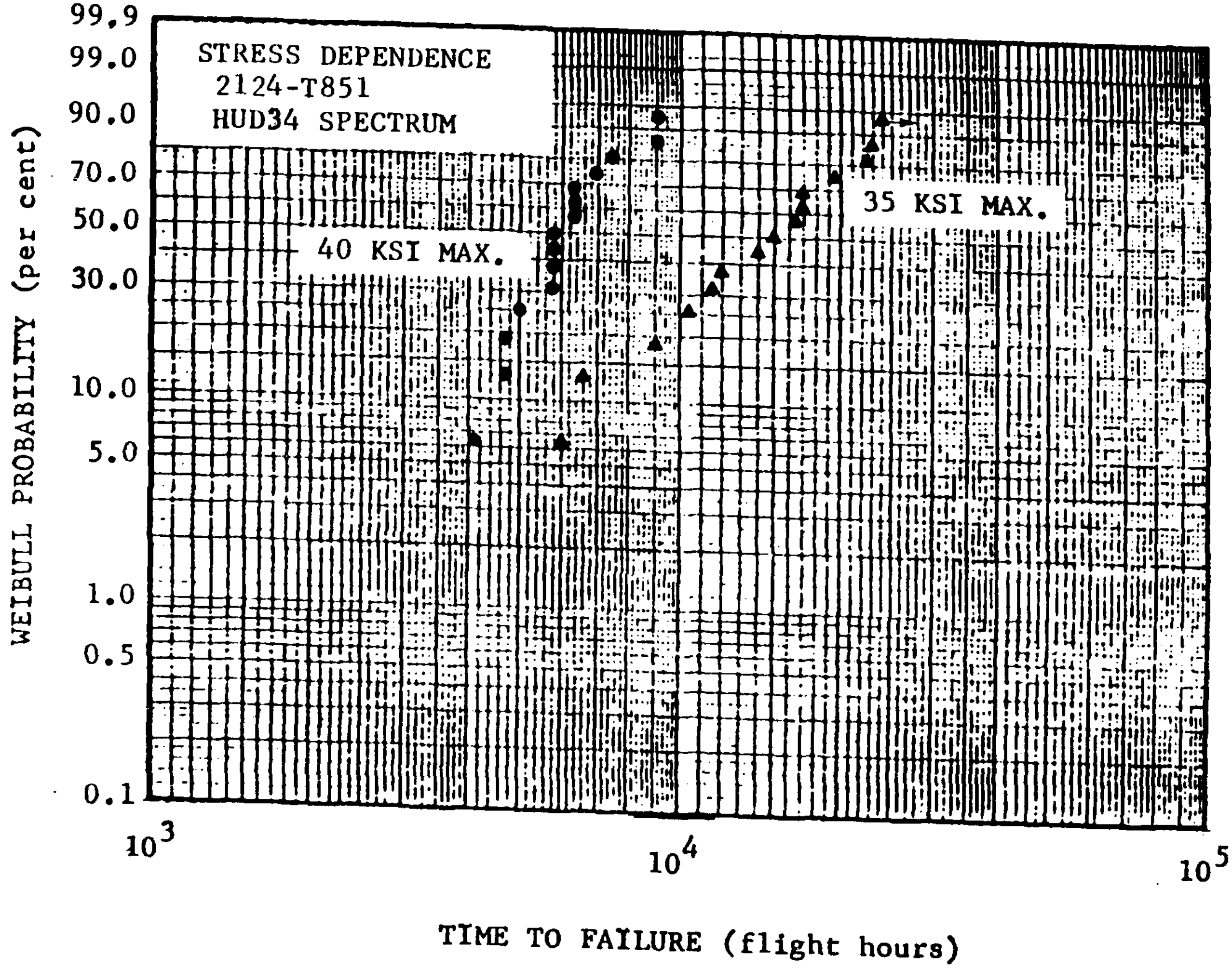

Figure 33. Time-To-Failure Plots Showing Stress Dependence

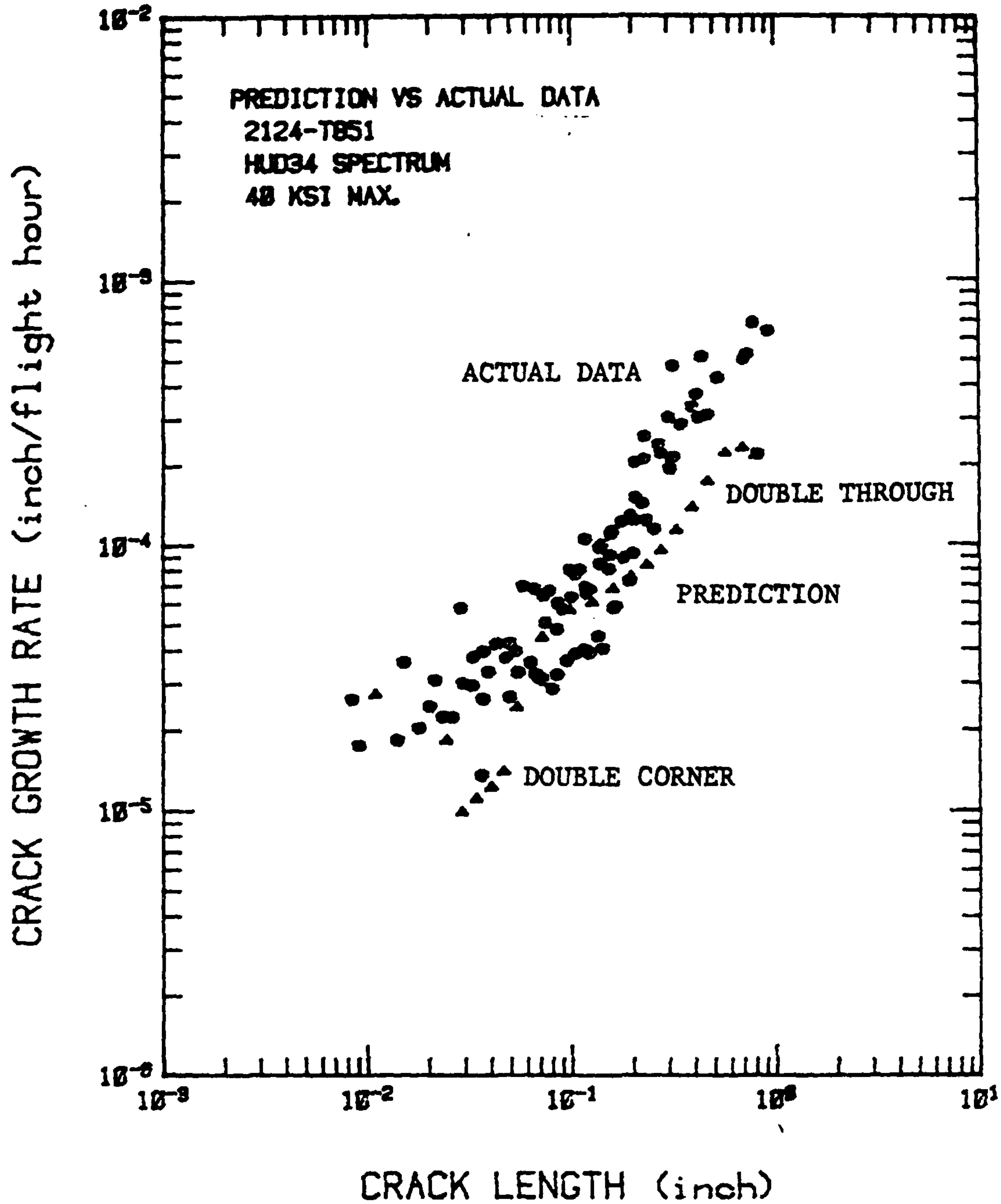

Figure 34. Crack Growth Rates For 2124-T851 Aluminum Alloy (HUD 34 Spectrum)

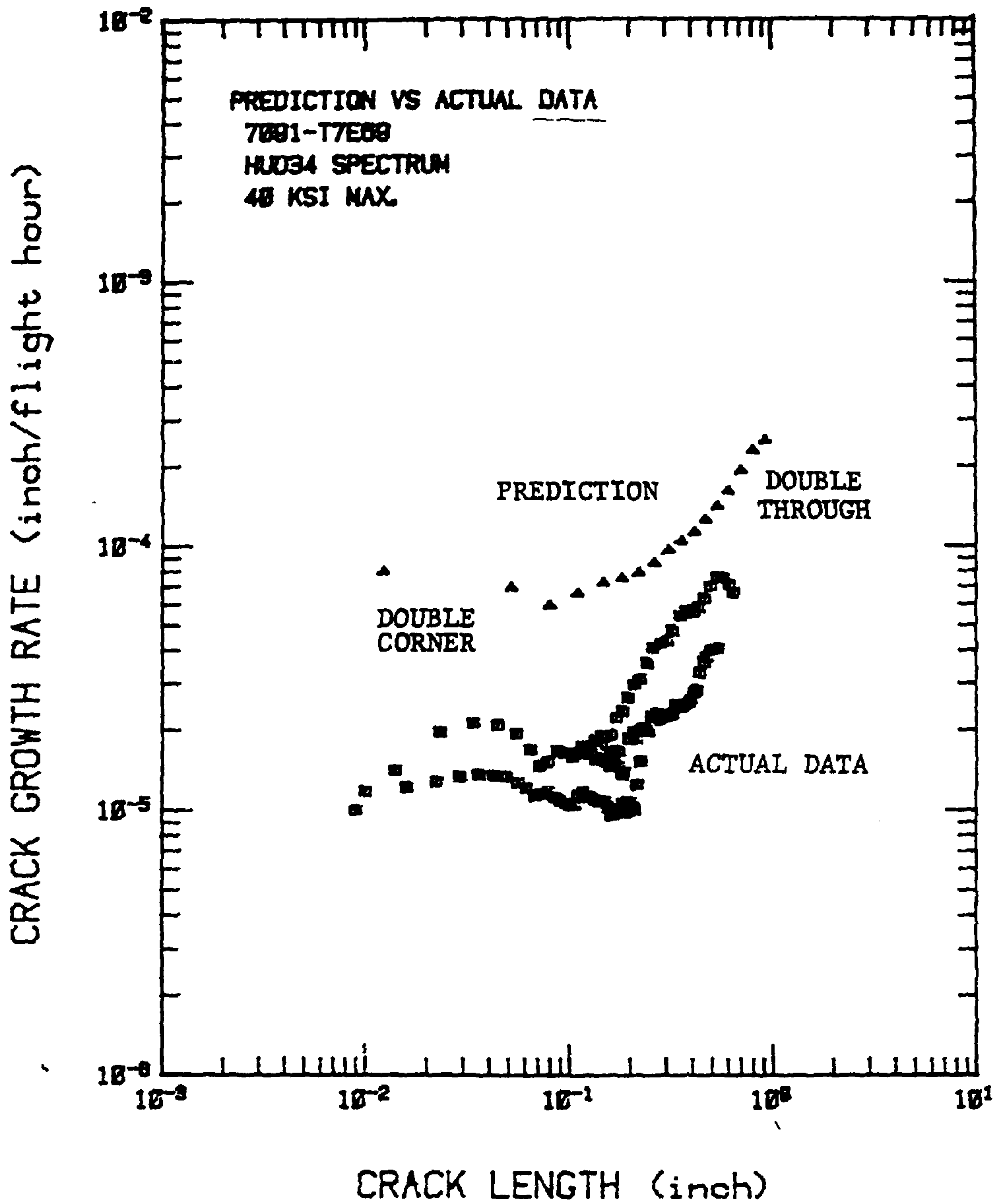

Figure 35. Crack Growth Rates For 7091-T7E69 Aluminum Alloy (HUD 34 Spectrum)

A comparison of crack growth rate as a function of crack length between the P/M materials and I/M alloys is shown in Figures 36-37. Comparisons are shown for both HUD34 and NOR 1 spectra. Crack growth rates were determined from eq. 2 where a(t) is the crack size at time t, and Q and b are constants that were determined from the least square fit of all log da/dt vs. log a pairs of the sample. Values of Q and b for all data sets are listed in Table 9. Individual Q and b values for all test coupons are listed in Appendix B.

A slower crack growth rate is observed in the RST materials especially at larger crack lengths. The poorest crack growth rate performance was obtained in 2124-T851 plate for tests conducted under both the HUD34 and NOR1 spectra. Crack growth rates in the 7091-forged material were intermediate between the 7091-extruded material and 2124-T851 (Figure 36). Crack growth rate comparisons between CW67-T7E91 and 7091-T7E91 were dependent on the billets from which the CW67 material had been extruded. Extrusions from billets #514570 and #514571 showed inferior crack propagation characteristics compared to 7091-T7E69 (Figures 36-37). However, CW67 test coupons fabricated from the billet #514553-2 showed superior crack growth rate compared to 7091-T7E91.

Crossover effects are observed in comparing spectrum crack growth rates of the RST materials with 7475-T7351 plate run under the NOR1 spectrum. For smaller crack lengths, the crack growth resistance of 7475-T7351 is superior, while at larger crack lengths, the crack propagation behavior of the P/M-T7E69 material is better. These results are consistent with constant amplitude crack growth comparisons between 7091-T7E69 and 7475-T7351 where it was found that for low ΔK values, 7475 had superior crack growth resistance, and at high values of stress intensity factor, 7091 had better resistance [24]. The ranking between P/M and I/M aluminum alloys in spectrum fatigue crack growth resistance has been found to be strongly dependent on the type of load histories encountered [25].

Additional crack growth curves based on the "Initial Fatigue Quality" (IFQ) Model are presented in Section 5. The technique used in generating these crack growth curves was presented in Section IV.

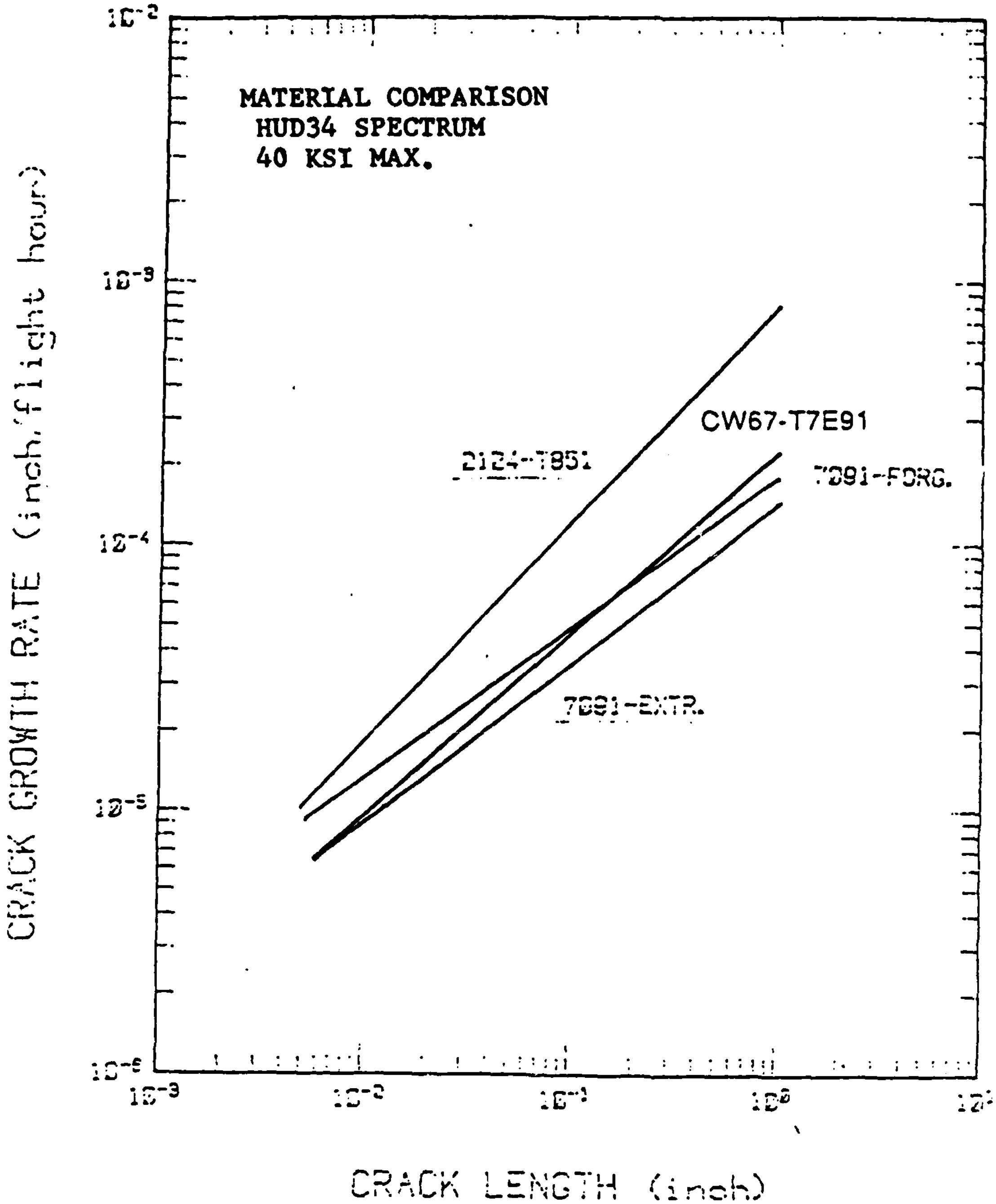

Figure 36. Crack Growth Rates of 2124-T851, 7091-T7E69, CW67-T7E91, and 7091-Forgings As A Function Of Crack Length Under The HUD 34 Spectrum

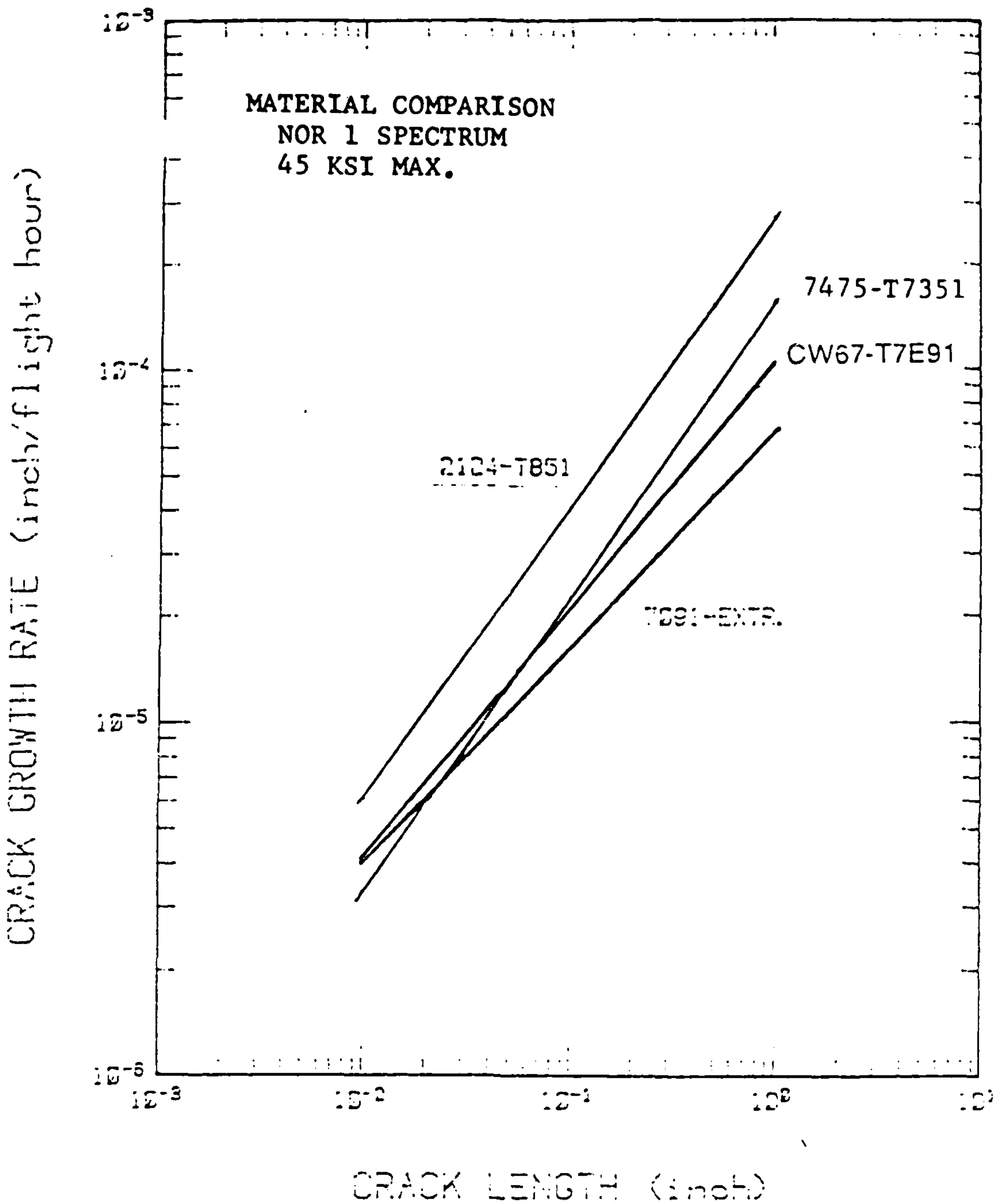

Figure 37. Crack Growth Rates Of 2124-T851, 7475-T7351, 7091-T7E69, and CW67-T7E91 As A Function Of Crack Length Under The NOR 1 Spectrum

Additional crack growth curves based on the "Initial Fatigue Quality" (IFQ) Model are presented in Section 5. The technique used in generating these crack growth curves was presented in Section IV.

5.3.3 Time-To-Crack-Initiation (TTCI)

The time required for an initial defect to become a fatigue crack of size 0.150 inch was used to define the arbitrary crack size a_0 in this program. This value was easily obtainable from fractographic results.

As presented in Section IV, observed TTCI values are known to be fit very well by a three-parameter Weibull distribution. Therefore, a fractographically observed TTCI distribution can be expressed as shown in Eq. (1). The parameter T is a random variable indicating TTCI, α is the shape parameter, β is the scale parameter, and ϵ is the lower bound of TTCI.

Eq (1) may be transformed into:

$$\log \left\{ -\ln\left[1-F_T(t)\right]\right\} = \alpha \log (t-\epsilon) - \alpha \log \beta \qquad (7)$$

Eq. (7) shows that $-\ln[1-F_T(t)]$ vs. $(t-\epsilon)$ is plotted as a straight line on log-log scale paper.

Figures 38-42 show the TTCI distributions obtained from this program. Each data point represents the $-\ln[1 - 1/(n+1)]$ vs. $(\text{TTCI} - \epsilon)$ pair for each specimen, where $i/(n+1)$ is the TTCI rank of the specimen within the individual data set. The straight line in Figures 38-42 is the $F_T(t)$ distribution giving the best least squares fit to the plotted $-\ln[1-F_T(t)]$ vs. $(\text{TTCI} - \epsilon)$. $F_T(t)$ can be calculated from Eq. (1) using the parameters α, β, and ϵ. The parameters α and β are presented in Table 9. The parameter ϵ was equal to zero for all analyses. The slopes of the straight lines in Figures 38-42 are directly related to the parameter α. As mentioned earlier, the parameter α is not expected to be a function of the spectrum type and stress level. Therefore, a set of identical test specimens is expected to have the same slope even though tested under various spectrum types and stress levels.

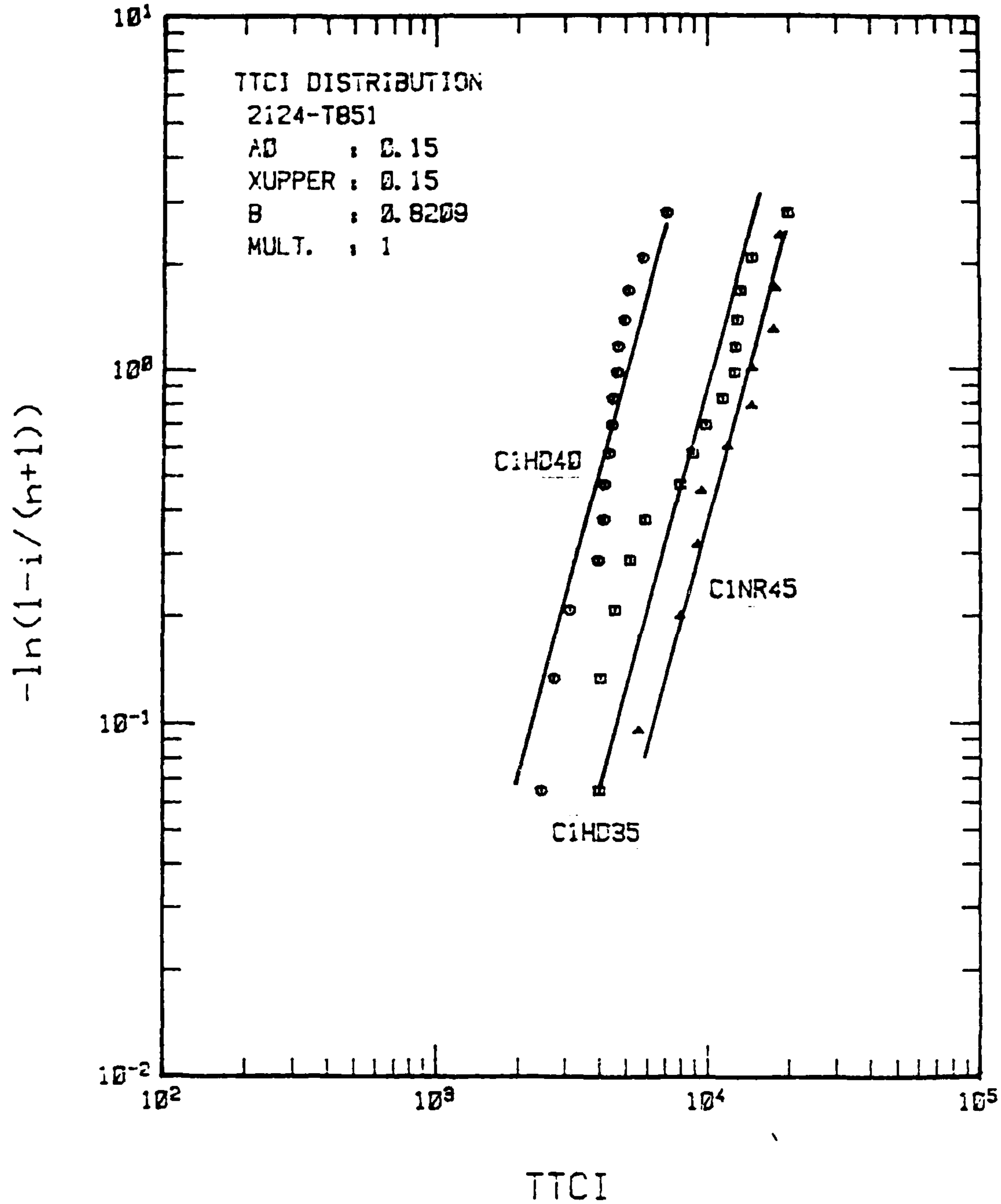

Figure 38. TTCI Distributions For 2124-T851 Aluminum Alloy

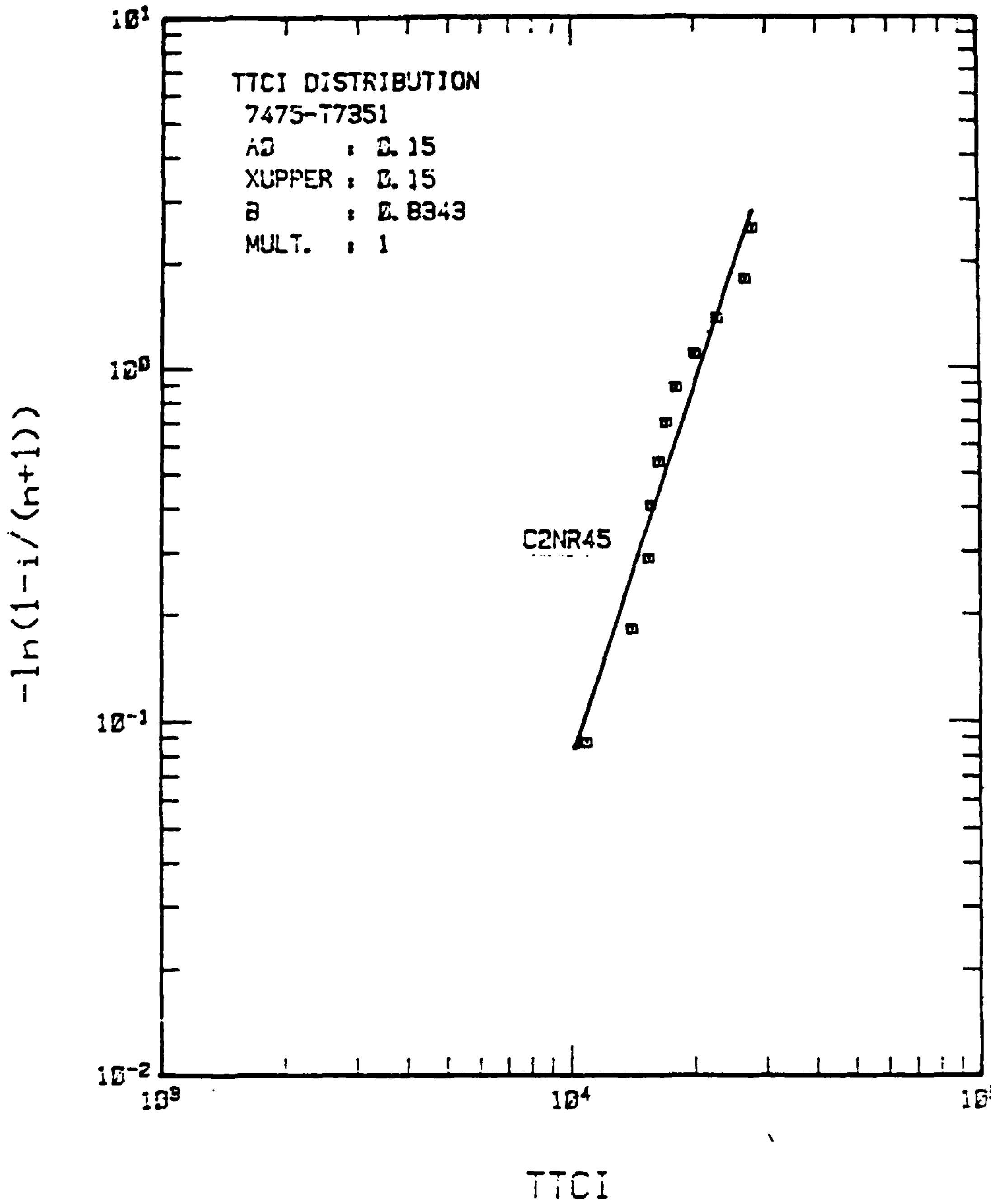

Figure 39. TTCI Distributions For 7475-T7351 Aluminum Alloy

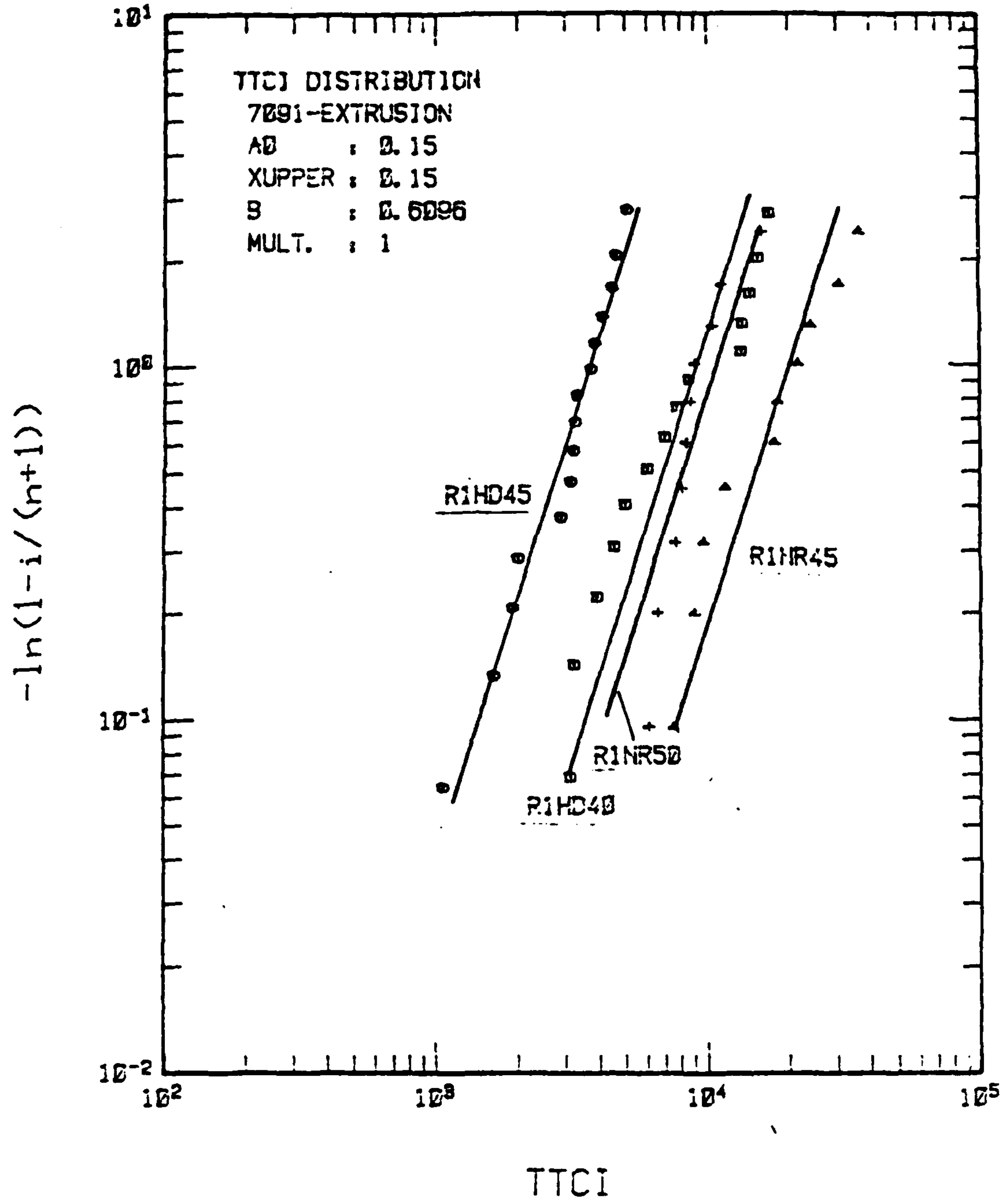

Figure 40. TTCI Distributions For 7091-Extrusion

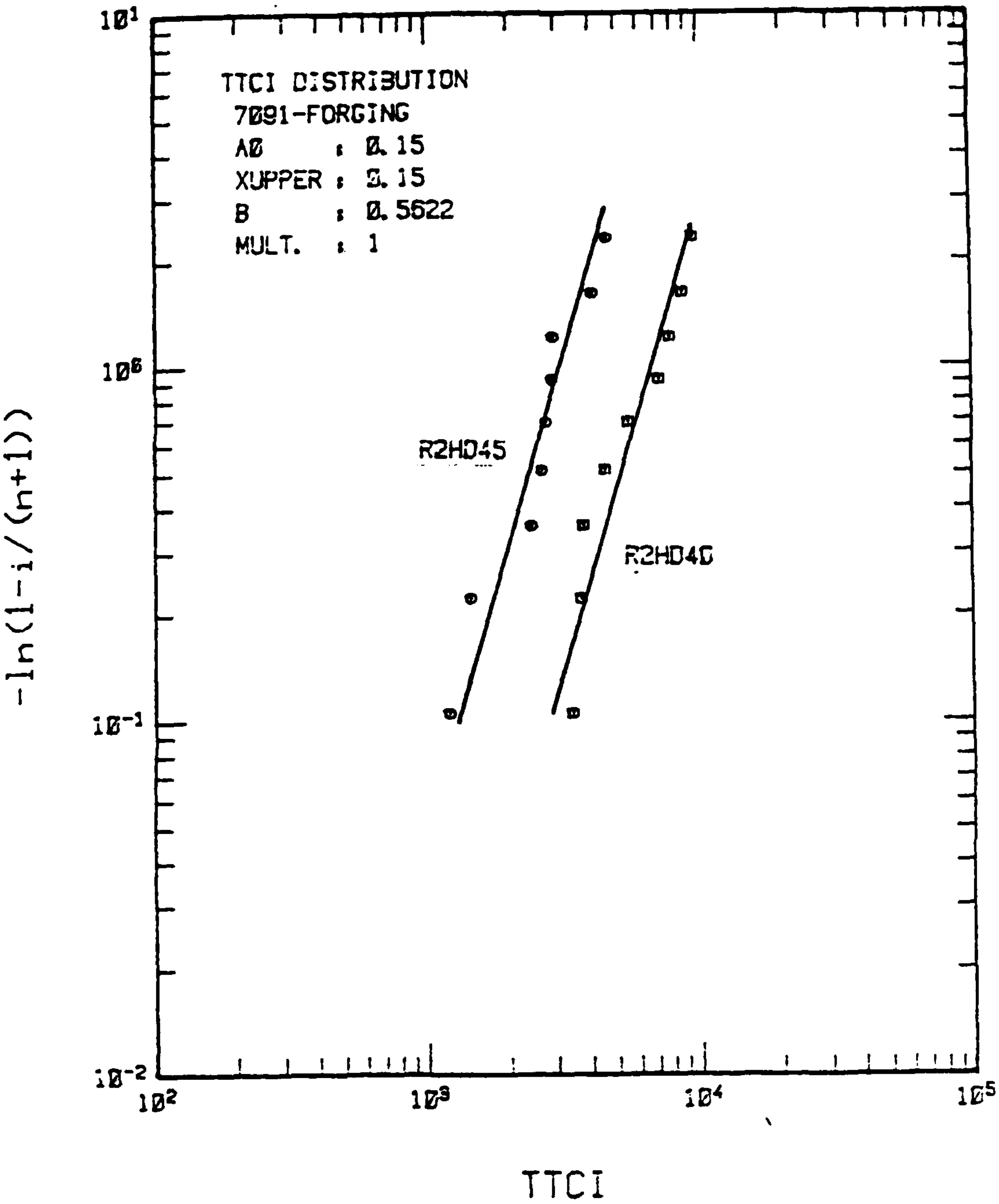

Figure 41 . TTCI Distributions For 7091-Forging

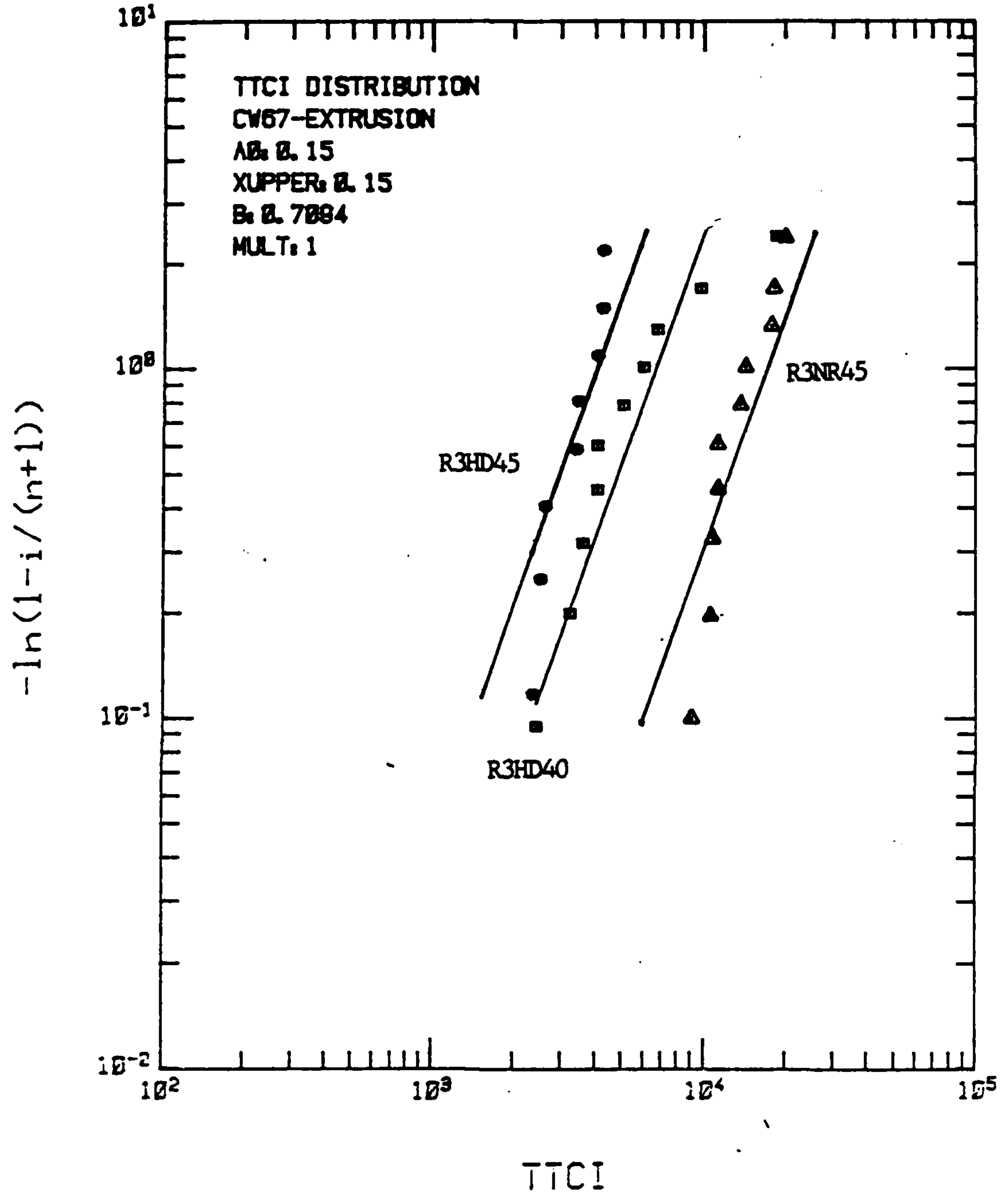

Figure 42. TTCI Distributions For CW67-Extrusion

The observed TTCI values are fit quite well by a three-parameter Weibull distribution. The data points from two different types of spectra and two different stress levels are fit well by TTCI distributions with the same slope.

A comparison of materials based on TTCI results are shown in Figures 43-44. Superior crack initiation resistance is obtained in the 7091 P/M material. Increased scatter is observed in this alloy, however. The poorest performing 7091-T7E69 specimens performed only slightly better than the poorest 2124-T851 coupons under both spectra. Crossover effects between 7475-T7351 and 7091-T7E69 were observed in the TTCI data for the NOR1 spectrum, also. This crossover effect, however, was due to the increased scatter in the experimental data for 7091-extrusions as compared to the I/M 7475-T7351 material. The control of inclusions in the RS P/M alloys will be expected to strongly influence crack initiation. By proper control, the worst performing P/M specimens would be eliminated therefore reducing the experimental scatter.

The TTCI distribution for CW67 extruded material tested under the HUD34 spectrum was similar to 7091-forged specimens (Figure 43). Better performing CW67-T7E91 and 7091-forged specimens had TTCI values intermediate between 2124-T851 and 7091-T7E69 extruded specimens. For CW67 specimens tested under the NOR1 specimens, a relatively small scatter in TTCI values was obtained (Figure 44). Poorer performing CW67 coupons had improved TTCI values over 7091-TE69 extruded material and 2124-T851 plate.

5.3.4 Measurements of EIFS Distribution

As described in Section 4.2, the EIFS distribution can be derived from the TTCI distribution by extrapolating TTCI backward using an assumed crack growth equation (Eq. 2). In that particular equation, a(t) is the crack size at time t, Q and b are constants. The EIFS distribution can be written as (Eq. 4), where x is a random variable indicating a(o), the crack size at time zero (or EIFS), c is b-1, and x_u is the upper bound of the EIFS distribution which is defined in Eq. 5. Eq. (4) can be used to find the probability that the EIFS is less than a given size, x, using parameters for any structural concept found in Table 9.

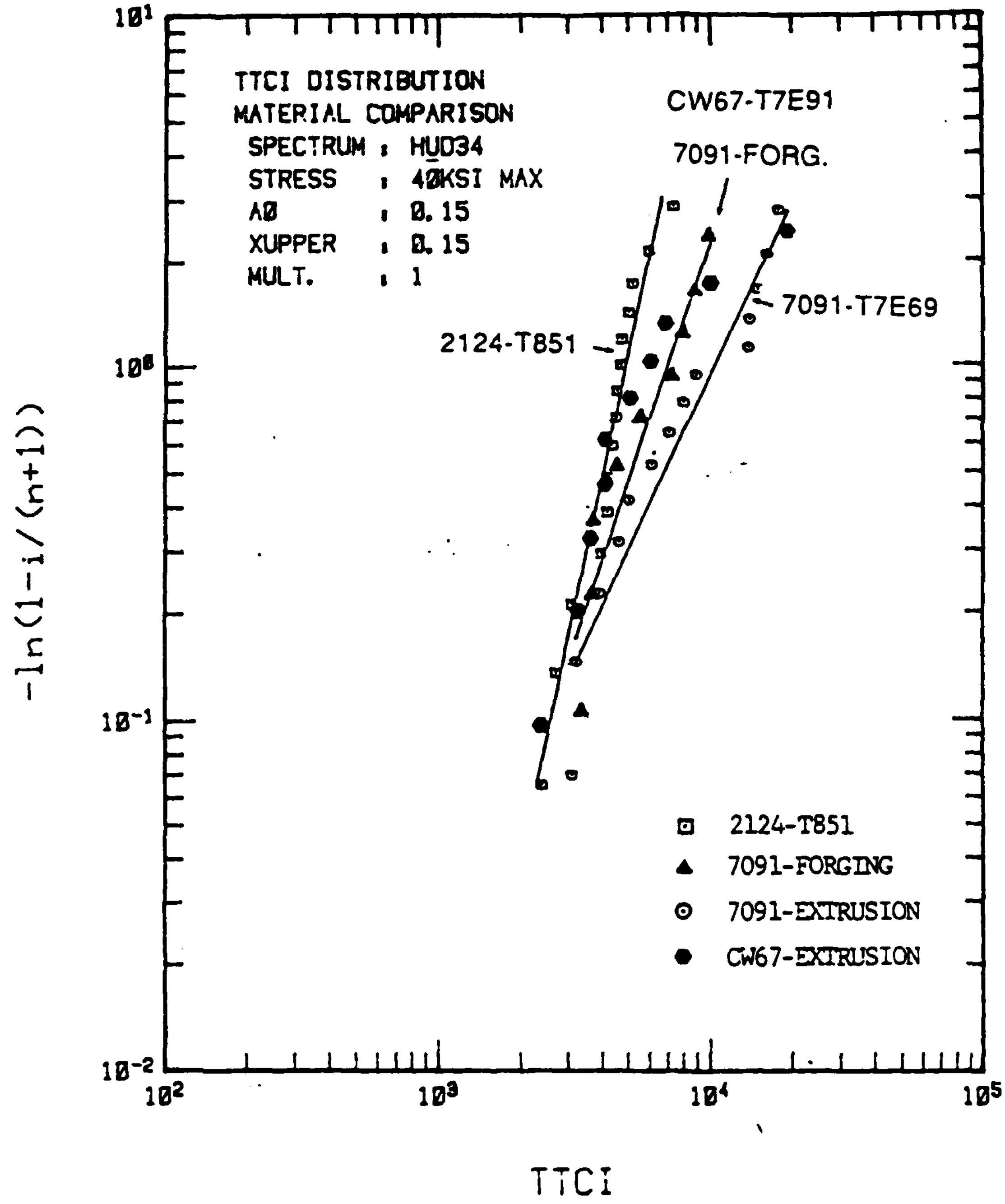

Figure 43. TTCI Comparisons For Three Aluminum Alloys (HUD 34 Spectrum)

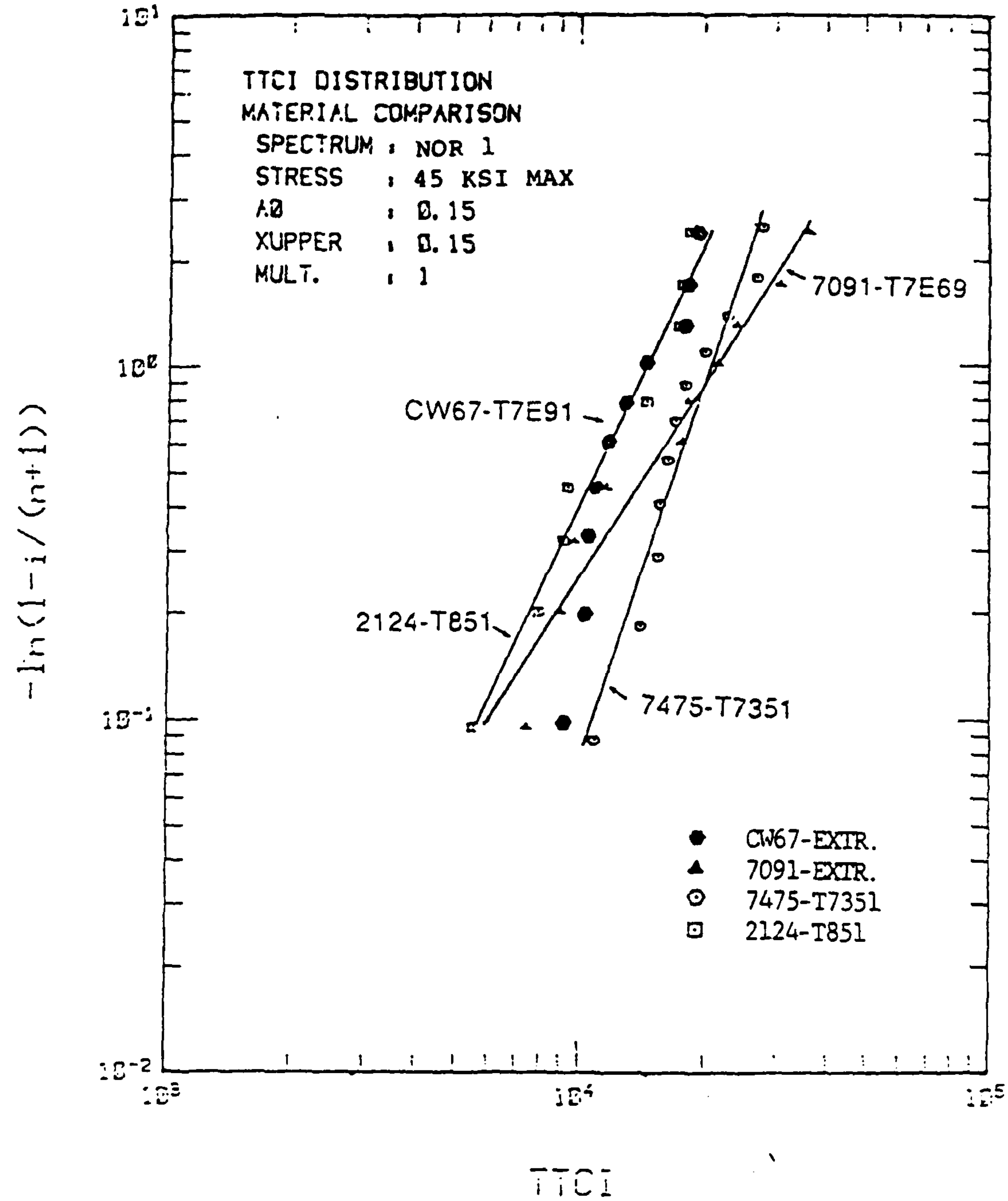

Figure 44. TTCI Comparisons For Four Aluminum Alloys (NOR 1 Spectrum)

Individual EIFS values for all test coupons are listed in Appendix B. In some instances the EIFS for a specimen may be given as a negative number. This, in effect, causes the analysis to predict that some time is required to reach a crack length of zero. We interpret this physically to mean that some time was required to initiate fatigue cracks in our unflawed specimens. In these cases the backward extrapolation of the crack growth curve can intersect the abcissa at positive time, or intersect the ordinate at negative crack size. For such cases, x in Eq. (4) is negative so that Eq. (4) is undefined. This can be remedied by using Eq. (8) whenever x is negative.

$$F_{a(o)}(x) = \exp\left|-\left[\frac{-(-x)^{-c} - x_u^{-c}}{cQ\beta}\right]^{\alpha}\right| \tag{8}$$

Eq. (4) may be transformed into:

$$\log\left[-\ln F_{a(0)}(x)\right] = \alpha \log\left(x^{-c} - x_u^{-c}\right) - \alpha \log cQ\beta \tag{9}$$

Eq. (9) shows that $-\ln F_{a(o)}(x)$ vs. $(x^{-c} - x_u^{-c})$ is plotted as a straight line on log-log paper. The slope of the straight line is directly related to the parameter α. Figures 45-49 show the EIFS distributions obtained from this program. Each data point in Figures 45-49 represents the $-\ln(i/n=1)$ vs. $(\mathrm{EIFS}^{-c} - x_u^{-c})$ pair for each specimen, where $i/(n+l)$ is the EIFS rank of the specimen among the set of identical test specimens. The straight lines in Figures 45-49 are plotted from $-\ln F_{a(o)}(x)$ vs. $(x^{-c} - x_u^{-c})$. $F_{a(o)}(x)$ can be calculated from Eq. (4) using the parameters Q, b, α, β, and x_u presented in Table 9.

As shown in Figures 45-49, the experimental EIFS distributions (data points) are reasonably fit by the best fit EIFS function (straight lines) given by Eq. (4). For a given set of identical test specimens, all the data points obtained from different test conditions merge more or less into a single EIFS distribution. This tends to confirm the assumption that the EIFS distribution is generic, as described in Section 4.2.

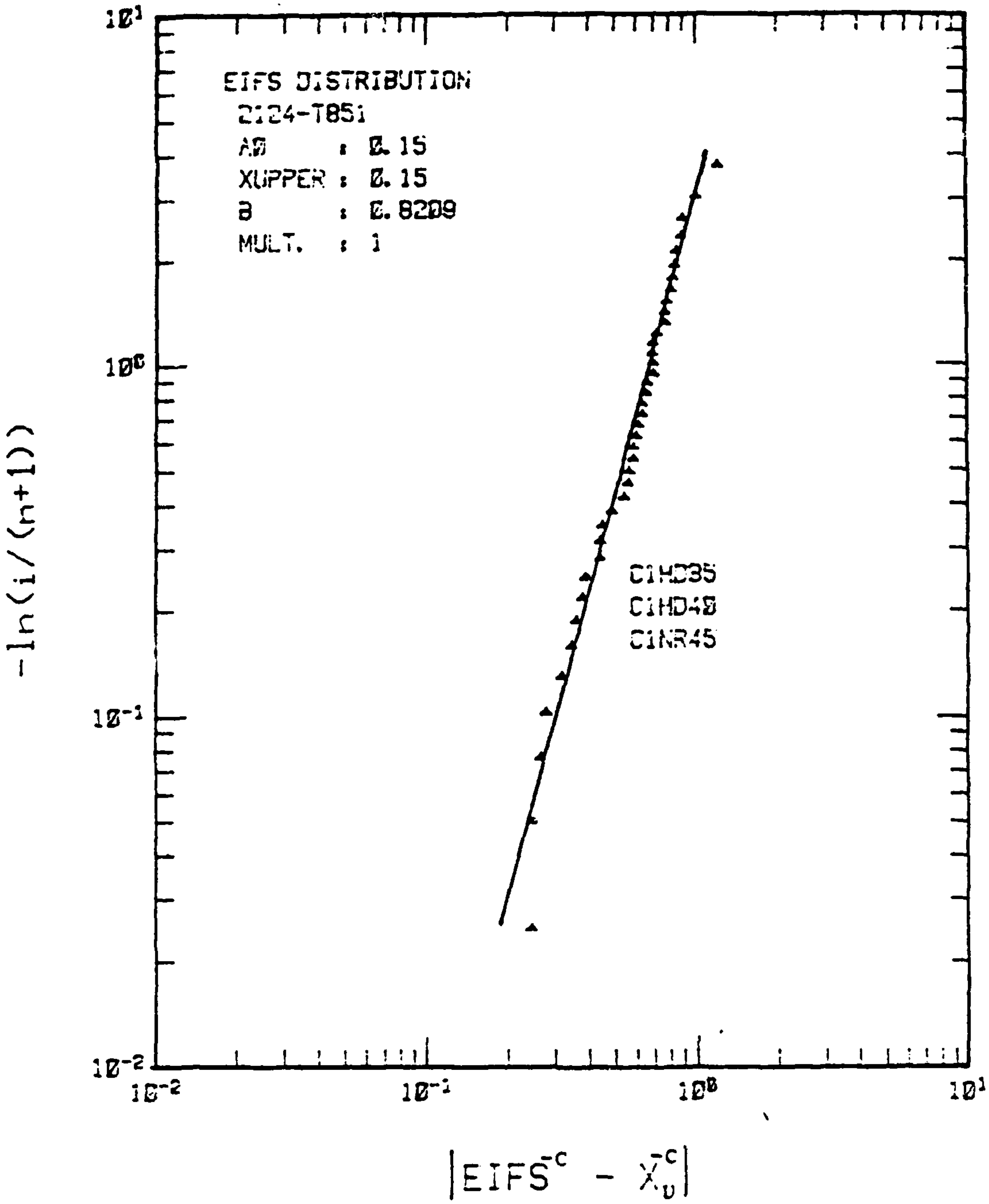

Figure 45. EIFS Distributions For 2124-T851 Aluminum Alloy

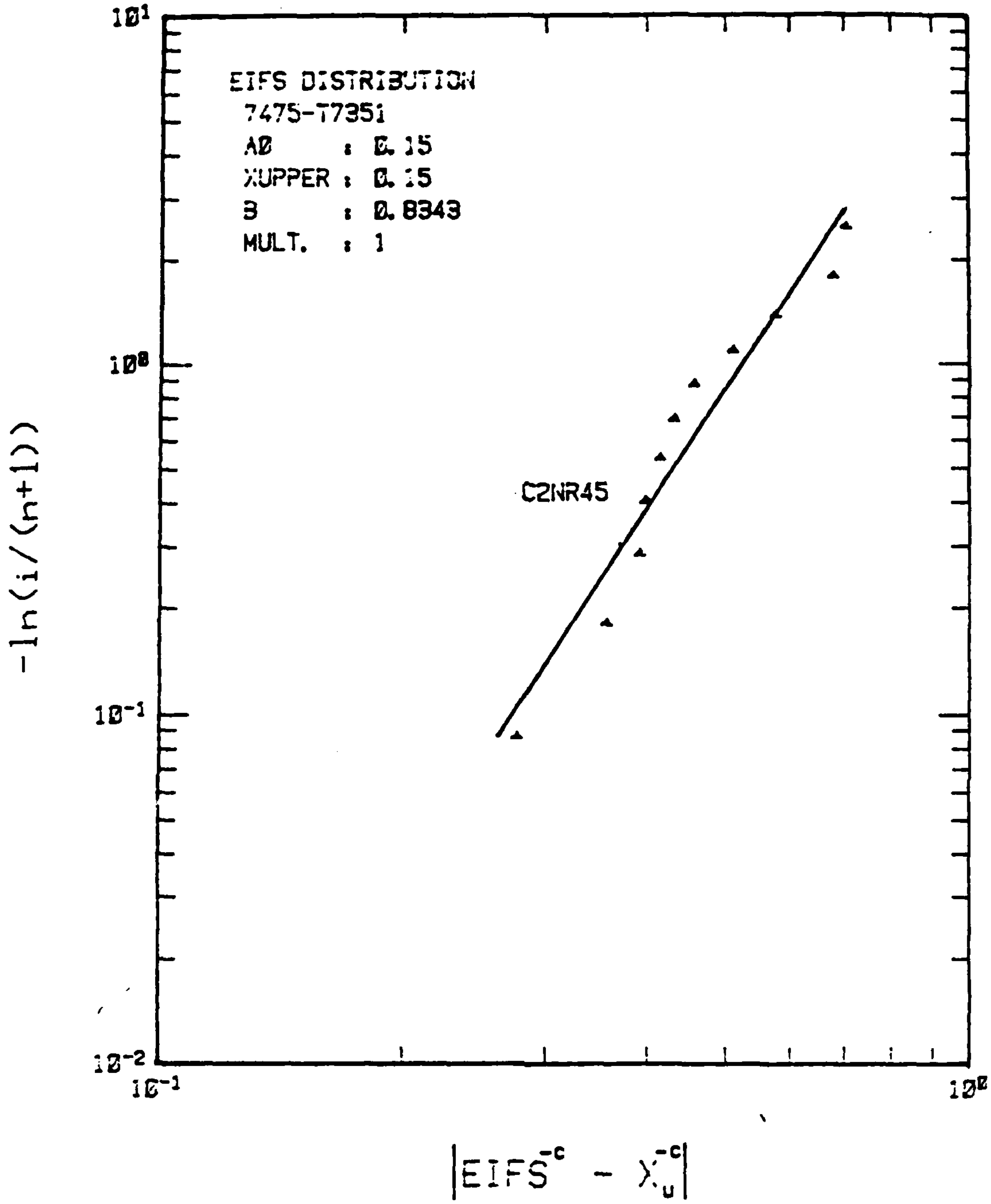

Figure 46. EIFS Distributions For 7475-T7351 Aluminum Alloy

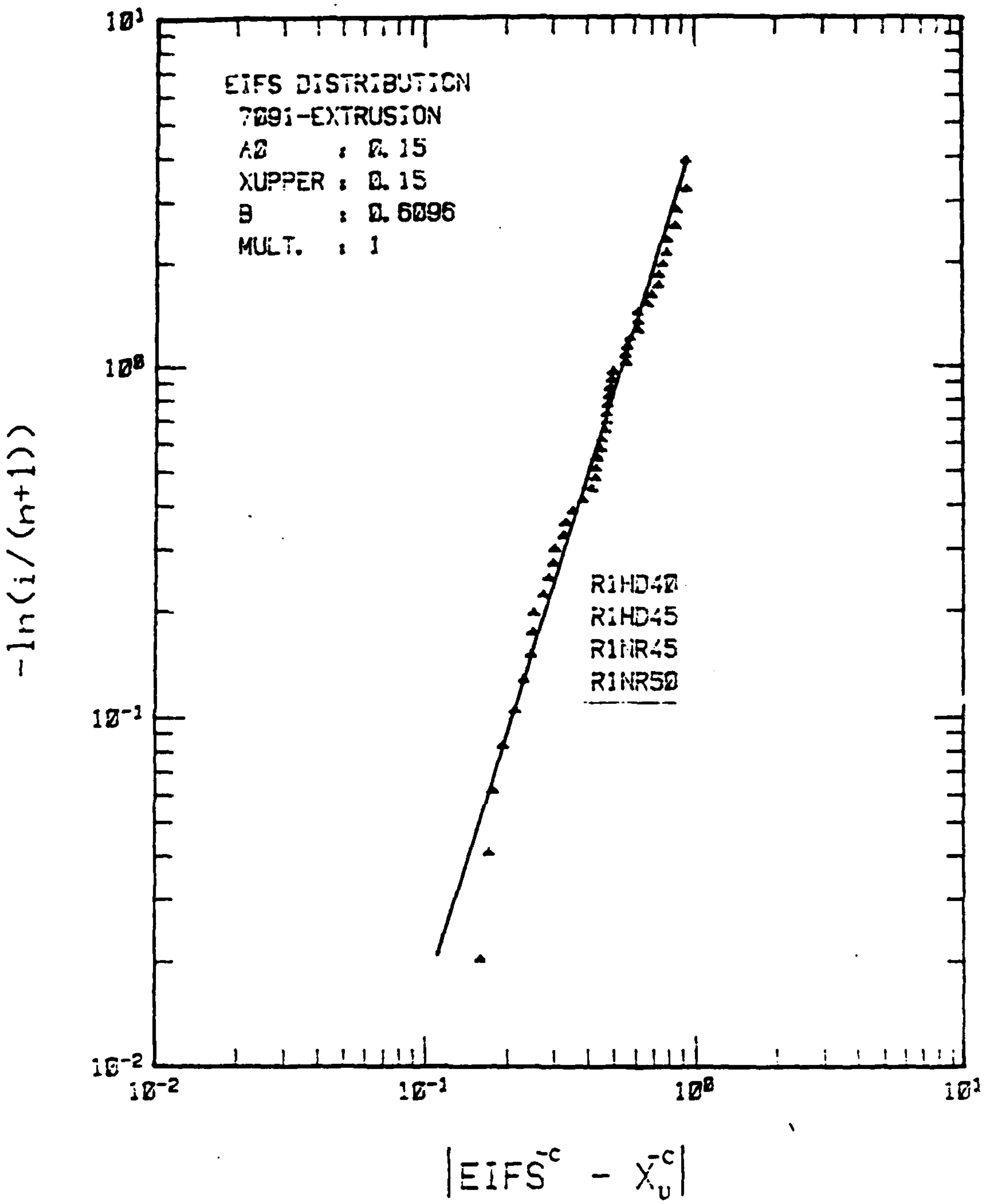

Figure 47. EIFS Distributions For 7091-Extrusion

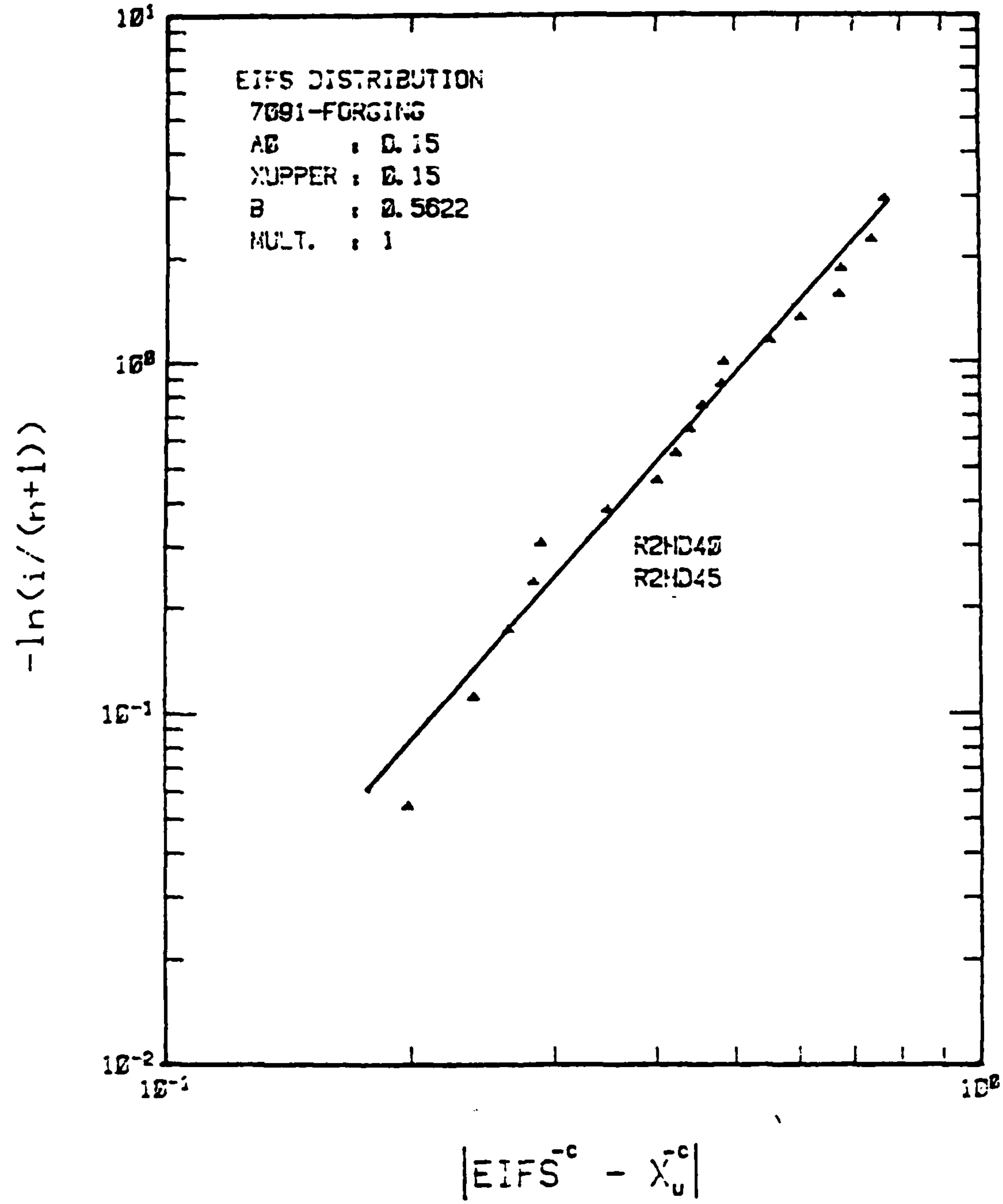

Figure 48. EIFS Distributions For 7091-Forging

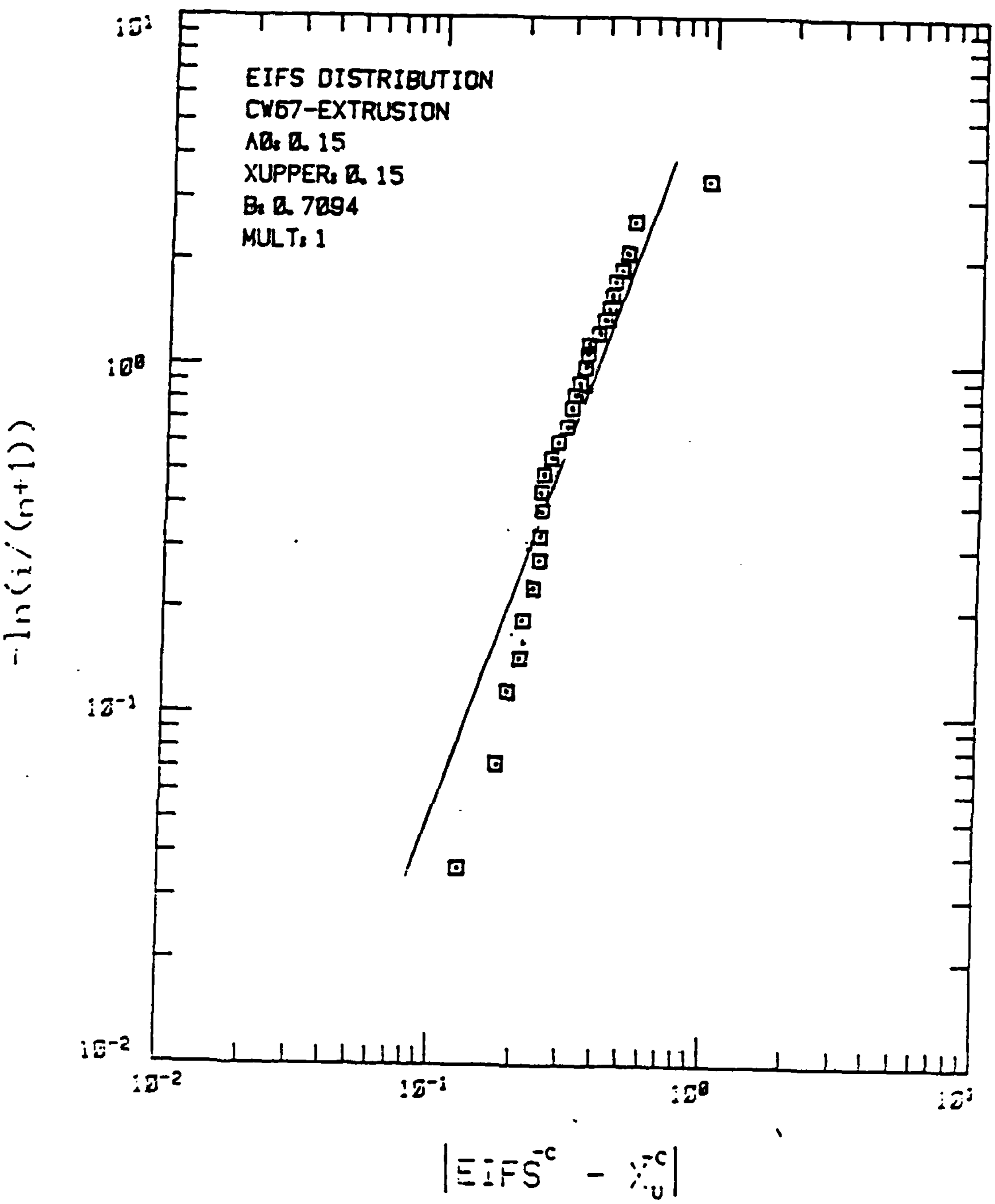

Figure 49. EIFS Distributions For CW67-Extrusion

On comparing EIFS values of RST materials with I/M alloys, EIFS values of 7091-T7E69 extrusions were considerably less than 2124-T851 plate. This difference is reflected in Table 11 where the average TTCI and EIFS values are shown for the different spectra. The average EIFS values for 7475-T7351 plate tested under the NOR1 spectrum were intermediate between 7091-T7E69 extrusions and CW67-T7E91 extrusions with the 7091-T7E69 material having the smallest EIFS values. Average EIFS values for 7091-forgings were slightly higher than initial flaw sizes obtained for 7091-extrusions.

Comparisons of $|EIFS^{-c} - x_u^{-c}|$ distributions between P/M alloys and I/M alloys are shown in Figures 50-52. Comparisons are shown for both the tension-compression HUD34 spectrum and tensile-dominated NOR1 spectrum. As mentioned previously, the EIFS distribution plots for a given material are fairly independent of spectrum.

On comparing 7091 extruded material with 7475-T7351 material, crossover effects are also observed in the EIFS distributions. Again, the crossover effect is due to greater scatter in the 7091-extrusion experimental data. The poorer performing 7091-extrusion coupons have larger EIFS values than the poorer 7475-T7351 specimens. Correspondingly, the better performing 7091-T7E69 coupons have lower EIFS values than 7475-T7351.

5.4 DURABILITY ANALYSIS BASED ON IFQ MODEL

5.4.1 Crack Growth Modeling

Using the Initial Fatigue Quality (IFQ) model, the crack growth rate over the crack size range of interest is assumed to be expressed as Eq. 2, where a(t) is the crack size at time t, and Q and b are constants that are determined from the least square fit of all log da/dt vs. log a pairs of the sample.

Integrating Eq. (2) from t = o to t = t will give the time required for an initial defect to become a fatigue crack of size a(t):

$$t = -\frac{1}{cQ}\left[a^{-c}(t) - a^{-c}(0)\right] \tag{10}$$

TABLE 11. AVERAGE TTCI AND EIFS OF EACH MATERIAL

- UNDER HUD34, 40 KSI

	AVG. TTCI	AVG. EIFS
2124-T851	4396 FLT. HOURS	3.5980×10^{-4} INCH
7091-EXTR.	8756	-1.0847×10^{-2}
7091-FORG.	6015	-8.0123×10^{-3}
CW67-EXTR.	6358	-8.0224×10^{-4}

- UNDER NOR1, 45 KSI

	AVG. TTCI	AVG. EIFS
2124-T851	12643	1.4831×10^{-3} INCH
7475-T7351	18657	1.4404×10^{-3}
7091-EXTR.	18636	-9.4831×10^{-3}
CW67-EXTR.	13467	4.644×10^{-3}

- UNDER HUD34, 45 KSI

	AVG. TTCI	AVG. EIFS
7091-EXTR.	3227	1.0233×10^{-3} INCH
7091-FORG.	2786	8.2078×10^{-3}
CW67-EXTR.	3373	4.4522×10^{-3}

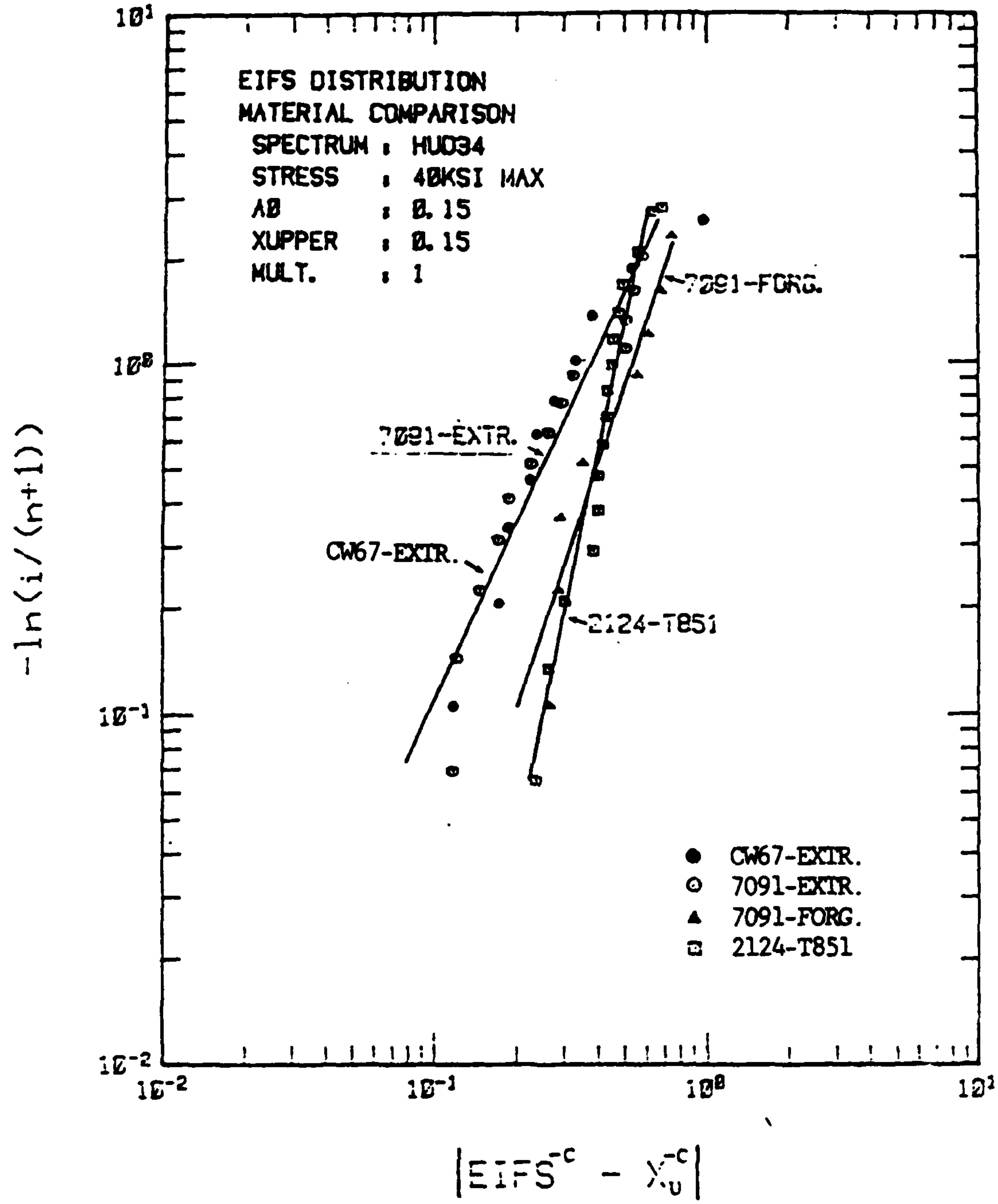

Figure 50. EIFS Comparisons For Three Aluminum Alloys (HUD 34 Spectrum)

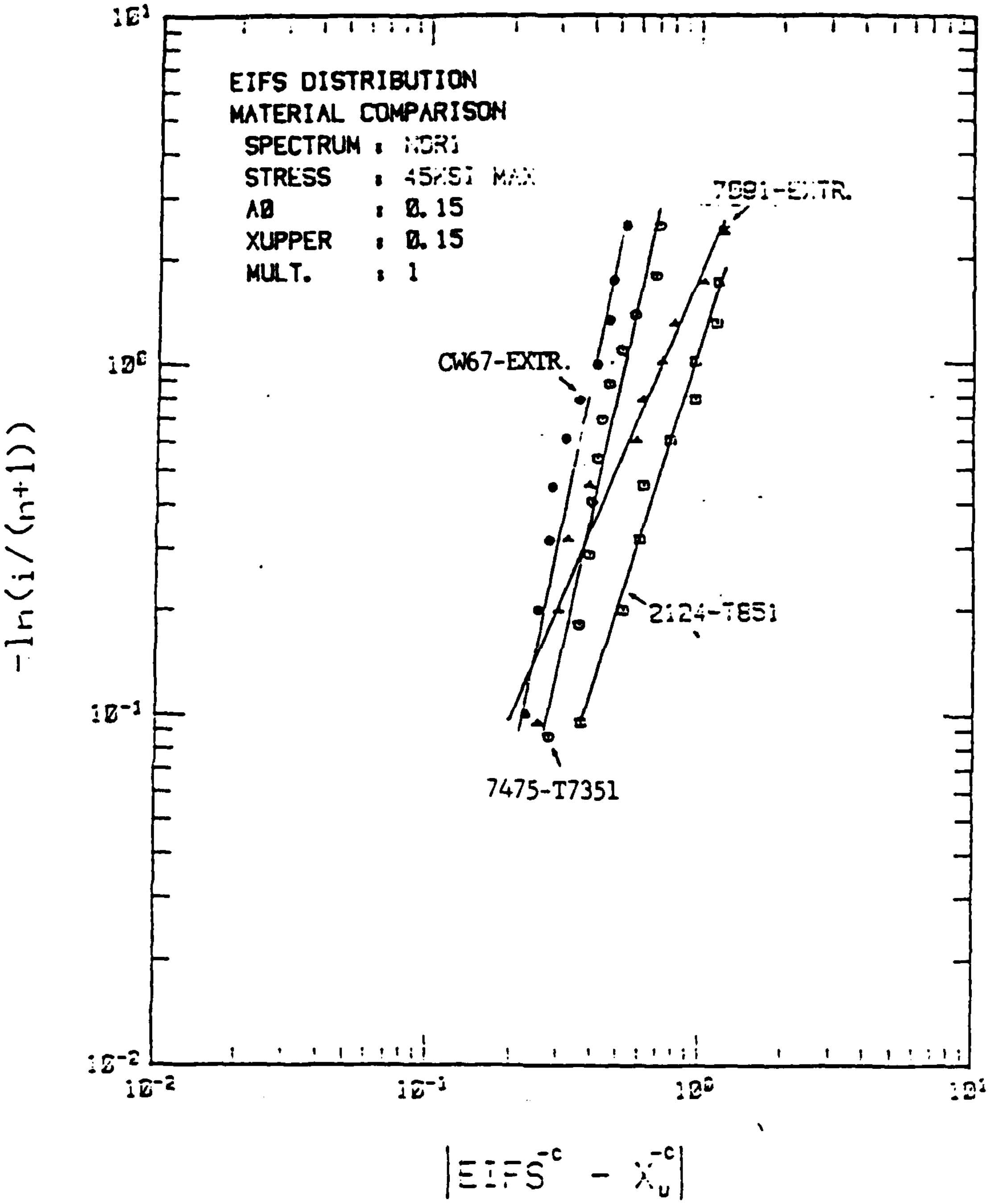

Figure 51. EIFS Comparisons For Four Aluminum Alloys (NOR 1 Spectrum)

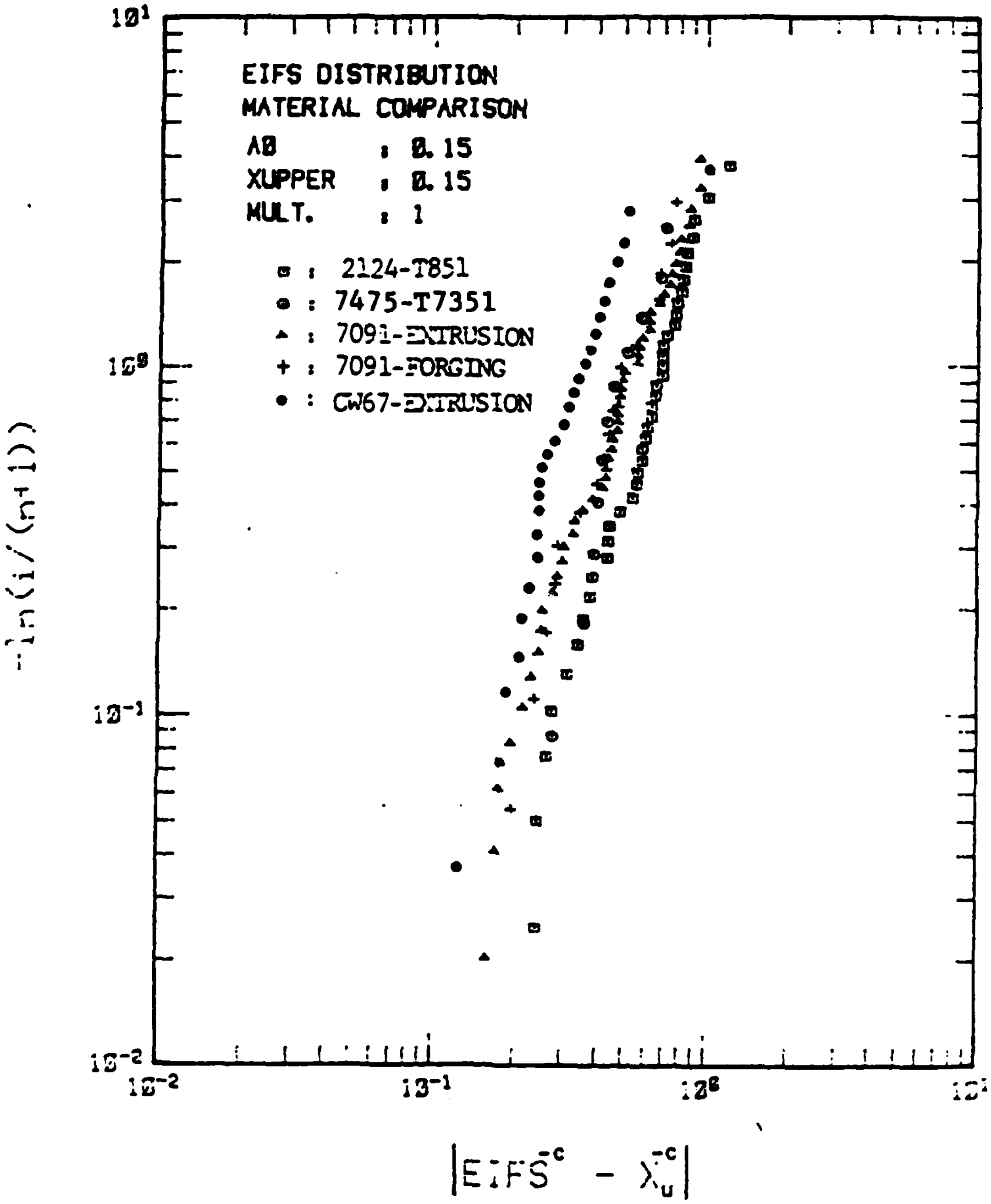

Figure 52. EIFS Comparisons (Pooled Data)

Using Eq. (10) the crack growth behavior of P/M alloys can be compared to I/M samples assuming the a(o) or EIFS values are known. By using an average EIFS value for each data set (Table 11), the following crack growth curves shown in Figures 53-55 can be generated. Results are shown for coupons tested under both the HUD34 and NOR1 test spectra. Eq. 10 can also be used to calculate time-to-failure (TTF). In this case, at t = 0, a = a(0), which is the EIFS. At t = TTF, a = a(TTF), which is the crack size at failure, or critical crack size, a_{crit}. Calculated TTF values can be obtained from Figures 53-55 and compared to experimental values (Table 10). Relatively good agreement was obtained between calculated values of TTF and experimental average values.

Results from Figures 53-55 show superior crack growth resistance for the P/M aluminum alloys. The poorest crack growth behavior was obtained in 2124-T851 for coupons tested under both the HUD34 and NOR1 test spectra (Figures 53-54). The best crack growth life was obtained in 7091-T7E69 extruded material for tests conducted under NOR1 spectrum and HUD34 spectrum (40 ksi maximum stress). For tests conducted under the HUD 34 spectrum with a maximum stress of 45 ksi, maximum flight hours was obtained from the CW67-T7E91 material (Fig. 55). In this set of experiments, all of the CW67 test coupons were fabricated from the #514553-2 billet.

5.4.2 Reliability and Figure of Merit

The durability of structures depends on both the EIFS distribution and crack growth rate. These two elements must be combined in order to judge their relative importance. A recommended method for properly considering both the EIFS distribution and the crack growth rate is to combine them to compute the flaw distribution after a desired service interval. This technique was used in the "Initial Quality of Advanced Joining Concepts" program [5]. The flaw distribution after service (FDAS) can be computed by transforming (1) and (4) to obtain:

$$
\begin{aligned}
F_{a(T)}(x) &= P\,[\,a(T) \le x\,] \\
&= \exp\left\{-\left[\frac{x^{-c}-a_o^{-c}+cQT(T-\epsilon)}{cQ\beta}\right]^{\alpha}\right\} \qquad (11)
\end{aligned}
$$

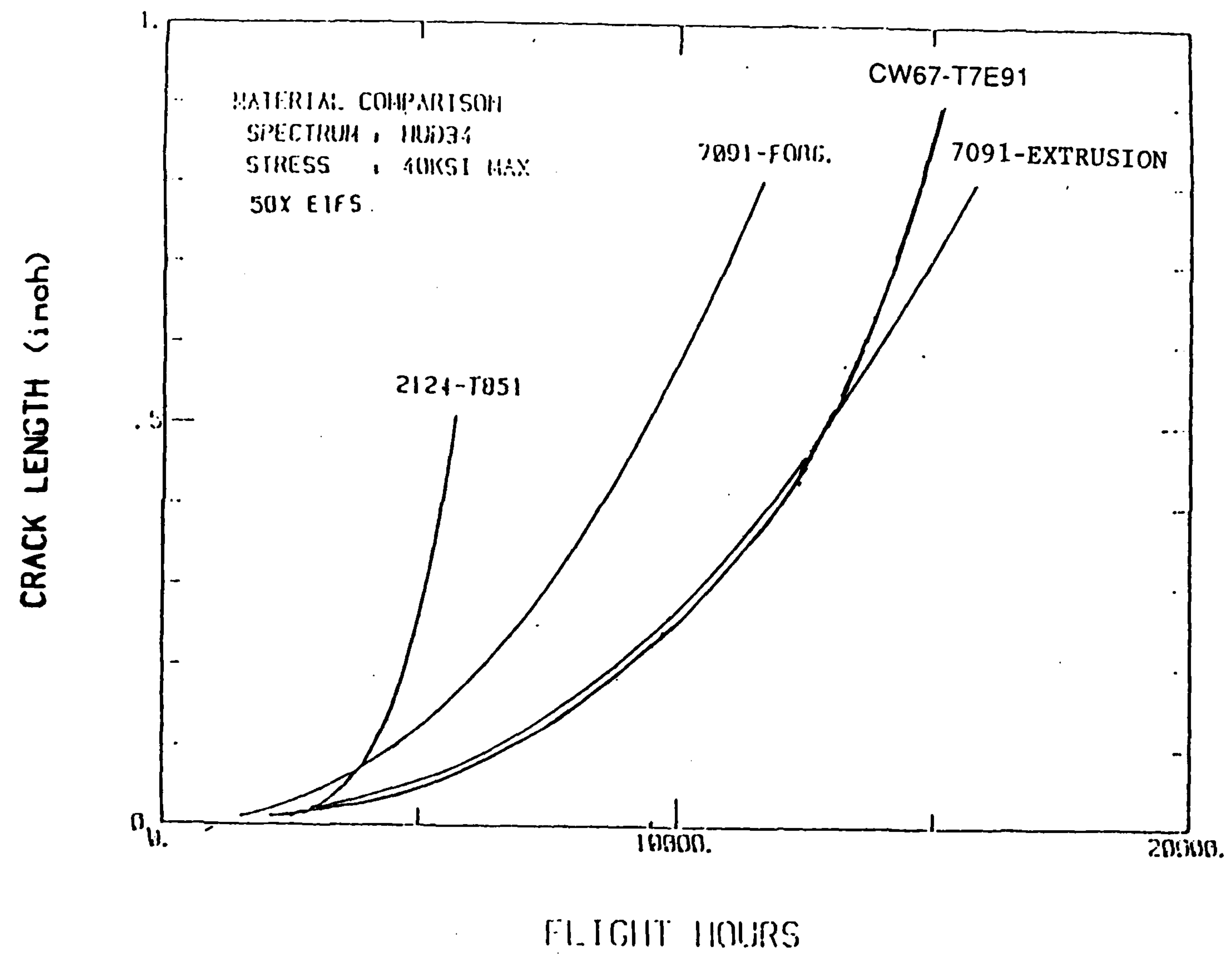

Figure 53. Crack Growth Comparisons In Three Aluminum Alloys (HUD 34 Spectrum, Maximum Stress = 40 ksi)

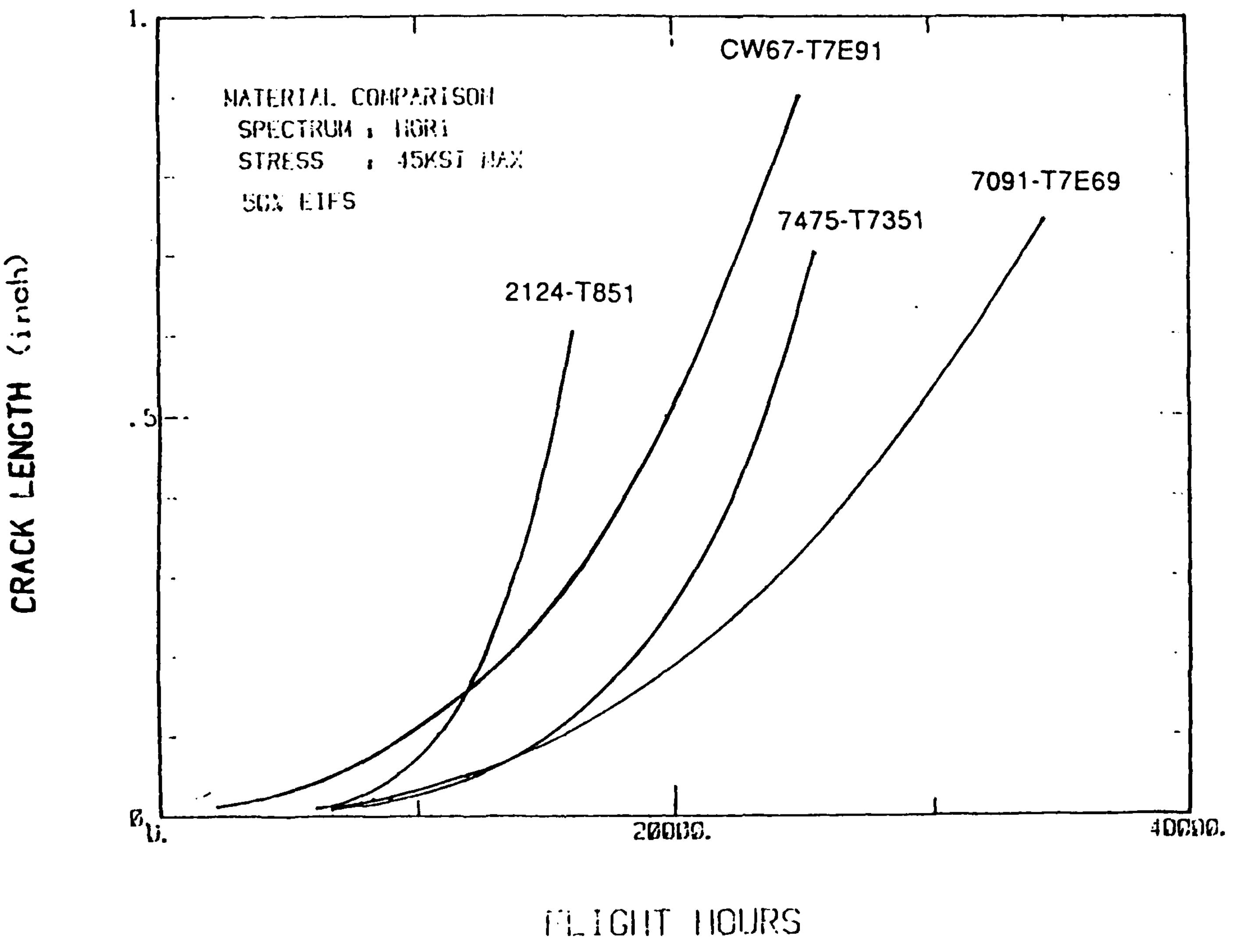

Figure 54. Crack Growth Comparisons In Four Aluminum Alloys (NOR 1 Spectrum)

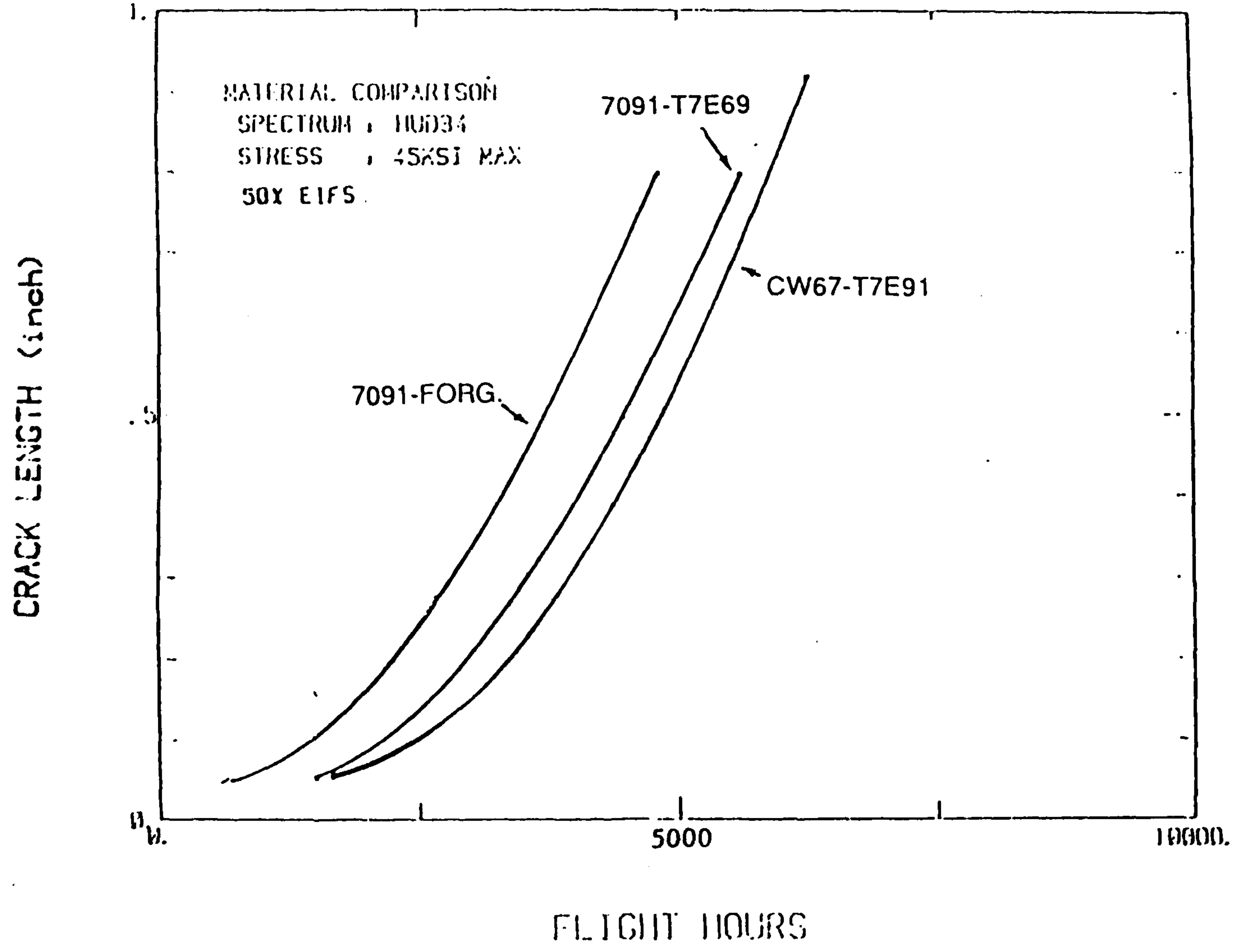

Figure 55. Crack Growth Comparisons In P/M Aluminum Alloys (HUD 34 Spectrum, Maximum Stress = 45 ksi)

where $F_{a(T)}(x)$ is the distribution of flaws after time T.

Equation (11) can be used to find the cumulative flaw distribution for any conditions. The parameters a_0, α, and β are given in Table 9. The lower bound of TTCI, ϵ, was set equal to zero in all of our analysis. The parameters Q and c (where c=b-1) describe crack growth, which is a function of geometry and loading. These are already known for the test conditions of this program and are also given in Table 9. They can also be calculated using any valid crack growth prediction, such as a cycle-by-cycle computer analysis. The parameter x in Equation(11)can represent any flaw size of interest. If flaw sizes are extended to the critical crack size in Equation 11, $x = a_{crit}$, reliability of both RST structures and ingot metallurgy materials may be calculated at any service time.

From previous studies [5,12,18] it is shown that characteristic crack growth rate, Q, can be given as a function of stress level, σ, by:

$$Q = A\sigma^{B} \tag{12}$$

for a reasonable range of σ. Equation (12) provides the means for determining the effect of spectrum stress on structural performance. If Q is experimentally determined for two different stress levels, the constants A and B can be determined from Equation (12). Values of Q can then be calculated for any stress level.

Equations (11) and (12) were used to generate reliabilities and results are plotted in Figures 56-57 for the HUD34 spectrum at 16,000 flight hours and Figs. 58-59 for the NOR1 spectrum at 27,000 flight hours. Since aircraft structural reliabilities less than 90 percent are generally of little interest, a closer look at the regions of interest are shown in Figure 57 and Figure 59. These results indicate that at high reliabilities, P/M alloys can tolerate the most stress, or that the RST structures can be operated at higher stresses than the conventional I/M aluminum alloys.

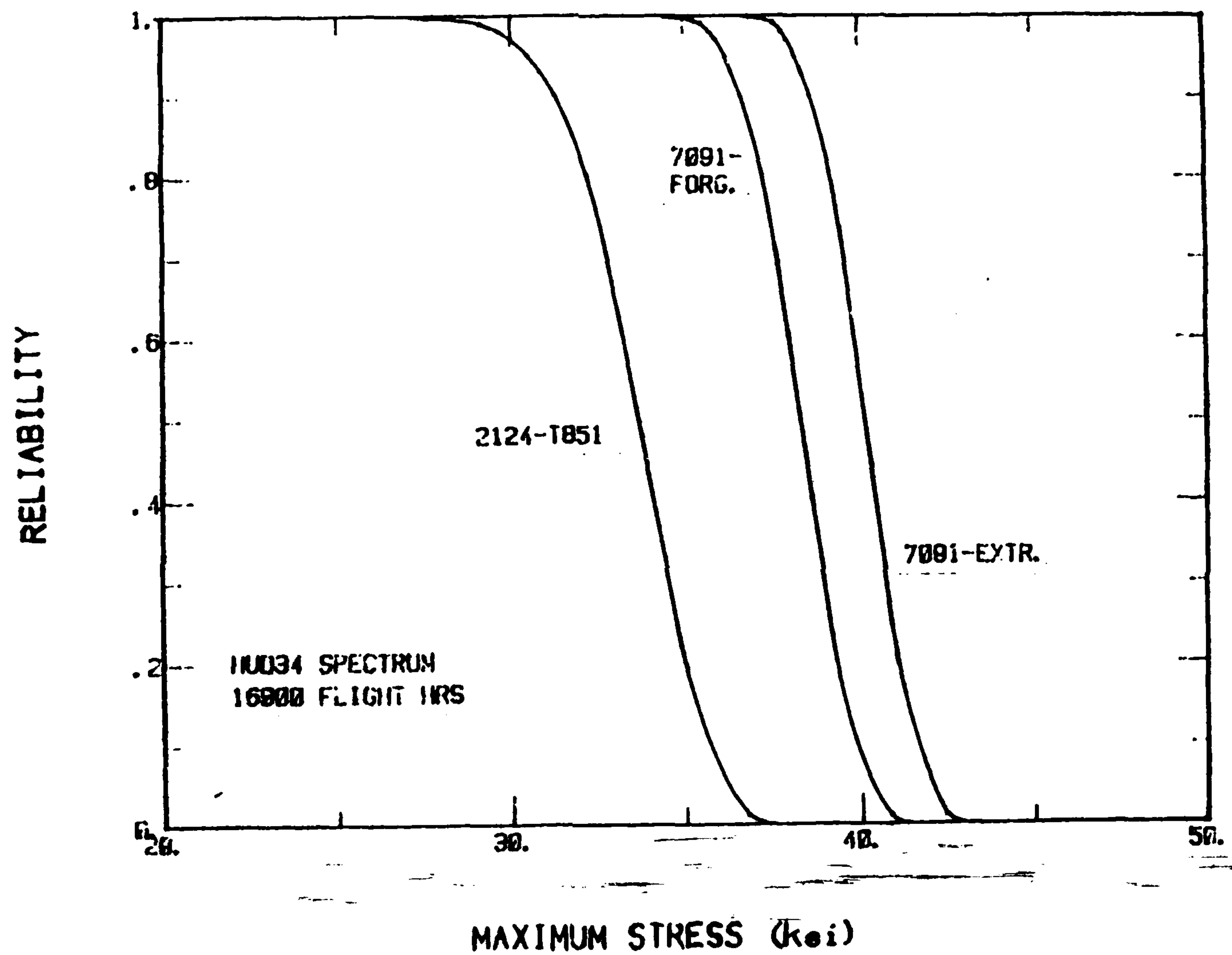

Figure 56. Comparison Of Structural Reliability Of P/M Aluminum Alloys Versus I/M Aluminum Alloys (HUD 34 Spectrum At 16,000 Flight Hours)

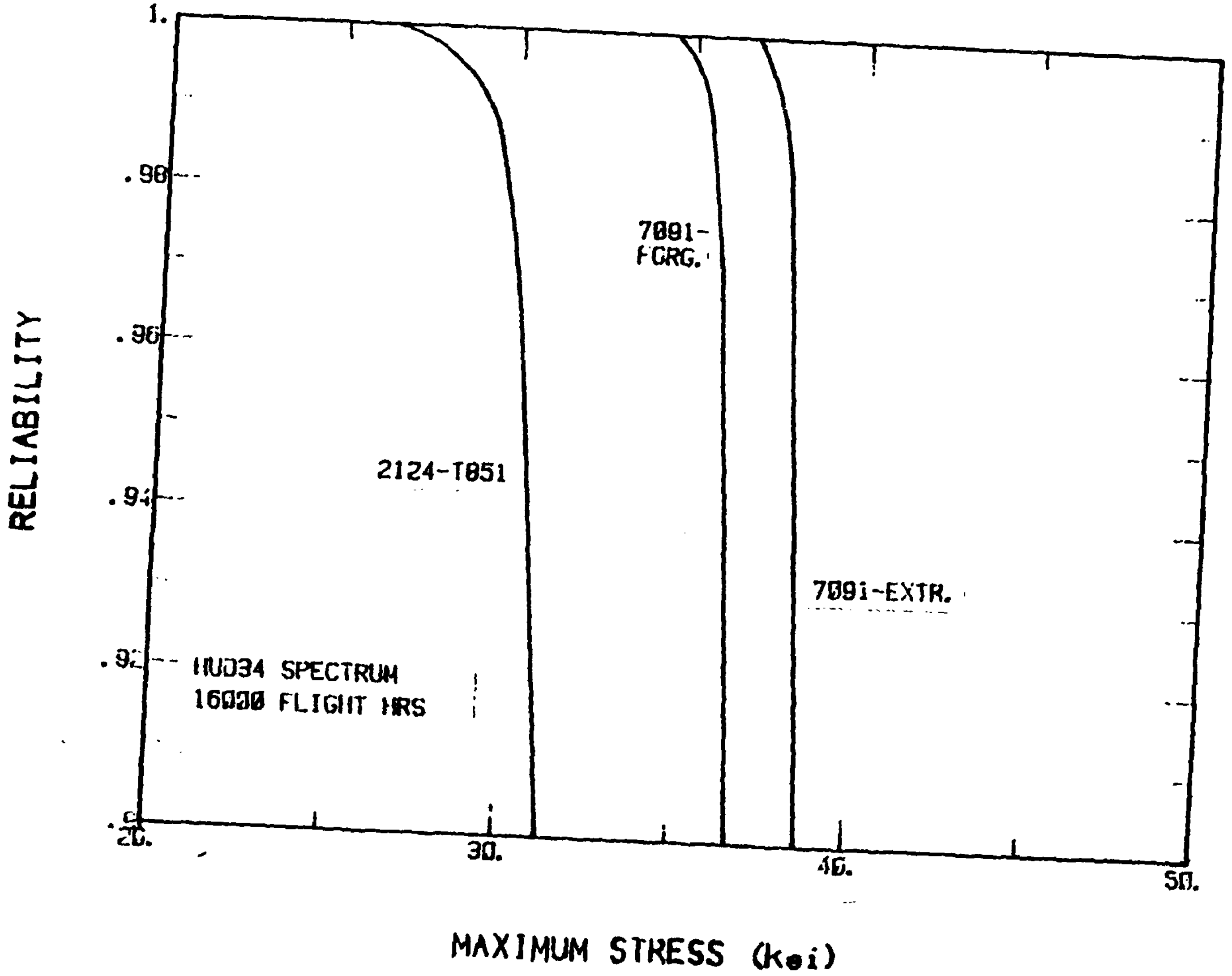

Figure 57. Comparison Of Reliability Above 90 Percent For Three Aluminum Alloys (HUD 34 Spectrum)

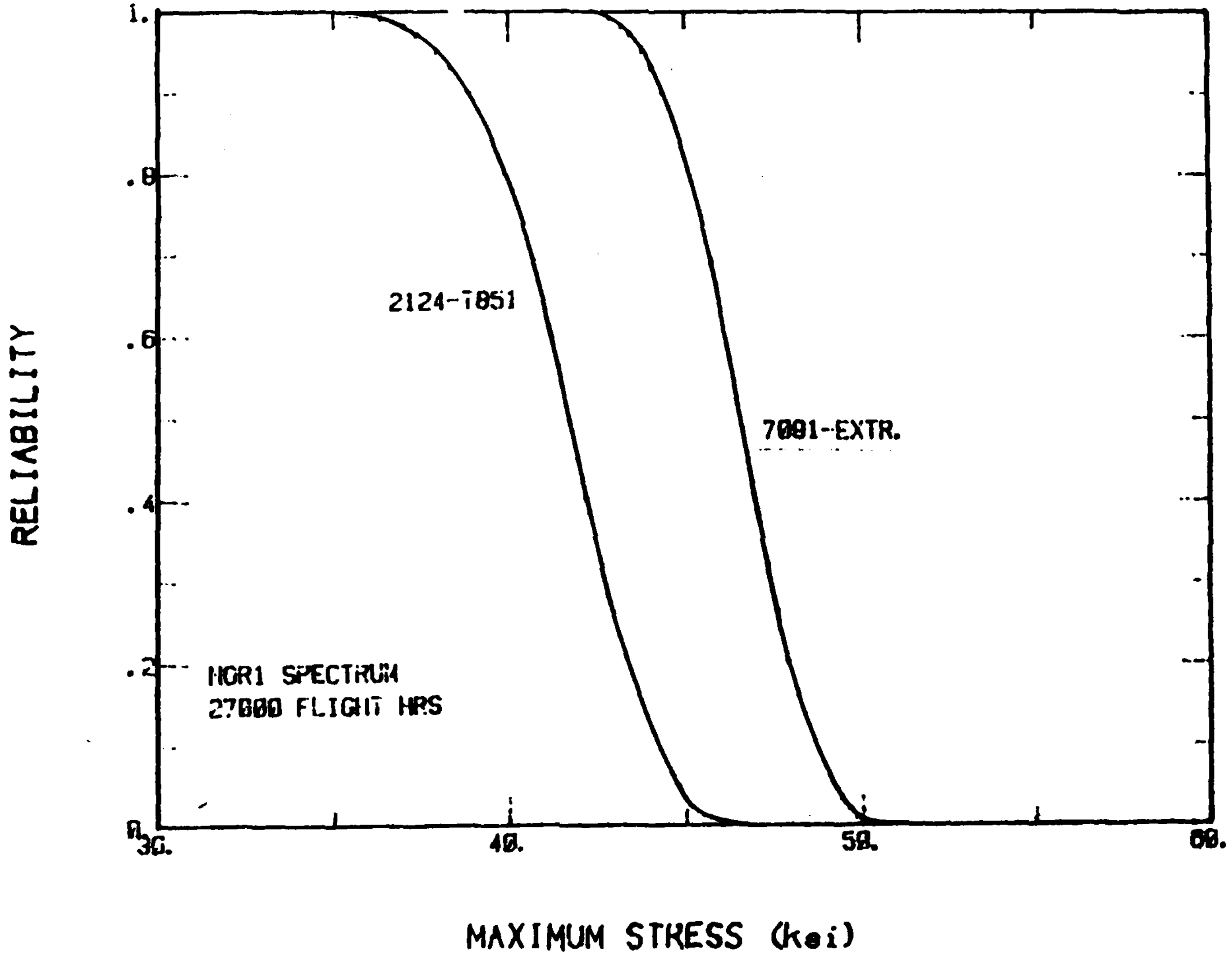

Figure 58. Comparison Of Structural Reliability Of P/M Aluminum Alloys Versus I/M Aluminum Alloys (NOR 1 Spectrum At 27,000 Flight Hours)

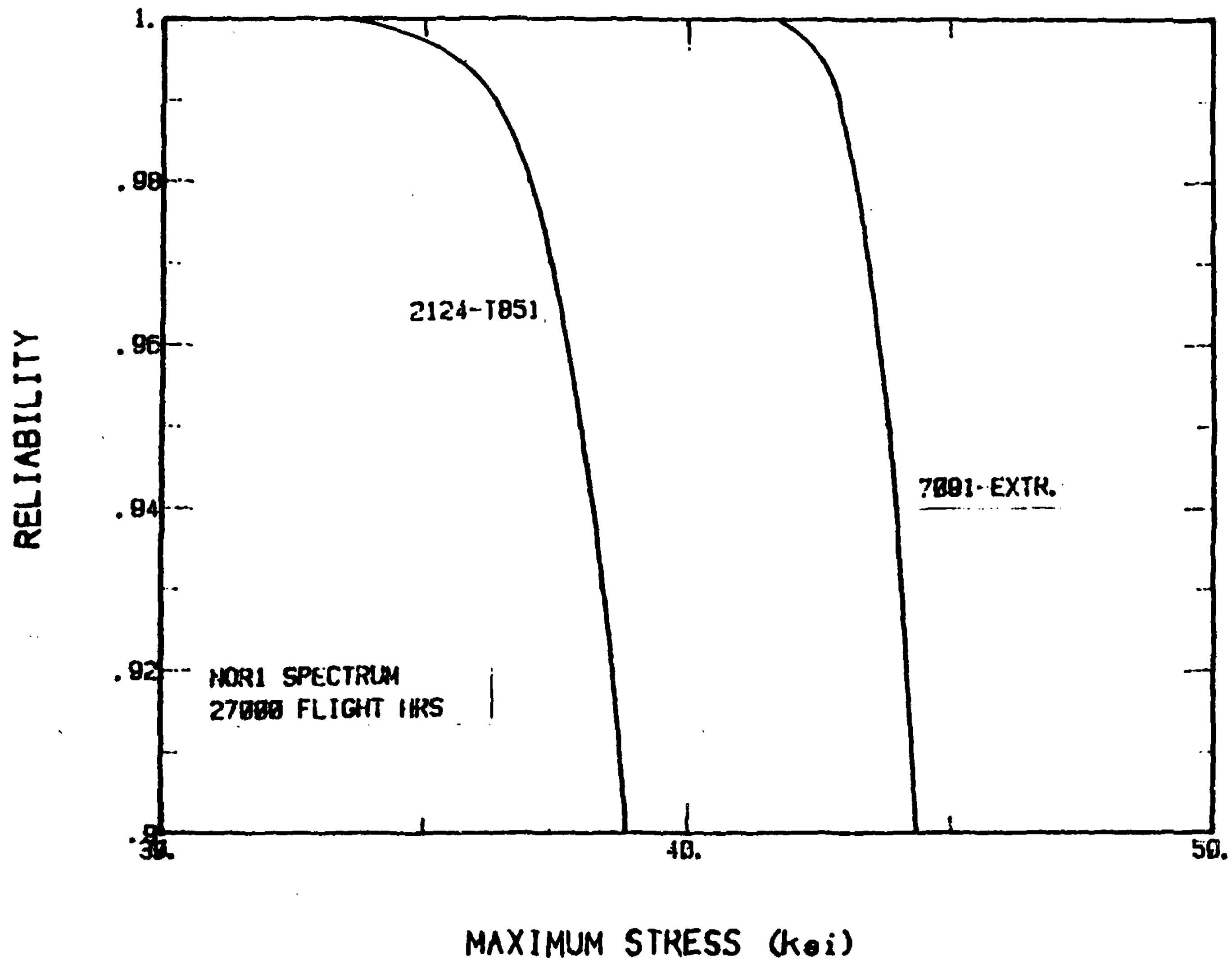

Figure 59. Comparison Of Reliability Above 90 Percent Of 7091-Extrusion and 2124-T951 Plate (NOR 1 Spectrum)

In these examples, the information desired is the probability that a flaw is less than a_{crit} after 16,000 flight hours (2 lifetimes) of the HUD34 spectrum and 27,000 flight hours of the NOR1 spectrum. A durability analysis such as used in this section for comparing structural reliability of P/M aluminum alloys versus I/M aluminum alloys (Figures 56-59) can be used for making "figure of merit" comparisons. This method gives quantitative, statistically based information for design comparison with relatively little effort.

In addition to durability comparisons, designers must often consider other factors in making "figure of merit" comparisons. These factors include density, strength, stiffness, corrosion resistance, cost, and availability of material. Studies have been conducted on determining how improvements in various properties affect weight savings in aircraft structures [26]. Results of these studies are shown in Figure 60. For example, a 10 percent weight savings can be achieved by a 10% decrease (improvement) in density, by a 30 percent increase in strength or by a 45 percent increase in stiffness. Depending on the specific component, damage-tolerance and fatigue are properties where improvements can also lead to weight savings.

The effects of the various engineering parameters will change in relative importance depending on both the mission of the aircraft and the governing failure mode (tension, compression, or other modes). The modulus of elasticity and the compression yield strength are more important in compression-critical structures, particularly in thin sections, and the fatigue resistance, fracture toughness, and tensile strength are more important in tension-critical applications.

For structural components requiring high strength plus excellent corrosion resistance, RST P/M aluminum alloys are particularly appealing. For example, P/M alloys offer between 10 to 20 percent greater strength than 7075-T73 which is commonly used in these applications. This translates into at least a 5 percent weight savings (Figure 60). However, when specific strength (strength/density) is considered, some of the potential weight savings is lost. Based on density comparisons, the density of CW67 is 0.104 lb./in.^{3}. The density of 7475 is 0.101 lb./in.^{3} and that of 2124 material is 0.100 lb./in.^{3}. Based on density comparisons alone,

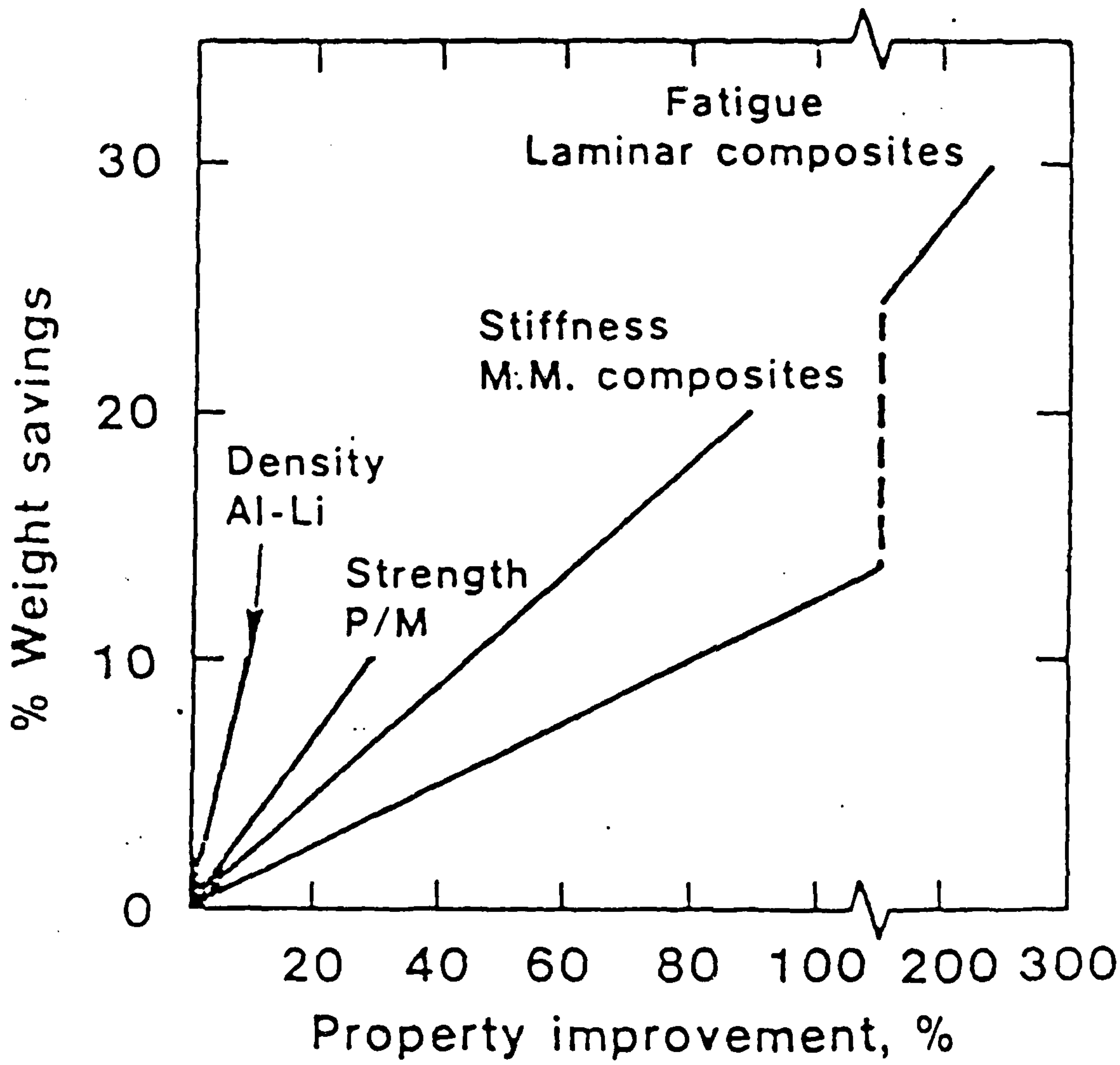

FIGURE 60. Effect Of Property Improvements On Weight Saving

weight penalty of approximately 3 percent is obtained by replacing conventional I/M alloys such as 7475 and 2124 with an RST P/M alloy such as CW67.

The cost of P/M products remains higher than those produced from standard ingot metallurgy. Therefore, their applications are limited to components where superior performance requirements must justify their use. The growth of P/M alloys has also been constrained by the size of billets available for processing into wrought products. In the past, RST P/M billets have been restricted to 300 lb. capacity. However, in the future this capacity can be raised to 4,000 lb. [27]. This should ease some of the past problems related to obtaining sufficient material.

5.5 SEVERITY OF SPECTRUM

A comparison of the HUD34 spectrum with the NOR1 spectrum in terms of spectrum severity is shown in Figure 60. A TTCI comparison for 7091-T7E91 extrusion tested at a maximum stress level of 45 ksi is shown. Much faster crack initiation is observed for the material tested under the HUD34 spectrum. These results are consistent with high compressive loads which are present in the HUD34 spectrum causing crack initiation to occur at an earlier stage.

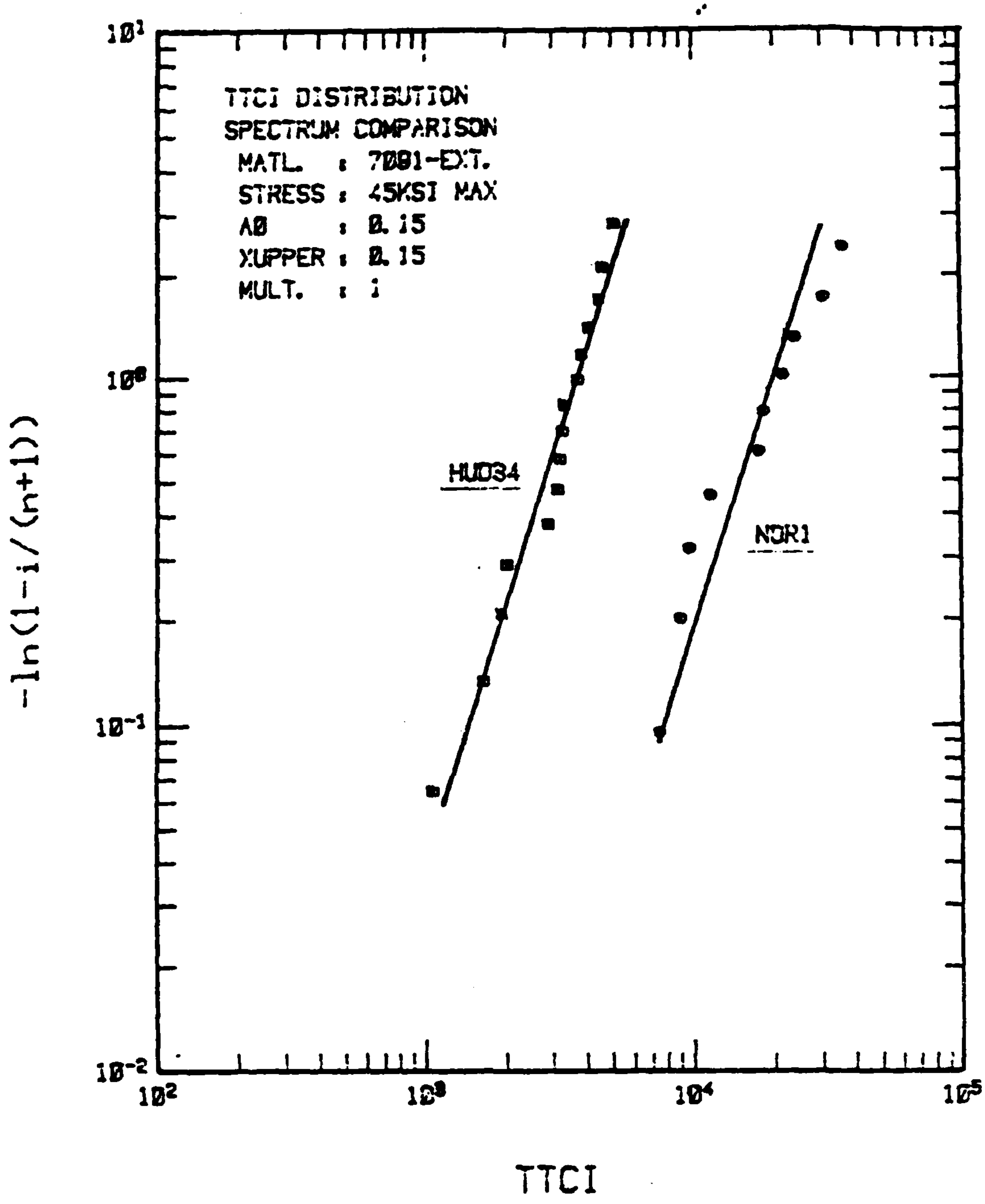

Figure 61. TTCI Distributions Of 7091-Extrusion Showing Comparison Of Load Spectra

8. Superior crack initiation resistance was observed in the higher ranked P/M specimens, especially extruded 7091-T7E69. However, lower ranked 7091-T7E69 test coupons exhibited little improvement in crack initiation resistance over I/M alloys tested. The control of inclusions in the RS P/M alloys will be expected to strongly influence crack initiation. By proper control, the worst performing P/M specimens would be eliminated therefore reducing the experimental scatter.

9. Experimental EIFS distributions of P/M and I/M materials were reasonably fit by a best fit EIFS function.

10. A fairly large variation in fatigue properties was observed in CW67 extruded material. Test coupons from one billet had significantly better durability than extrusions obtained from two other billets. These results emphasize the need for using material from different billets when generating design test data.

11. None of the inspection techniques provided correlations of NDI parameters with spectrum fatigue performance. It was concluded that the size of the flaws which influenced fatigue performance are smaller than can be detected with the NDI techniques used in these studies.

SECTION VII

RECOMMENDATIONS

1. High strength RST P/M aluminum alloys should be considered for usage in structures where I/M aluminum alloys such as 2124-T851 and 7475-T7351 are currently used. Potential weight savings exist with the RST aluminum alloys due to the improvement in fatigue properties. The type of spectrum loading needs to be considered when comparing RST P/M aluminum alloys with I/M aluminum alloys, however.

2. The high tensile strength, excellent corrosion resistance, good fracture toughness, and slow crack growth at large crack sizes, make CW67 particularly attractive for aerospace applications. However, the cause of variation in fatigue properties from billet to billet needs to be investigated. Testing material from different billets is recommended when generating design test data.

3. Effects of anisotropy in basic mechanical properties of CW67 on spectrum fatigue performance needs to be examined.

4. Durability and damage tolerance specification, based on the IFQ model should be considered for both RST P/M structures and conventional I/M structures. These methods based on element level testing, provide an effective compromise between the deterministic analysis and limited testing on the one hand, and very high costs associated with multiple structural tests, on the other.

5. Mechanisms responsible for the reduction in fatigue life of the forged material compared to extruded material needed to be investigated further. Correlations between parameters such as grain flow, forging variables, residual stress, etc. with fatigue properties need to be established.

REFERENCES

1. MIL-A-87221 (USAF) "Military Specification: General Specification for Aircraft Structures," February, 1985.

2. MIL-A-83444 (USAF), "Airplane Damage Tolerance Requirements," July 1974.

3. MIL-A-8866B (USAF), "Airplane Strength and Rigidity Reliability Requirements, Repeated Loads and Fatigue," August 1975.

4. MIL-A-8867B (USAF), "Airplane Strength and Rigidity Ground Tests," August 1975.

5. W. R. Garver, D. Y. Lee and K. M. Koepsel, "Initial Quality of Advanced Joining Concepts - Final Report," AFWAL-TR-84-3066, December 1984.

6. W. M. Griffith and J. S. Santner, "Effect of Defects in Aluminum P/M, in High Strength Powder Metallurgy Aluminum Alloys," TMS-AIME, 1982, PP125-146.

7. B. Quist, presented at Air Force/Industry Aluminum Cooperative Testing Meeting, June 4, 1984.

8. G. W. Kuhlman, "High Strength and Elevated Temperature Alloy Forgings for Aerospace Applications," Metal Powder Report Conference on PM Aerospace Materials, Berne, Switzerland, MPR Publishing (November 1984).

9. G. J. Hildeman, D. J. Brownhill, D. K. Denzer and A. Hafeez, "7XXX P/M Alloy Development," WESTEC Conference Symposium on Advanced 7XXX P/M and I/M Alloys, Los Angeles, CA (March 1983).

10. A. Hafeez,"Corrosion Resistance of Wrought P/M Alloys," Alcoa Techbrief (March 1985).

REFERENCES (Continue)

11. J. W. Morrow, F. C. Nordquist, and T. E. Coyle, "Test Results of Spectrum/Environmental Fatigue Testing to Determine the Crack Growth Rates of Flaws in 7475, 2124 and 2024 Aluminum Alloys and 6Al-4V-Titanium," General Dynamics, Fort Worth Division Report, 16PR925, 10 June 1978.

12. P. J. Noronha, S. P. Henslee, D. E. Gordon, F. R. Wolanski, and B. G. W. Yee, "Fastener Hole Quality-Final Report," AFFDL-TR-78-206, December 1978.

13. C. O. Ruud and C. S. Barrett, "Use of Cr K-Beta X-Rays and Position Sensitive Detection for Residual Stress Measurement in Stainless Steel Pipe," Advances in X-Ray Analysis, Vol. 22, p. 247, 1979.

14. S. Forness, "Fracture Mechanics Methodology Update," General Dynamics, Fort Worth Division ERR-FW-2219, May 1982.

15. J. C. Newman and I. S. Raju, "Analysis of Surface Cracks in Finite Plates Under Tension or Bending Loads," NASA TP 1578, Dec. 1979.

16. J. C. Newman and I. S. Raju, "Stress Intensity Factors for Two Symmetrical Corner Cracks," ASTM STP 677, C. W. Smith, Ed., 1979, pp. 411-430.

17. J. B. Chang, R. M. Hiyama, J. Szamossi, "Improved Methods for Predicting Spectrum Loading Effects," AFWAL-TR-81-3092, Volume I, Technical Summary, Air Force Flight Dynamics Laboratory, November 1981.

18. S. D. Manning, J. N. Yang, M. Shinozuka, D. E. Gordon, S. M. Speaker, and B. G. W. Yee, "Durability Methods Development, Volume V," Air Force Flight Dynamics Laboratory, AFFDL-TR-79-3118, Vol. V, 1982.

19. S. D. Manning, J. N. Yang, and J. W. Norris "USAF Durability Design Handbook: Guidelines for the Analysis and Design of Durable Aircraft Structures," Air Force Flight Dynamics Laboratory, AFFDL-TR-99-3118, Vol. XI, February 1983.

REFERENCES (Concluded)

20. D. A. Virkler, B. W. Hillberry, and P. V. Goel, "The Statistical Nature of Fatigue Crack Propagation-Final Report," AFFDL-TR-78-43, April 1978.

21. S. D. Manning, S. M. Speaker, and D. E. Gordon, "Durability Methods Development Volume VII - Phase II Documentation," AFFDL-TR-79-3118, January 1984.

22. S. D. Manning and J. N. Yang, "Advanced Durability Analysis Volume I - Analytical Methods," AFWAL-TR-86-3017, Volume I, July 1987.

23. D. Y. Lee and D. E. Gordon, "Cyclic Stability of Aluminum Alloys - Strain Ratio Effect," Presented at TMS-AIME Meeting at Denver, Colorado on 26 February 1987.

24. D. Y. Lee and W. R. Garver, "Fatigue Performance of P/M and I/M Aluminum Alloys - Stress Ratio Effect," Presented at TMS-AIME Meeting at Detroit, Michigan on 19 September 1984.

25. D. Y. Lee, D. E. Gordon, and W. R. Garver, "Structural Performance of RSP P/M Aluminum Alloys Under Spectrum Loading," Presented at WESTEC Meeting, Los Angeles, California.

26. J. C. Ekwall, E. J. Rhodes, and G. G. Wald, "Methodology for Evaluating Aircraft Weight Savings from Basic Material Properties," ASTM STP 761, Symposium on Design of Fatigue and Fracture Resistant Structures, 327-44, 1980.

27. R. H. Graham, Aluminum Company of America, Alcoa Laboratories, Private Communication, October 1987.

LIST OF SYMBOLS

SYMBOL	DESCRIPTION
RST	Rapidly Solidified Technology
RSP	Rapid Solidification Processing
P/M	Powder Metallurgy
I/M	Ingot Metallurgy
OOR	Out-Of-Roundness
FTSD	Film-To-Source-Distance
FCGR	Fatigue Crack Growth Rate
FCG	Fatigue Crack Growth
a	Crack Length
a_o	Crack Length at t = TTCI
$a(o)$	EIFS
a_{crit}	a(TTF), Critical Crack Size
b	Crack Growth Parameter
c	$= b-1$
EIFS	Equivalent Initial Flaw Size
$F_{a(o)}(x)$	$= P[a(o) < x]$
$F_T(t)$	$= P[T < t]$
FDAS	= Flaw Distribution After Service
i	Subscript Representing an Individual Specimen
I	Subscript Representing an Individual Data Set

LIST OF SYMBOLS (Continued)

SYMBOL	DESCRIPTION
IFQ	Initial Fatigue Quality
P[]	Probability
Q	Crack Growth Parameter
Q_i	Q for Specimen Using Pooled b
Q_I	Q Obtained from Pooled Data Set
t	Time
T	A Random Variable Indicating TTCI
TTCI	Time to Crack Initiation
TTF	Time to Failure
x	A Random Variable indicating EIFS
x_u	Upper bound of EIFS
α	Shape Parameter of TTCI Distribution
β	Scale Parameter of TTCI Distribution
ϵ	Lower Bound of TTCI Distribution
*	Superscript Representing a Pooled Data Set

APPENDIX A

Fractographic Crack Growth Data

Measured crack growth data for all of the data sets are listed in this section. Crack sizes are given in inches and time is given in flight hours. Data set notations used are listed in Table A-1. For example, C1HD35 refers to 2124-T851 material tested under the HUD 34 spectrum with a maximum stress of 35 ksi.

A I – POOLED DATA SETS FOR EIFS DETERMINATION

POOLED DATA SET	INDIVIDUAL DATA SET	NO OF SPECIMENS
2124-T851	C1HD35	15
	C1HD40	15
	C1NR45	10
7475-T7351	C2NR45	11
7091-EXTRUSION	R1HD40	14
	R1HD45	15
	R1NR45	10
	R1NR50	10
7091-FORGING	R2HD40	9
	R2HD45	9
CW67-EXTRUSION	R3HD40	10
	R3HD45	8
	R3NR45	10

2124-T851
HUD 34 SPECTRUM
35 KSI MAXIMUM STRESS

C1HD35-01

Point	Hours	Length
1	500.	0.0071
2	1000.	0.0196
3	1500.	0.0370
4	2000.	0.0624
5	2500.	0.0829
6	3000.	0.1024
7	3500.	0.1259
8	4000.	0.1483
9	4500.	0.1794
10	5000.	0.2267
11	5500.	0.2921
12	6000.	0.6314

C1HD35-02

Point	Hours	Length
1	2000.	0.0092
2	2500.	0.0247
3	3000.	0.0446
4	3500.	0.0601
5	4000.	0.0757
6	4500.	0.1451
7	5000.	0.2945
8	5500.	0.3811
9	6000.	0.6729
10	6500.	0.8741

C1HD35-03

Point	Hours	Length
1	2000.	0.0290
2	2500.	0.0441
3	3000.	0.0611
4	3500.	0.0766
5	4000.	0.0954
6	4500.	0.1131
7	5000.	0.1413
8	5500.	0.1719
9	6000.	0.2093
10	6500.	0.2673
11	7000.	0.3859
12	7500.	0.5147
13	8000.	0.6378
14	8500.	0.7813
15	9000.	0.8869

C1HD35-04

Point	Hours	Length
1	1500.	0.0207
2	2000.	0.0312
3	2500.	0.0436
4	3000.	0.0600
5	3500.	0.0759
6	4000.	0.0936
7	4500.	0.1086
8	5000.	0.1236
9	5500.	0.1384
10	6000.	0.1532
11	6500.	0.1727
12	7000.	0.1959
13	7500.	0.2242
14	8000.	0.2700
15	8500.	0.3267
16	9000.	0.4274
17	9500.	0.6035
18	10000.	0.7887
19	10500.	0.8285

C1HD35-05

Point	Hours	Length
1	3500.	0.0268
2	4000.	0.0391
3	4500.	0.0496
4	5000.	0.0606
5	5500.	0.0743
6	6000.	0.0840
7	6500.	0.0978
8	7000.	0.1166
9	7500.	0.1348
10	8000.	0.1516
11	8500.	0.1707
12	9000.	0.1963
13	9500.	0.2279
14	10000.	0.2588
15	10500.	0.3192
16	11000.	0.4226
17	11500.	0.8224

C1HD35-06

Point	Hours	Length
1	5500.	0.0548
2	6000.	0.0696
3	6500.	0.0847
4	7000.	0.0957
5	7500.	0.1076
6	8000.	0.1195
7	8500.	0.1372
8	9000.	0.1580
9	9500.	0.1889
10	10000.	0.2289
11	10500.	0.2882
12	11000.	0.3690
13	11500.	0.5576
14	12000.	0.8309

C1HD35-07

Point	Hours	Length
1	7000.	0.0313
2	7500.	0.0404
3	8000.	0.0542
4	8500.	0.0687
5	9000.	0.0806
6	9500.	0.0921
7	10000.	0.1058
8	10500.	0.1216
9	11000.	0.1373
10	11500.	0.1552
11	12000.	0.1799
12	12500.	0.2037
13	13000.	0.2862
14	13500.	0.4169
15	14000.	0.5829

C1HD35-08

Point	Hours	Length
1	4500.	0.0297
2	5000.	0.0360
3	5500.	0.0434
4	6000.	0.0534
5	6500.	0.0604
6	7000.	0.0676
7	7500.	0.0776
8	8000.	0.0921
9	8500.	0.1060
10	9000.	0.1211
11	9500.	0.1364
12	10000.	0.1589
13	10500.	0.1746
14	11000.	0.1869
15	11500.	0.2096
16	12000.	0.2293
17	12500.	0.2582
18	13000.	0.2771
19	13500.	0.3096
20	14000.	0.3492
21	14500.	0.4100
22	15000.	0.5156

C1HD35-09

Point	Hours	Length
1	9000.	0.0635
2	9500.	0.0733
3	10000.	0.0839
4	10500.	0.0980
5	11000.	0.1096
6	11500.	0.1191
7	12000.	0.1323
8	12500.	0.1480
9	13000.	0.1665
10	13500.	0.1818
11	14000.	0.1969
12	14500.	0.2091
13	15000.	0.2244
14	15500.	0.2447
15	16000.	0.3504
16	16500.	0.6172

C1HD35-10

Point	Hours	Length
1	4000.	0.0198
2	4500.	0.0262
3	5000.	0.0329
4	5500.	0.0392
5	6000.	0.0455
6	6500.	0.0517
7	7000.	0.0585
8	7500.	0.0658
9	8000.	0.0733
10	8500.	0.0809
11	9000.	0.0888
12	9500.	0.0955
13	10000.	0.1007
14	10500.	0.1078
15	11000.	0.1155
16	11500.	0.1238
17	12000.	0.1345
18	12500.	0.1461
19	13000.	0.1589
20	13500.	0.1704
21	14000.	0.1839
22	14500.	0.1972
23	15000.	0.2178
24	15500.	0.2417
25	16000.	0.2695
26	16500.	0.3051
27	17000.	0.8268

C1HD35-11

Point	Hours	Length
1	6500.	0.0228
2	7000.	0.0290
3	7500.	0.0385
4	8000.	0.0457
5	8500.	0.0514
6	9000.	0.0590
7	9500.	0.0684
8	10000.	0.0784
9	10500.	0.0890
10	11000.	0.1033
11	11500.	0.1137
12	12000.	0.1261
13	12500.	0.1386
14	13000.	0.1553
15	13500.	0.1752
16	14000.	0.2015
17	14500.	0.2242
18	15000.	0.2664
19	15500.	0.3051
20	16000.	0.3767
21	16500.	0.4760
22	17000.	0.7895

C1HD35-12

Point	Hours	Length
1	8500.	0.0519
2	9000.	0.0593
3	9500.	0.0659
4	10000.	0.0729
5	10500.	0.0794
6	11000.	0.0886
7	11500.	0.0964
8	12000.	0.1030
9	12500.	0.1104
10	13000.	0.1183
11	13500.	0.1290
12	14000.	0.1396
13	14500.	0.1481
14	15000.	0.1568
15	15500.	0.1680
16	16000.	0.1845
17	16500.	0.2030
18	17000.	0.2214
19	17500.	0.2368
20	18000.	0.2706
21	18500.	0.3216
22	19000.	0.4181
23	19500.	0.7850

C1HD35-14

Point	Hours	Length
1	10500.	0.0811
2	11000.	0.0954
3	11500.	0.1088
4	12000.	0.1201
5	12500.	0.1308
6	13000.	0.1431
7	13500.	0.1594
8	14000.	0.1788
9	14500.	0.2020
10	15000.	0.2239
11	15500.	0.2494
12	16000.	0.2759
13	16500.	0.3042
14	17000.	0.3341
15	17500.	0.3594
16	18000.	0.3913
17	18500.	0.4178
18	19000.	0.4701
19	19500.	0.5087
20	20000.	0.5680
21	20500.	0.6437
22	21000.	0.6975
23	21500.	0.7400
24	22000.	0.7778
25	22500.	0.8149
26	23000.	0.8494

C1HD35-13

Point	Hours	Length
1	500.	0.1078
2	1000.	0.1141
3	1500.	0.1171
4	2000.	0.1235
5	2500.	0.1302
6	3000.	0.1364
7	3500.	0.1432
8	4000.	0.1503
9	4500.	0.1558
10	5000.	0.1596
11	5500.	0.1631
12	6000.	0.1667
13	6500.	0.1724
14	7000.	0.1788
15	7500.	0.1834
16	8000.	0.1887
17	8500.	0.1917
18	9000.	0.1956
19	9500.	0.1997
20	10000.	0.2047
21	10500.	0.2096
22	11000.	0.2119
23	11500.	0.2184
24	12000.	0.2271
25	12500.	0.2350
26	13000.	0.2435
27	13500.	0.2493
28	14000.	0.2598
29	14500.	0.2658
30	15000.	0.2741
31	15500.	0.2837
32	16000.	0.2951
33	16500.	0.3048
34	17000.	0.3096
35	17500.	0.3256
36	18000.	0.3397
37	18500.	0.3534
38	19000.	0.3698
39	19500.	0.3921
40	20000.	0.4088
41	20500.	0.4496
42	21000.	0.4947
43	21500.	0.5410
44	22000.	0.5739
45	22500.	0.6137

C1HD35-15

Point	Hours	Length
1	18000.	0.1268
2	18500.	0.1336
3	19000.	0.1394
4	19500.	0.1471
5	20000.	0.1567
6	20500.	0.1643
7	21000.	0.1718
8	21500.	0.1852
9	22000.	0.1984
10	22500.	0.2152
11	23000.	0.2376
12	23500.	0.2513
13	24000.	0.2754

2124-T851

HUD 34 SPECTRUM

40 KSI MAXIMUM STRESS

C1HD40-01

Hours	Length
500.	0.0274
1000.	0.0457
1500.	0.0649
2000.	0.0869
2500.	0.1285
3000.	0.1802
3500.	0.4236
4000.	0.6378

C1HD40-02

Hours	Length
500.	0.0196
1000.	0.0362
1500.	0.0523
2000.	0.0831
2500.	0.1107
3000.	0.1432
3500.	0.1747
4000.	0.2663
4500.	0.3167

C1HD40-03

Hours	Length
2000.	0.0152
2500.	0.0332
3000.	0.0528
3500.	0.0727
4000.	0.1166
4500.	0.1777

C1HD40-04

Hours	Length
500.	0.0362
1000.	0.0430
1500.	0.0782
2000.	0.1096
2500.	0.1584
3000.	0.2219
3500.	0.3015
4000.	0.5234
4500.	0.7260
4809.	0.9219

C1HD40-05

Hours	Length
500.	0.0141
1000.	0.0233
1500.	0.0365
2000.	0.0496
2500.	0.0631
3000.	0.0855
3500.	0.1232
4000.	0.1526
4500.	0.2041
5000.	0.2759
5500.	0.4259

C1HD40-06

Hours	Length
1500.	0.0090
2000.	0.0196
2500.	0.0328
3000.	0.0486
3500.	0.0654
4000.	0.0947
4500.	0.1645
5000.	0.2188
5500.	0.4148

C1HD40-07

Hours	Length
2500.	0.0287
3000.	0.0575
3500.	0.0982
4000.	0.1380
4500.	0.1826
5000.	0.2275
5500.	0.3934

C1HD40-08

Hours	Length
3000.	0.0691
3500.	0.0849
4000.	0.1168
4500.	0.1540
5000.	0.2079
5500.	0.3047

C1HD40-09

Point	Hours	Length
1	1500.	0.0202
2	2000.	0.0325
3	2500.	0.0497
4	3000.	0.0748
5	3500.	0.1002
6	4000.	0.1378
7	4500.	0.1976
8	5000.	0.2672
9	5500.	0.4370
10	6000.	0.7782

C1HD40-10

Point	Hours	Length
1	4000.	0.0910
2	4500.	0.1193
3	5000.	0.1566
4	5500.	0.2288
5	6000.	0.4124

C1HD40-11

Point	Hours	Length
1	3000.	0.0258
2	3500.	0.0370
3	4000.	0.0653
4	4500.	0.1050
5	5000.	0.1423
6	5500.	0.2052
7	6000.	0.3473

C1HD40-12

Point	Hours	Length
1	2500.	0.0230
2	3000.	0.0375
3	3500.	0.0708
4	4000.	0.0975
5	4500.	0.1378
6	5000.	0.1908
7	5500.	0.3518
8	6000.	0.4616
9	6500.	0.6973

C1HD40-13

Point	Hours	Length
1	500.	0.0084
2	1000.	0.0215
3	1500.	0.0392
4	2000.	0.0547
5	2500.	0.0721
6	3000.	0.0855
7	3500.	0.1044
8	4000.	0.1239
9	4500.	0.1432
10	5000.	0.1643
11	5500.	0.2017
12	6000.	0.2565
13	6500.	0.3165
14	7000.	0.4705

C1HD40-14

Point	Hours	Length
1	4000.	0.0102
2	4500.	0.0255
3	5000.	0.0372
4	5500.	0.0665
5	6000.	0.0916
6	6500.	0.1173
7	7000.	0.1439
8	7500.	0.1792
9	8000.	0.2477
10	8488.	0.2773

C1HD40-15

Point	Hours	Length
1	1500.	0.0091
2	2000.	0.0179
3	2500.	0.0295
4	3000.	0.0479
5	3500.	0.0668
6	4000.	0.0804
7	4500.	0.0953
8	5000.	0.1167
9	5500.	0.1354
10	6000.	0.1615
11	6500.	0.1928
12	7000.	0.2340
13	7500.	0.3162
14	8000.	0.7058
15	8500.	0.8153

C1NR45-02

Point	Hours	Length
1	3164.	0.0114
2	4218.	0.0232
3	5273.	0.0388
4	6328.	0.0653
5	7383.	0.1140
6	8436.	0.2480
7	9479.	0.3700

C1NR45-03

Point	Hours	Length
1	2109.	0.0107
2	3164.	0.0164
3	4219.	0.0315
4	5273.	0.0450
5	6328.	0.0621
6	7383.	0.0772
7	8437.	0.1084
8	9492.	0.1564
9	10534.	0.2803

C1NR45-04

Point	Hours	Length
1	1055.	0.0166
2	2110.	0.0209
3	3164.	0.0290
4	4219.	0.0384
5	5274.	0.0523
6	6328.	0.0645
7	7383.	0.0905
8	8438.	0.1154
9	9492.	0.1773
10	10547.	0.2920
11	11170.	0.6571

C1NR45-05

Point	Hours	Length
1	5273.	0.0071
2	6328.	0.0120
3	7383.	0.0207
4	8436.	0.0289
5	9492.	0.0368
6	10547.	0.0472
7	11601.	0.0595
8	12656.	0.0807
9	13500.	0.1084
10	14554.	0.1521
11	15609.	0.2954
12	16018.	0.6800

C1NR45-06

Point	Hours	Length
1	6328.	0.0064
2	7383.	0.0138
3	8437.	0.0172
4	9493.	0.0252
5	10547.	0.0406
6	11601.	0.0580
7	12656.	0.0848
8	13500.	0.1071
9	14555.	0.1510
10	15609.	0.1992
11	16664.	0.2488
12	16968.	0.3244

C1NR45-07

Point	Hours	Length
1	4219.	0.0166
2	5274.	0.0242
3	6328.	0.0384
4	7383.	0.0523
5	8438.	0.0649
6	9492.	0.0820
7	10547.	0.1072
8	11602.	0.1433
9	12656.	0.1780
10	13500.	0.2331
11	14555.	0.2939
12	15610.	0.3505
13	16654.	0.4722
14	17719.	0.5729
15	17768.	0.7871

C1NR45-08

Point	Hours	Length
1	5273.	0.0089
2	6328.	0.0134
3	7383.	0.0176
4	8436.	0.0248
5	9492.	0.0312
6	10547.	0.0384
7	11601.	0.0476
8	12656.	0.0563
9	13500.	0.0669
10	14554.	0.0764
11	15609.	0.0921
12	16664.	0.1228
13	17719.	0.1505
14	18773.	0.1912
15	19828.	0.2500
16	20883.	0.4100
17	21398.	0.8500

C1NR45-09

Point	Hours	Length
1	3164.	0.0089
2	4218.	0.0119
3	5273.	0.0167
4	6328.	0.0232
5	7383.	0.0290
6	8436.	0.0356
7	9492.	0.0421
8	10547.	0.0476
9	11601.	0.0564
10	12656.	0.0663
11	13500.	0.0780
12	14554.	0.0918
13	15609.	0.1120
14	16664.	0.1340
15	17719.	0.1570
16	18773.	0.1920
17	19828.	0.2400
18	20883.	0.3420
19	21704.	0.8600

C1NR45-10

oint	Hours	Length
1	13500.	0.0160
2	14555.	0.0310
3	15610.	0.0531
4	16664.	0.0929
5	17719.	0.1217
6	18774.	0.1673
7	19828.	0.2336
8	20883.	0.4137
9	21821.	0.5215

C1NR45-01

Point	Hours	Length
1	3164.	0.0280
2	4218.	0.0500
3	5273.	0.1300
4	6328.	0.2100
5	7372.	0.6000

7475-T7351
NOR 1 SPECTRUM
45 KSI MAXIMUM STRESS

C2NR45-01

Point	Hours	Length
1	2109.	0.0093
2	3164.	0.0147
3	4218.	0.0218
4	5273.	0.0316
5	6328.	0.0445
6	7383.	0.0590
7	8436.	0.0798
8	9492.	0.1045
9	10547.	0.1394
10	11601.	0.1684
11	12656.	0.2021
12	13500.	0.2412
13	14554.	0.2951
14	15609.	0.3847
15	16664.	0.5450
16	17705.	0.8300

C2NR45-03

Point	Hours	Length
1	7383.	0.0234
2	8436.	0.0322
3	9492.	0.0473
4	10547.	0.0622
5	11601.	0.0833
6	12656.	0.1110
7	13500.	0.1352
8	14554.	0.1614
9	15609.	0.1943
10	16664.	0.2306
11	17719.	0.2663
12	18773.	0.3062
13	19829.	0.3564
14	20883.	0.4251
15	21937.	0.5384
16	22979.	0.7100

C2NR45-02

Point	Hours	Length
1	4218.	0.0089
2	5273.	0.0143
3	6328.	0.0205
4	7383.	0.0284
5	8436.	0.0362
6	9492.	0.0452
7	10547.	0.0551
8	11601.	0.0663
9	12656.	0.0786
10	13500.	0.0963
11	14554.	0.1140
12	15609.	0.1323
13	16664.	0.1586
14	17719.	0.1933
15	18773.	0.2310
16	19828.	0.2853
17	20883.	0.3585
18	21937.	0.4650
19	22979.	0.6020

C2NR45-04

Point	Hours	Length
1	5273.	0.0145
2	6328.	0.0191
3	7383.	0.0256
4	8436.	0.0314
5	9492.	0.0383
6	10547.	0.0492
7	11601.	0.0672
8	12656.	0.0985
9	14554.	0.1312
10	15609.	0.1534
11	16664.	0.1817
12	17719.	0.2158
13	18773.	0.2540
14	19828.	0.3036
15	20883.	0.3866
16	21937.	0.4869
17	22979.	0.6290

C2NR45-05

Point	Hours	Length
1	3164.	0.0040
2	4218.	0.0071
3	5273.	0.0114
4	6328.	0.0159
5	7383.	0.0235
6	8436.	0.0306
7	9492.	0.0374
8	10547.	0.0453
9	11601.	0.0549
10	12656.	0.0652
11	13500.	0.0784
12	14554.	0.0950
13	15609.	0.1184
14	16664.	0.1410
15	17719.	0.1643
16	18773.	0.1942
17	19828.	0.2333
18	20883.	0.2796
19	21937.	0.3433
20	22992.	0.4350
21	24047.	0.5920
22	25089.	0.8400

C2NR45-07

Point	Hours	Length
1	5273.	0.0064
2	6328.	0.0108
3	7383.	0.0156
4	8436.	0.0211
5	9493.	0.0272
6	10547.	0.0377
7	11601.	0.0476
8	12656.	0.0584
9	13500.	0.0705
10	14554.	0.0840
11	15609.	0.1015
12	16664.	0.1192
13	17719.	0.1429
14	18773.	0.1635
15	19828.	0.1882
16	20883.	0.2227
17	21937.	0.2661
18	22992.	0.3174
19	24047.	0.3809
20	25101.	0.4812
21	26144.	0.6620

C2NR45-06

Point	Hours	Length
1	15609.	0.1481
2	16664.	0.1650
3	17718.	0.1802
4	18773.	0.1885
5	19828.	0,2071
6	20882.	0,2308
7	21937.	0,2725
8	22992.	0.3034
9	24046.	0.3673
10	25101.	0.4609
11	25256.	0.5586

C2NR45-08

Point	Hours	Length
1	15610.	0.0143
2	16664.	0.0219
3	17719.	0.0312
4	18774.	0.0481
5	19828.	0.0692
6	20883.	0.0896
7	21938.	0.1199
8	22992.	0.1579
9	24047.	0.1976
10	25102.	0.2388
11	26156.	0.2965
12	27000.	0.3740
13	28055.	0.4782
14	29095.	0.6011

C2NR45-09

Point	Hours	Length
1	11602.	0.0209
2	12656.	0.0316
3	13500.	0.0468
4	14554.	0.0619
5	15609.	0.0740
6	16664.	0.0920
7	17718.	0.1077
8	18773.	0.1158
9	19828.	0.1416
10	20882.	0.1679
11	21937.	0.1941
12	22992.	0.2100
13	24046.	0.2372
14	25101.	0.2736
15	26156.	0.3207
16	27000.	0.4377
17	28055.	0.7900
18	29095.	0.8179

C2NR45-11

Point	Hours	Length
1	21937.	0.0817
2	22992.	0.0967
3	24047.	0.1117
4	25101.	0.1274
5	26156.	0.1406
6	28054.	0.1771
7	29109.	0.2027
8	30164.	0.2286
9	31218.	0.2581
10	32273.	0.2903
11	33328.	0.3323
12	34382.	0.3876
13	35437.	0.4581
14	36492.	0.5774
15	37534.	0.7322

C2NR45-10

Point	Hours	Length
1	19828.	0.0143
2	20883.	0.0197
3	21938.	0.0284
4	22992.	0.0475
5	24047.	0.0647
6	25102.	0.0776
7	26156.	0.0912
8	27000.	0.1203
9	28035.	0.1620
10	29110.	0.2045
11	30164.	0.2689
12	31219.	0.3429
13	32260.	0.6272

MATERIAL	SPECTRUM	STRESS
7091-EXTRUSION	HUD34	40

R1HD40-01

Point	Hours	Length
1	1000.	0.0218
2	1500.	0.0379
3	2000.	0.0743
4	2500.	0.1055
5	3000.	0.1417
6	3500.	0.1734
7	4000.	0.2107
8	4500.	0.2472
9	5000.	0.2872
10	5500.	0.3263
11	6000.	0.3590
12	6500.	0.4183
13	7000.	0.5070
14	7500.	0.5974
15	8000.	0.6719
16	8500.	0.8546

R1HD40-03

Point	Hours	Length
1	500.	0.0202
2	1000.	0.0371
3	1500.	0.[illegible]702
4	2000.	0.1003
5	2500.	0.1225
6	3000.	0.1408
7	3500.	0.1664
8	4000.	0.1854
9	4500.	0.2063
10	5000.	0.2251
11	5500.	0.2497
12	6000.	0.2794
13	6500.	0.3097
14	7000.	0.3484
15	7500.	0.4231
16	8000.	0.4971
17	8500.	0.5729
18	9000.	0.6234
19	9500.	0.7022
20	10000.	0.7826
21	10500.	0.[illegible]98

R1HD40-02

Point	Hours	Length
1	1000.	0.0081
2	1500.	0.0214
3	2000.	0.0366
4	2500.	0.0492
5	3000.	0.0646
6	3500.	0.0953
7	4000.	0.1137
8	4500.	0.1321
9	5000.	0.1501
10	5500.	0.1665
11	6000.	0.1911
12	6500.	0.212[illegible]
13	7000.	0.2373
14	7500.	0.2900
15	8000.	0.3730
16	8500.	0.4429
17	9000.	0.5009
18	9500.	0.7679

R1HD40-04

Point	Hours	Length
1	1000.	0.0149
2	1500.	0.0307
3	2000.	0.0561
4	2500.	0.0775
5	3000.	0.1040
6	3500.	0.1286
7	4000.	0.1567
8	4500.	0.1885
9	5000.	0.2236
10	5500.	0.2663
11	6000.	0.3124
12	6500.	0.3635
13	7000.	0.4170
14	7500.	0.46[illegible]
15	8000.	0.5269
16	8500.	0.5836
17	9000.	0.6414
18	9500.	0.6982
19	10000.	0.7363
20	10500.	0.7732
21	11000.	0.8159

R1HD40-05

Point	Hours	Length
1	1000.	0.0146
2	1500.	0.0240
3	2000.	0.0315
4	2500.	0.0371
5	3000.	0.0440
6	3500.	0.0524
7	4000.	0.0610
8	4500.	0.0704
9	5000.	0.0785
10	5500.	0.0868
11	6000.	0.0954
12	6500.	0.1040
13	7000.	0.1119
14	7500.	0.1212
15	8000.	0.1377
16	8500.	0.1473
17	9000.	0.1581
18	9500.	0.1709
19	10000.	0.1864
20	10500.	0.2025
21	11000.	0.2173
22	11500.	0.2280
23	12000.	0.2560
24	12500.	0.2879
25	13000.	0.3070
26	13500.	0.3247
27	14000.	0.4553
28	14500.	0.5461
29	15000.	0.6552
30	15500.	0.7679
31	15954.	0.8218

R1HD40-06

Point	Hours	Length
1	2500.	0.0480
2	3000.	0.0601
3	3500.	0.0766
4	4000.	0.0[illegible]58
5	4500.	0.1113
6	5000.	0.1217
7	5500.	0.1339
8	6000.	0.1498
9	6500.	0.1624
10	7000.	0.1765
11	7500.	0.1915
12	8000.	0.2053
13	8500.	0.2180
14	9000.	0.2350
15	9500.	0.2534
16	10000.	0.2678
17	10500.	0.2844
18	11000.	0.3031
19	11500.	0.3242
20	12000.	0.3503
21	12500.	0.3737
22	13000.	0.4019
23	13500.	0.4327
24	14000.	0.4664
25	14500.	0.5057
26	15000.	0.5575
27	15500.	0.6002
28	16000.	0.6453
29	16500.	0.6900
30	17000.	0.7240
31	17500.	0.7600
32	18000.	0.7995
33	18500.	0.8780

R1HD40-07

Point	Hours	Length
1	7000.	0.0090
2	7500.	0.0140
3	8000.	0.0232
4	8500.	0.0338
5	9000.	0.0446
6	9500.	0.0549
7	10000.	0.0640
8	10500.	0.0718
9	11000.	0.0787
10	11500.	0.0870
11	12000.	0.0955
12	12500.	0.1034
13	13000.	0.1113
14	13500.	0.1198
15	14000.	0.1286
16	14500.	0.1361
17	15000.	0.1440
18	15500.	0.1517
19	16000.	0.1593
20	16500.	0.1664
21	17000.	0.1750
22	17500.	0.1831
23	18000.	0.1886
24	18500.	0.1935

R1HD40-08

Point	Hours	Length
1	1500.	0.0223
2	2000.	0.0403
3	2500.	0.0708
4	3000.	0.0939
5	3500.	0.1140
6	4000.	0.1315
7	4500.	0.1482
8	5000.	0.1632
9	5500.	0.1781
10	6000.	0.1931
11	6500.	0.2098
12	7000.	0.2247
13	7500.	0.2390
14	8000.	0.2566
15	8500.	0.2726
16	9000.	0.2910
17	9500.	0.3080
18	10000.	0.3283
19	10500.	0.3487
20	11000.	0.3730
21	11500.	0.4009
22	12000.	0.4261
23	12500.	0.4533
24	13000.	0.4800
25	13500.	0.5134
26	14000.	0.5449
27	14500.	0.5626
28	15000.	0.5928
29	15500.	0.6413
30	16000.	0.6846
31	16500.	0.7292
32	17000.	0.7745
33	17500.	0.8225
34	18000.	0.9119
35	18500.	0.9477
36	19000.	0.9889

R1HD40-09

)

Point	Hours	Length
1	500.	0.0119
2	1000.	0.0242
3	1500.	0.0363
4	2000.	0.0469
5	2500.	0.0576
6	3000.	0.0670
7	3500.	0.0779
8	4000.	0.0894
9	4500.	0.1016
10	5000.	0.1139
11	5500.	0.1227
12	6000.	0.1328
13	6500.	0.1419
14	7000.	0.1506
15	7500.	0.1621
16	8000.	0.1723
17	8500.	0.1845
18	9000.	0.1984
19	9500.	0.2133
20	10000.	0.2287
21	10500.	0.2448
22	11000.	0.2657
23	11500.	0.2866
24	12000.	0.3077
25	12500.	0.3283
26	13000.	0.3539
27	13500.	0.3768
28	14000.	0.4063
29	14500.	0.4367
30	15000.	0.4727
31	15500.	0.5126
32	16000.	0.5507
33	16500.	0.5818
34	17000.	0.6108
35	17500.	0.6341
36	18000.	0.6591
37	18500.	0.6897
38	19000.	0.7184
39	19500.	0.7417
40	20000.	0.7651
41	20500.	0.7930

R1HD40-10

Point	Hours	Length
1	5000.	0.0101
2	5500.	0.0160
3	6000.	0.0223
4	6500.	0.0288
5	7000.	0.0357
6	7500.	0.0424
7	8000.	0.0493
8	8500.	0.0558
9	9000.	0.0620
10	9500.	0.0679
11	10000.	0.0734
12	10500.	0.0794
13	11000.	0.0852
14	11500.	0.0906
15	12000.	0.0961
16	12500.	0.1012
17	13000.	0.1065
18	13500.	0.1117
19	14000.	0.1179
20	14500.	0.1234
21	15000.	0.1291
22	15500.	0.1346
23	16000.	0.1400
24	16500.	0.1453
25	17000.	0.1508
26	17500.	0.1561
27	18000.	0.1611
28	18500.	0.1657
29	19000.	0.1706
30	19500.	0.1755
31	20000.	0.1803
32	20500.	0.1855
33	21000.	0.1908
34	21500.	0.1960
35	22000.	0.2015
36	22500.	0.2067
37	23000.	0.2117
38	23500.	0.2166
39	24000.	0.2242

R1HD40-11

Point	Hours	Length
1	6000.	0.0080
2	6500.	0.0154
3	7000.	0.0239
4	7500.	0.0336
5	8000.	0.0409
6	8500.	0.0486
7	9000.	0.0576
8	9500.	0.0725
9	10000.	0.0840
10	10500.	0.0937
11	11000.	0.1030
12	11500.	0.1117
13	12000.	0.1218
14	12500.	0.1308
15	13000.	0.1411
16	13500.	0.1515
17	14000.	0.1608
18	14500.	0.1706
19	15000.	0.1815
20	15500.	0.1920
21	16000.	0.2029
22	16500.	0.2142
23	17000.	0.2243
24	17500.	0.2362
25	18000.	0.2472
26	18500.	0.2583
27	19000.	0.2688
28	19500.	0.2793
29	20000.	0.2907
30	20500.	0.3027
31	21000.	0.3162
32	21500.	0.3281
33	22000.	0.3412
34	22500.	0.3550
35	23000.	0.3709
36	23500.	0.3860
37	24000.	0.4031

R1HD40-12

Point	Hours	Length
1	11500.	0.1170
2	12000.	0.1257
3	12500.	0.1343
4	13000.	0.1440
5	13500.	0.1533
6	14000.	0.1617
7	14500.	0.1725
8	15000.	0.1840
9	15500.	0.1960
10	16000.	0.2106
11	16500.	0.2258
12	17000.	0.2417
13	17500.	0.2617
14	18000.	0.2826
15	18500.	0.3042
16	19000.	0.3260
17	19500.	0.3517
18	20000.	0.3798
19	20500.	0.4083
20	21000.	0.4352
21	21500.	0.4666
22	22000.	0.4982
23	22500.	0.5366
24	23000.	0.5739
25	23500.	0.6121
26	24000.	0.6452

R1HD40-13

Point	Hours	Length
1	8500.	0.1600
2	9000.	0.1682
3	9500.	0.1755
4	10000.	0.1828
5	10500.	0.1893
6	11000.	0.1968
7	11500.	0.2080
8	12000.	0.2165
9	12500.	0.2265
10	13000.	0.2367
11	13500.	0.2468
12	14000.	0.2564
13	14500.	0.2693
14	15000.	0.2796
15	15500.	0.2911
16	16000.	0.3018
17	16500.	0.3133
18	17000.	0.3244
19	17500.	0.3364
20	18000.	0.3491
21	18500.	0.3613
22	19000.	0.3735
23	19500.	0.3863
24	20000.	0.3988
25	20500.	0.4124
26	21000.	0.4263
27	21500.	0.4407
28	22000.	0.4592
29	22500.	0.4767
30	23000.	0.4968
31	23500.	0.5168
32	24000.	0.5372

R1HD40-14

Point	Hours	Length
1	6000.	0.0433
2	6500.	0.0473
3	7000.	0.0497
4	7500.	0.0524
5	8000.	0.0557
6	8500.	0.0592
7	9000.	0.0632
8	9500.	0.0693
9	10000.	0.0752
10	10500.	0.0862
11	11000.	0.0921
12	11500.	0.0980
13	12000.	0.1056
14	12500.	0.1131
15	13000.	0.1213
16	13500.	0.1309
17	14000.	0.1418
18	14500.	0.1533
19	15000.	0.1659
20	15500.	0.1795
21	16000.	0.1959
22	16500.	0.2147
23	17000.	0.2315
24	17500.	0.2502
25	18000.	0.2718
26	18500.	0.2931
27	19000.	0.3176
28	19500.	0.3417
29	20000.	0.3693
30	20500.	0.3973
31	21000.	0.4281
32	21500.	0.4646
33	22000.	0.5020
34	22500.	0.5429
35	23000.	0.5831
36	23500.	0.6275
37	24000.	0.6628

7091-T7E69 EXT.

HUD 34 SPECTRUM

45 KSI MAXIMUM STRESS

R1HD45-01

Point	Hours	Length
1	500.	0.0498
2	1000.	0.1361
3	1500.	0.3453
4	2000.	0.8851

R1HD45-03

Point	Hours	Length
1	1000.	0.0130
2	1500.	0.0246
3	2000.	0.0418
4	2500.	0.0793
5	3000.	0.1300
6	3500.	0.2606
7	4000.	0.3968
8	4500.	0.6693

R1HD45-04

Point	Hours	Length
1	500.	0.0158
2	1000.	0.0351
3	1500.	0.0843
4	2000.	0.1468
5	2500.	0.2176
6	3000.	0.2660
7	3500.	0.3466
8	4000.	0.4751
9	4500.	0.6657

R1HD45-06

Point	Hours	Length
1	2000.	0.0189
2	2500.	0.0433
3	3000.	0.0655
4	3500.	0.0944
5	4000.	0.1387
6	4500.	0.1918
7	5000.	0.2948
8	5500.	0.4015
9	6000.	0.8454

R1HD45-07

Point	Hours	Length
1	1000.	0.0244
2	1500.	0.0412
3	2000.	0.0582
4	2500.	0.0970
5	3000.	0.1283
6	3500.	0.1742
7	4000.	0.2190
8	4500.	0.2780
9	5000.	0.3448
10	5500.	0.4280
11	6000.	0.5486
12	6500.	0.6695
13	7000.	0.7640
14	7373.	0.9300

R1HD45-08

Point	Hours	Length
1	500.	0.0093
2	1000.	0.0202
3	1500.	0.0457
4	2000.	0.0717
5	2500.	0.0980
6	3000.	0.1280
7	3500.	0.1635
8	4000.	0.1999
9	4500.	0.2414
10	5000.	0.3011
11	5500.	0.3744
12	6000.	0.4680
13	6500.	0.5421
14	7000.	0.6388
15	7500.	0.7717

R1HD45-09

Point	Hours	Length
1	500.	0.0065
2	1000.	0.0157
3	1500.	0.0393
4	2000.	0.0589
5	2500.	0.0863
6	3000.	0.1269
7	3500.	0.1963
8	4000.	0.2625
9	4500.	0.3000
10	5000.	0.3629
11	5500.	0.4578
12	6000.	0.5197
13	6500.	0.6327
14	7000.	0.7139
15	7500.	0.7867

R1HD45-10

Point	Hours	Length
1	1000.	0.0056
2	1500.	0.0159
3	2000.	0.0286
4	2500.	0.0565
5	3000.	0.0758
6	3500.	0.1109
7	4000.	0.1239
8	4500.	0.1564
9	5000.	0.1903
10	5500.	0.2494
11	6000.	0.2954
12	6500.	0.3484
13	7000.	0.4284
14	7500.	0.5586
15	8000.	0.6906
16	8500.	0.7844

R1HD45-11

Point	Hours	Length
1	1500.	0.0213
2	2000.	0.0489
3	2500.	0.0793
4	3000.	0.1101
5	3500.	0.1373
6	4000.	0.1661
7	4500.	0.1979
8	5000.	0.2313
9	5500.	0.2762
10	6000.	0.3194
11	6500.	0.3763
12	7000.	0.4527
13	7500.	0.5625
14	8000.	0.6624
15	8500.	0.7276
16	9000.	0.7977

R1HD45-12

Point	Hours	Length
1	1000.	0.0307
2	1500.	0.0640
3	2000.	0.0961
4	2500.	0.1277
5	3000.	0.1567
6	3500.	0.1827
7	4000.	0.2114
8	4500.	0.2427
9	5000.	0.2827
10	5500.	0.3222
11	6000.	0.3760
12	6500.	0.4374
13	7000.	0.4995
14	7500.	0.5771
15	8000.	0.6672
16	8500.	0.7225
17	9000.	0.7759

R1HD45-14

Point	Hours	Length
1	1000.	0.0162
2	1500.	0.0446
3	2000.	0.0654
4	2500.	0.0908
5	3000.	0.1121
6	3500.	0.1356
7	4000.	0.1553
8	4500.	0.1766
9	5000.	0.1936
10	5500.	0.2230
11	6000.	0.2494
12	6500.	0.2767
13	7000.	0.3077
14	7500.	0.3371
15	8000.	0.3743
16	8500.	0.4203
17	9000.	0.4545
18	9500.	0.5027
19	10000.	0.5532
20	10500.	0.6097
21	11000.	0.6541

R1HD45-15

Point	Hours	Length
1	1000.	0.0124
2	1500.	0.0246
3	2000.	0.0451
4	2500.	0.0711
5	3000.	0.0887
6	3500.	0.1069
7	4000.	0.1225
8	4500.	0.1438
9	5000.	0.1672
10	5500.	0.1918
11	6000.	0.2146
12	6500.	0.2333
13	7000.	0.2673
14	7500.	0.2975
15	8000.	0.3314
16	8500.	0.3750
17	9000.	0.4170
18	9500.	0.4667
19	10000.	0.5264
20	10500.	0.5629
21	11000.	0.6062
22	11500.	0.6396
23	12000.	0.6912
24	12500.	0.7414
25	13000.	0.7963
26	13260.	0.8722

7091-T7E69 EXT.

NOR 1 SPECTRUM

45 KSI MAXIMUM STRESS

R1NR45-01

Point	Hours	Length
1	2109.	0.0092
2	3164.	0.0195
3	4218.	0.0375
4	5273.	0.0650
5	6328.	0.1060
6	7383.	0.1451
7	8436.	0.2119
8	9492.	0.2709
9	10547.	0.3793
10	11601.	0.5860
11	12647.	0.6921

R1NR45-04

Point	Hours	Length
1	5273.	0.0164
2	6328.	0.0276
3	7383.	0.0427
4	8436.	0.0604
5	9492.	0.0862
6	10547.	0.1176
7	11601.	0.1487
8	12656.	0.1760
9	13500.	0.2160
10	14554.	0.2600
11	15609.	0.3050
12	16664.	0.3600
13	17719.	0.4700
14	18773.	0.5800
15	19815.	0.7100

R1NR45-02

Point	Hours	Length
1	5273.	0.0070
2	6328.	0.0176
3	7383.	0.0335
4	8436.	0.0817
5	9492.	0.1353
6	10547.	0.2134
7	11601.	0.3366
8	12656.	0.4734
9	14540.	0.7309

R1NR45-05

Point	Hours	Length
1	12656.	0.0113
2	13500.	0.0145
3	14554.	0.0189
4	15609.	0.0248
5	16664.	0.0320
6	17719.	0.0408
7	18773.	0.0535
8	19828.	0.0723
9	20883.	0.1107
10	21937.	0.1900
11	22992.	0.2700
12	24047.	0.3800
13	25101.	0.4900
14	26156.	0.5700
15	27000.	0.6600
16	28054.	0.7600

R1NR45-03

Point	Hours	Length
1	2110.	0.0062
2	3164.	0.0043
3	4219.	0.0115
4	5274.	0.0275
5	6328.	0.0335
6	7383.	0.0653
7	8438.	0.1233
8	9492.	0.1729
9	10547.	0.2246
10	11603.	0.2981
11	12656.	0.3773
12	13500.	0.3752
13	14555.	0.5456
14	15595.	0.7287

R1NR45-06

Point	Hours	Length
1	9492.	0.0180
2	10547.	0.0260
3	11601.	0.0350
4	12656.	0.0480
5	13500.	0.0600
6	14554.	0.0730
7	15609.	0.0990
8	16664.	0.1280
9	17719.	0.1524
10	18773.	0.1772
11	19828.	0.2042
12	20883.	0.2334
13	21937.	0.2732
14	22992.	0.3147
15	24047.	0.3736
16	25101.	0.4500
17	26156.	0.5500
18	27000.	0.6500
19	28054.	0.7500
20	29095.	0.8800

R1NR45-07

Point	Hours	Length
1	7383.	0.0089
2	8436.	0.0121
3	9492.	0.0160
4	10547.	0.0216
5	11601.	0.0291
6	12656.	0.0381
7	13500.	0.0498
8	14554.	0.0615
9	15609.	0.0811
10	16664.	0.1063
11	17719.	0.1342
12	18773.	0.1631
13	19828.	0.1921
14	20883.	0.2227
15	21937.	0.2576
16	22992.	0.2995
17	24047.	0.3381
18	25101.	0.3900
19	26156.	0.4920
20	27000.	0.5510
21	28054.	0.6100
22	29109.	0.6900
23	30153.	0.7600

R1NR45-08

Point	Hours	Length
1	6328.	0.0125
2	7383.	0.0177
3	8436.	0.0227
4	9492.	0.0292
5	10547.	0.0351
6	11601.	0.0418
7	12656.	0.0481
8	13500.	0.0549
9	14554.	0.0617
10	15609.	0.0718
11	16664.	0.0807
12	17719.	0.0904
13	18773.	0.1009
14	19828.	0.1113
15	20883.	0.1211
16	21937.	0.1310
17	22992.	0.1405
18	24047.	0.1507
19	25101.	0.1610
20	26156.	0.1725
21	27000.	0.1862
22	28054.	0.1999
23	29109.	0.2198
24	30164.	0.2444
25	31218.	0.2708
26	32273.	0.2983
27	33328.	0.3284
28	34382.	0.3840
29	35437.	0.4400
30	36492.	0.5050
31	37547.	0.5900
32	38589.	0.6600

R1NR45-09

Point	Hours	Length
1	18773.	0.0173
2	19828.	0.0207
3	20883.	0.0260
4	21937.	0.0319
5	22992.	0.0376
6	24047.	0.0415
7	25101.	0.0509
8	26156.	0.0612
9	28054.	0.0913
10	29109.	0.1180
11	30164.	0.1384
12	31218.	0.1657
13	32273.	0.1919
14	33328.	0.2214
15	34382.	0.2712
16	35437.	0.3305
17	36492.	0.4169
18	37547.	0.5083
19	38601.	0.5931
20	39656.	0.6752
21	40500.	0.7473

7091-T7E69
NOR I SPECTRUM
50 KSI MAXIMUM STRESS

R1NR50-01

Point	Hours	Length
1	4218.	0.0347
2	5273.	0.0553
3	6328.	0.0781
4	7383.	0.1141
5	8436.	0.1788
6	9492.	0.2903
7	10547.	0.4526
8	11589.	.7390

R1NR50-02

Point	Hours	Length
1	2109.	0.0143
2	3164.	0.0351
3	4218.	0.0663
4	5273.	0.1079
5	6328.	0.1656
6	7383.	0.2284
7	8436.	0.3005
8	9492.	0.4049
9	10547.	0.5360
10	11589.	0.6827

R1NR50-03

Point	Hours	Length
1	3164.	0.0230
2	4218.	0.0521
3	5273.	0.0935
4	6328.	0.1387
5	7383.	0.1878
6	8436.	0.2751
7	9492.	0.4628
8	10547.	0.7523
9	11589.	0.8299

R1NR50-04

Point	Hours	Length
1	3164.	0.0196
2	4218.	0.0349
3	5273.	0.0515
4	6328.	0.0719
5	7383.	0.0957
6	8436.	0.1318
7	9492.	0.1643
8	10547.	0.2999
9	11601.	0.4604
10	12647.	0.6146

R1NR50-05

Point	Hours	Length
1	2109.	0.0046
2	3164.	0.0164
3	4218.	0.0296
4	5273.	0.0496
5	6328.	0.0747
6	7383.	0.1108
7	8436.	0.1527
8	9492.	0.2015
9	10547.	0.2545
10	11601.	0.3227
11	12656.	0.4244
12	14554.	0.6573
13	15490.	0.7844

R1NR50-06

Point	Hours	Length
1	3164.	0.0242
2	4218.	0.0406
3	5273.	0.0677
4	6328.	0.0978
5	7383.	0.1364
6	8436.	0.1810
7	9492.	0.2296
8	10547.	0.2907
9	11601.	0.3819
10	12656.	0.4775
11	14554.	0.6654
12	15595.	0.7328

R1NR50-07

Point	Hours	Length
1	4218.	0.0197
2	5273.	0.0392
3	6328.	0.0733
4	7383.	0.1070
5	8436.	0.1408
6	9492.	0.1769
7	10547.	0.2176
8	11601.	0.2617
9	12656.	0.3456
10	14554.	0.5527
11	15595.	0.6934

R1NR50-08

Point	Hours	Length
1	4218.	0.0174
2	5273.	0.0328
3	6328.	0.0489
4	7383.	0.0738
5	8436.	0.0933
6	9492.	0.1230
7	10547.	0.1526
8	11601.	0.2100
9	12656.	0.2754
10	14554.	0.4833
11	15609.	0.6460
12	16664.	0.7468

R1NR50-09

Point	Hours	Length
1	6328.	0.0088
2	7383.	0.0253
3	8436.	0.0483
4	9492.	0.0859
5	10547.	0.1226
6	11601.	0.1544
7	12656.	0.2081
8	14554.	0.3124
9	15609.	0.4287
10	16664.	0.5600
11	17705.	0.6187

R1NR50-10

Point	Hours	Length
1	9492.	0.0291
2	10547.	0.0397
3	11601.	0.0511
4	12656.	0.0647
5	14554.	0.1023
6	15609.	0.1381
7	16664.	0.1751
8	17719.	0.2531
9	18773.	0.3374
10	19828.	0.4598
11	20274.	0.7920

7091-FORGING
HUD 34 SPECTRUM
40 KSI MAXIMUM STRESS

R2HD40-01

Point	Hours	Length
1	1000.	0.0[illegible]45
2	1500.	0.0329
3	2000.	0.0501
4	2500.	0.0784
5	3000.	0.1128
6	3500.	0.1420
7	4000.	0.1640
8	4500.	0.1967
9	5000.	0.2324
10	5500.	0.2568
11	6000.	0.2911
12	6500.	0.3335
13	7000.	0.3943
14	7500.	0.4726
15	8000.	0.5744
16	8500.	0.8140

R2HD40-03

Point	Hours	Length
1	500.	0.0137
2	1000.	0.0270
3	1500.	0.0502
4	2000.	0.0775
5	2500.	0.[illegible]
6	3000.	0.1267
7	3500.	0.1540
8	4000.	0.1848
9	4500.	0.2191
10	5000.	0.2552
11	5500.	0.2999
12	6000.	0.3457
13	6500.	0.3779
14	7000.	0.4181
15	7500.	0.4831
16	8000.	0.5365
17	8500.	0.6237
18	9000.	0.6700
19	9500.	0.7448
20	10000.	0.8619

R2HD40-02

Point	Hours	Length
1	2000.	0.0442
2	2500.	0.0753
3	3000.	0.1056
4	3500.	0.1348
5	4000.	0.1663
6	4500.	0.2026
7	5000.	0.2390
8	5500.	0.2839
9	6000.	0.3293
10	6500.	0.3865
11	7000.	0.4433
12	7500.	0.5254
13	8000.	0.6071
14	8500.	0.7140
15	9000.	0.8177
16	9500.	0.9328

R2HD40-04

Point	Hours	Length
1	3000.	0.0239
2	3500.	0.0431
3	4000.	0.0604
4	4500.	0.0858
5	5000.	0.1165
6	5500.	0.1510
7	6000.	0.1973
8	6500.	0.2455
9	7000.	0.3020
10	7500.	0.3664
11	8000.	0.4443
12	8500.	0.5499
13	9000.	0.6579
14	9500.	0.7396
15	10000.	0.8246

R2HD40-05

Point	Hours	Length
1	1000.	0.0067
2	1500.	0.0128
3	2000.	0.0159
4	2500.	0.0260
5	3000.	0.0347
6	3500	0.0448
7	4000.	0.0553
8	4500.	0.0698
9	5000.	0.0856
10	5500.	0.1016
11	6000.	0.1164
12	6500.	0.1311
13	7000.	0.1448
14	7500.	0.1616
15	8000.	0.1812
16	8500.	0.2088
17	9000.	0.2435
18	9500.	0.2911
19	10000.	0.3393
20	10500.	0.4508
21	11000.	0.5552
22	11500.	0.6969

R2HD40-07

Point	Hours	Length
1	4000.	0.0051
2	4500.	0.0134
3	5000.	0.0252
4	5500.	0.0432
5	6000.	0.0617
6	6500.	0.0829
7	7000.	0.1[illegible]76
8	7500.	0.1322
9	8000.	0.1599
10	8500.	0.1918
11	9000.	0.2359
12	9500.	0.2831
13	10000.	0.3351
14	10500.	0.4090
15	11000.	0.5[illegible]74
16	11500.	0.6050
17	12000.	0.7950

R2HD40-06

Point	Hours	Length
1	1500.	0.0072
2	2000.	0.0236
3	2500.	0.0481
4	3000.	0.0721
5	3500.	0.0989
6	4000.	0.1246
7	4500.	0.1491
8	5000.	0.1769
9	5500.	0.2043
10	6000.	0.2352
11	6500.	0.2656
12	7000.	0.2973
13	7500.	0.3325
14	8000.	0.3678
15	8500.	0.4051
16	9000.	0.4370
17	9500.	0.4960
18	10000.	0.5538
19	10500.	0.6167
20	11000.	0.6932
21	11500.	0.7635
22	12000.	0.8208

R2HD40-08

Point	Hours	Length
1	8500.	0.0638
2	9000.	0.0840
3	9500.	0.1[illegible]03
4	10000.	0.1754
5	10500.	0.2232
6	11000.	0.2944
7	11500.	0.4172
8	12000.	0.5535
9	12500.	0.7369
10	13000.	0.8340
11	13500.	0.94[illegible]

R2HD40-09

Point	Hours	Length
1	3000.	0.0095
2	3500.	0.0185
3	4000.	0.0296
4	4500.	0.0378
5	5000.	0.0495
6	5500.	0.0623
7	6000.	0.0751
8	6500.	0.0889
9	7000.	0.1021
10	7500.	0.1153
11	8000.	0.1289
12	8500.	0.1435
13	9000.	0.1577
14	9500.	0.1731
15	10000.	0.1948
16	10500.	0.2143
17	11000.	0.2333
18	11500.	0.2517
19	12000.	0.2747
20	12500.	0.2942
21	13000.	0.3227
22	13500.	0.3466
23	14000.	0.3577
24	14500.	0.3915
25	15000.	0.4313
26	15500.	0.4621
27	16000.	0.5085
28	16500.	0.5328
29	17000.	0.5458
30	17500.	0.5632
31	18000.	0.5801

7091-FORGING
HUD 34 SPECTRUM
45 KSI MAXIMUM STRESS

R2HD45-01

Point	Hours	Length
1	500.	0.0509
2	1000.	0.1213
3	1500.	0.1931
4	2000.	0.2753
5	2500.	0.4093
6	3000.	0.5476
7	3500.	0.6718

R2HD45-02

Point	Hours	Length
1	500.	0.0203
2	1000.	0.0739
3	1500.	0.1668
4	2000.	0.2527
5	2500.	0.3530
6	3000.	0.4275
7	3500.	0.4909
8	4000.	0.5819
9	4500.	0.8602

R2HD45-03

Point	Hours	Length
1	500.	0.0223
2	1000.	0.0480
3	1500.	0.0703
4	2000.	0.0983
5	2500.	0.1343
6	3000.	0.2050
7	3500.	0.2965
8	4000.	0.5205
9	4500.	0.7326

R2HD45-04

Point	Hours	Length
1	500.	0.0147
2	1000.	0.0230
3	1500.	0.0398
4	2000.	0.0725
5	2500.	0.1077
6	3000.	0.1581
7	3500.	0.2275
8	4000.	0.2982
9	4500.	0.3937
10	5000.	0.[illegible]136

R2HD45-05

Point	Hours	Length
1	500.	0.0162
2	1000.	0.0414
3	1500.	0.0734
4	2000.	0.1113
5	2500.	0.1570
6	3000.	0.1966
7	3500.	0.2447
8	4000.	0.3005
9	4500.	0.4382
10	5000.	0.8223

R2HD45-06

Point	Hours	Length
1	500.	0.0063
2	1000.	0.0190
3	1500.	0.0520
4	2000.	0.0855
5	2500.	0.1141
6	3000.	0.1613
7	3500.	0.2489
8	4000.	0.3117
9	4500.	0.4215
10	5000.	0.5353
11	5411.	1.0000

R2HD45-07

Point	Hours	Length
1	500.	0.0146
2	1000.	0.0371
3	1500.	0.0674
4	2000.	0.1019
5	2500.	0.1350
6	3000.	0.1628
7	3500.	0.2055
8	4000.	0.2368
9	4500.	0.2900
10	5000.	0.3518
11	5500.	0.3889
12	6000.	0.4634
13	6500.	0.6065
14	7000.	0.7214

R2HD45-08

Point	Hours	Length
1	1500.	0.0198
2	2000.	0.0425
3	2500.	0.0618
4	3000.	0.0820
5	3500.	0.1129
6	4000.	0.1438
7	4500.	0.1816
8	5000.	0.2168
9	5500.	0.2732
10	6000.	0.3652
11	6500.	0.4842
12	7000.	0.6678
13	7488.	0.7994

R2HD45-09

Point	Hours	Length
1	2500.	0.0166
2	3000.	0.0448
3	3500.	0.0609
4	4000.	0.0923
5	4500.	0.1389
6	5000.	0.1794
7	5500.	0.2321
8	6000.	0.2916
9	6500.	0.4378
10	7000.	0.6479
11	7500.	0.7980

CW67-T7E91

HUD 34 SPECTRUM

40 KSI MAXIMUM STRESS

R3HD40-1

Point	Hours	Length
1	2000.	0.0111
2	2500.	0.0194
3	3000.	0.0289
4	3500.	0.0454
5	4000.	0.0667
6	4500.	0.0849
7	5000.	0.1042
8	5500.	0.1204
9	6000.	0.1332
10	6500.	0.1442
11	7000.	0.1547
12	7500.	0.1638
13	8000.	0.1726
14	8500.	0.1866
15	9000.	0.2015
16	9500.	0.2170
17	10000.	0.2363
18	10500.	0.2560
19	11000.	0.2755
20	11500.	0.3011
21	12000.	0.3271
22	12500.	0.3834
23	13000.	0.4247
24	13500.	0.4705
25	14000.	0.5183
26	14500.	0.5842
27	15000.	0.6157
28	15500.	0.6469
29	16000.	0.7161
30	16500.	0.7529
31	17000.	0.7834
32	17500.	0.8043
33	18000.	0.8232
34	18013.	0.9163

R3HD40-2

Point	Hours	Length
1	3000.	0.0262
2	3500.	0.0422
3	4000.	0.0630
4	4500.	0.0870
5	5000.	0.1084
6	5500.	0.1287
7	6000.	0.1500
8	6500.	0.1723
9	7000.	0.1943
10	7500.	0.2201
11	8000.	0.2508
12	8500.	0.2828
13	9000.	0.3136
14	9500.	0.3571
15	10000.	0.4008
16	10500.	0.4496
17	11000.	0.4977
18	11500.	0.5516
19	12000.	0.6048
20	12500.	0.6624
21	13000.	0.7185
22	13500.	0.7658
23	14000.	0.8044
24	14010.	0.9220

R3HD40-3

Point	Hours	Length
1	2000.	0.0261
2	2500.	0.0416
3	3000.	0.0623
4	3500.	0.0973
5	4000.	0.1423
6	4500.	0.1964
7	5000.	0.2525
8	5500.	0.3136
9	6000.	0.3748
10	6500.	0.4421
11	7000.	0.5371
12	7500.	0.5958
13	8000.	0.6739
14	8500.	0.7560
15	9000.	0.8129
16	9006.	0.9380

R3HD40-5

Point	Hours	Length
1	1500.	0.0253
2	2000.	0.0447
3	2500.	0.0707
4	3000.	0.0954
5	3500.	0.1183
6	4000.	0.1451
7	4500.	0.1694
8	5000.	0.1974
9	5500.	0.2292
10	6000.	0.2657
11	6500.	0.3017
12	7000.	0.3456
13	7500.	0.3906
14	8000.	0.4498
15	8500.	0.5115
16	9000.	0.5603
17	9500.	0.6271
18	10000.	0.6947
19	10500.	0.7640
20	11000.	0.8322
21	11500.	0.8789
22	11506.	0.9317

R3HD40-4

Point	Hours	Length
1	1000.	0.0181
2	1500.	0.0329
3	2000.	0.0472
4	2500.	0.0860
5	3000.	0.1133
6	3500.	0.1434
7	4000.	0.1733
8	4500.	0.2022
9	5000.	0.2380
10	5500.	0.2701
11	6000.	0.3064
12	6500.	0.3435
13	7000.	0.3812
14	7500.	0.4487
15	8000.	0.5208
16	8500.	0.5826
17	9000.	0.6437
18	9500.	0.6954
19	10000.	0.7347
20	10500.	0.7662
21	11000.	0.7992
22	11500.	0.8281
23	12000.	0.8905
24	12008.	0.9263

R3HD40-6

Point	Hours	Length
1	2000.	0.0157
2	2500.	0.0288
3	3000.	0.0429
4	3500.	0.0647
5	4000.	0.0923
6	4500.	0.1166
7	5000.	0.1463
8	5500.	0.1764
9	6000.	0.2064
10	6500.	0.2421
11	7000.	0.2759
12	7500.	0.3178
13	8000.	0.3614
14	8500.	0.4040
15	9000.	0.4519
16	9500.	0.5001
17	10000.	0.5531
18	10500.	0.6054
19	11000.	0.6590
20	11500.	0.7100
21	12000.	0.7537
22	12500.	0.7927
23	13000.	0.8276
24	13500.	0.8688
25	13509.	0.8890

R3HD40-7

Point	Hours	Length
1	1000.	0.0391
2	1500.	0.0688
3	2000.	0.1121
4	2500.	0.1551
5	3000.	0.1948
6	3500.	0.2344
7	4000.	0.2724
8	4500.	0.3187
9	5000.	0.3625
10	5500.	0.4235
11	6000.	0.5108
12	6500.	0.5737
13	7000.	0.6543
14	7500.	0.7149
15	8000.	0.8048
16	8500.	0.8467
17	9000.	0.8961
18	9006.	0.9314

R3HD40-9

Point	Hours	Length
1	14000.	0.0393
2	14500.	0.0539
3	15000.	0.0679
4	15500.	0.0800
5	16000.	0.0932
6	16500.	0.1085
7	17000.	0.1159
8	17500.	0.1242
9	18000.	0.1329
10	18500.	0.1488
11	19000.	0.1654
12	19500.	0.1806
13	20000.	0.2017

R3HD40-8

Point	Hours	Length
1	2000.	0.0352
2	2500.	0.0820
3	3000.	0.1322
4	3500.	0.1697
5	4000.	0.2147
6	4500.	0.2543
7	5000.	0.2930
8	5500.	0.3392
9	6000.	0.3889
10	6500.	0.4417
11	7000.	0.5002
12	7500.	0.5510
13	8000.	0.6205
14	8500.	0.6694
15	9000.	0.7126
16	9500.	0.7574
17	10000.	0.7841
18	10500.	0.8051
19	11000.	0.8223
20	11500.	0.8434
21	11508.	0.9043

R 3HD40-10

Point	Hours	Length
1	3000.	0.0124
2	3500.	0.0191
3	4000.	0.0269
4	4500.	0.0388
5	5000.	0.0502
6	5500.	0.0605
7	6000.	0.0716
8	6500.	0.0816
9	7000.	0.0919
10	7500.	0.1025
11	8000.	0.1134
12	8500.	0.1234
13	9000.	0.1338
14	9500.	0.1439
15	10000.	0.1564
16	10500.	0.1671
17	11000.	0.1792
18	11500.	0.1909
19	12000.	0.2070
20	12500.	0.2194
21	13000.	0.2346
22	13500.	0.2491
23	14000.	0.2644
24	14500.	0.2807
25	15000.	0.2954
26	15500.	0.3152
27	16000.	0.3358
28	16500.	0.3565
29	17000.	0.3792
30	17500.	0.4025
31	18000.	0.4284
32	18500.	0.4540
33	19000.	0.4853
34	19500.	0.5064
35	20000.	0.5340
36	20500.	0.5733
37	21000.	0.6001
38	21500.	0.6360
39	22000.	0.6685
40	22500.	0.6981
41	23000.	0.7339
42	23500.	0.7690
43	24000.	0.8055
44	24500.	0.8446
45	25000.	0.9039
46	25018.	0.9210

CW67-T7E91
HUD 34 SPECTRUM
45 KSI MAXIMUM STRESS

R3HD45-1

Point	Hours	Length
1	2000.	0.0474
2	2500.	0.0740
3	3000.	0.0941
4	3500.	0.1167
5	4000.	0.1399
6	4500.	0.1577
7	5000.	0.1806
8	5500.	0.2019
9	6000.	0.2249
10	6500.	0.2492
11	7000.	0.2596
12	7500.	0.2731
13	8000.	0.2863
14	8500.	0.3019
15	9000.	0.3211
16	9500.	0.3475
17	10000.	0.3716
18	10500.	0.3922
19	11000.	0.4180
20	11500.	0.4485
21	12000.	0.4826
22	12500.	0.5178
23	13000.	0.5563
24	13500.	0.5964
25	14000.	0.6402
26	14500.	0.6756
27	15000.	0.7182
28	15500.	0.7542
29	16000.	0.7737
30	16500.	0.7916
31	17000.	0.8113
32	17040.	0.9150

R3HD45-2

Point	Hours	Length
1	500.	0.0111
2	1000.	0.0455
3	1500.	0.0775
4	2000.	0.1231
5	2500.	0.1592
6	3000.	0.1956
7	3500.	0.2393
8	4000.	0.2858
9	4500.	0.3351
10	5000.	0.3873
11	5500.	0.4537
12	6000.	0.5100
13	6500.	0.5880
14	7000.	0.6480
15	7500.	0.7063
16	8000.	0.7745
17	8480.	0.9360

R3HD45-3

Point	Hours	Length
1	1500.	0.0408
2	2000.	0.0875
3	2500.	0.1376
4	3000.	0.1920
5	3500.	0.2606
6	4000.	0.3327
7	4500.	0.4060
8	5000.	0.4768
9	5500.	0.5597
10	6000.	0.6240
11	6500.	0.7070
12	7000.	0.8118
13	7040.	0.8834

R3HD45-4

Point	Hours	Length
1	1500.	0.0221
2	2000.	0.0442
3	2500.	0.0692
4	3000.	0.0947
5	3500.	0.1190
6	4000.	0.1450
7	4500.	0.1736
8	5000.	0.2047
9	5500.	0.2309
10	6000.	0.2600
11	6500.	0.2877
12	7000.	0.3153
13	7500.	0.3532
14	8000.	0.3943
15	8500.	0.4406
16	9000.	0.4803
17	9500.	0.5490
18	10000.	0.5878
19	10500.	0.6536
20	11000.	0.7196
21	11500.	0.7783
22	12000.	0.8380
23	12008.	0.92[illegible]0

R 3HD45-5

Point	Hours	Length
1	1500.	0.0196
2	2000.	0.0375
3	2500.	0.0660
4	3000.	0.1095
5	3500.	0.1540
6	4000.	0.2040
7	4500.	0.2630
8	5000.	0.3400
9	5500.	0.4260
10	6000.	0.5330
11	6500.	0.6060
12	7000.	0.6490
13	7500.	0.7190
14	8000.	0.8130
15	8494.	0.9170

R 3HD45-7

Point	Hours	Length
1	1000.	0.0314
2	1500.	0.0518
3	2000.	0.0981
4	2500.	0.1485
5	3000.	0.2049
6	3500.	0.2610
7	4000.	0.3140
8	4500.	0.3760
9	5000.	0.4710
10	5500.	0.5630
11	6000.	0.6460
12	6500.	0.7100
13	7000.	0.7720
14	7500.	0.8320
15	7520.	0.9400

R 3HD45-6

Point	Hours	Length
1	1000.	0.0205
2	1500.	0.0402
3	2000.	0.0574
4	2500.	0.0791
5	3000.	0.0995
6	3500.	0.1211
7	4000.	0.1397
8	4500.	0.1593
9	5000.	0.1821
10	5500.	0.2051
11	6000.	0.2324
12	6500.	0.2592
13	7000.	0.2863
14	7500.	0.3153
15	8000.	0.3440
16	8500.	0.3768
17	9000.	0.4105
18	9500.	0.4460
19	10000.	0.4746
20	10500.	0.5249
21	11000.	0.5841
22	11500.	0.6382
23	12000.	0.6857
24	12500.	0.7457
25	13000.	0.7881
26	13500.	0.8186
27	13998.	0.9087

R 3HD45-8

Point	Hours	Length
1	1500.	0.0290
2	2000.	0.0614
3	2500.	0.0944
4	3000.	0.1249
5	3500.	0.1563
6	4000.	0.1864
7	4500.	0.2191
8	5000.	0.2528
9	5500.	0.2908
10	6000.	0.3308
11	6500.	0.3650
12	7000.	0.4006
13	7500.	0.4780
14	8000.	0.5400
15	8500.	0.6120
16	9000.	0.6870
17	9500.	0.7640
18	10000.	0.8390
19	10007.	0.9110

CW67-T7E91

NOR 1 SPECTRUM

45 KSI MAXIMUM STRESS

R3NR45-1

Point	Hours	Length
1	9492.	0.0118
2	10547.	0.0184
3	11601.	0.0265
4	12656.	0.0370
5	13500.	0.0490
6	14554.	0.0678
7	15609.	0.0936
8	16664.	0.1284
9	17719.	0.1693
10	18773.	0.2177
11	19828.	0.2721
12	20883.	0.3344
13	21937.	0.3958
14	22992.	0.4570
15	24047.	0.5540
16	25101.	0.6583
17	26156.	0.7549
18	27000.	0.8280
19	27675.	0.9220

R3NR45-3

Point	Hours	Length
1	7383.	0.0236
2	8436.	0.0462
3	9492.	0.0916
4	10547.	0.1506
5	11601.	0.2118
6	12656.	0.2715
7	13500.	0.3270
8	14554.	0.3960
9	15609.	0.4970
10	16664.	0.5870
11	17719.	0.6990
12	18773.	0.7840
13	19575.	0.9300

R3NR45-2

Point	Hours	Length
1	11601.	0.0057
2	12656.	0.0130
3	13500.	0.0230
4	14554.	0.0330
5	15609.	0.0489
6	16664.	0.0701
7	17719.	0.0947
8	18773.	0.1255
9	19828.	0.1600
10	20883.	0.1972
11	21937.	0.2374
12	22992.	0.2802
13	24047.	0.3211
14	25101.	0.3682
15	26156.	0.4220
16	27000.	0.4800
17	28054.	0.5390
18	29109.	0.6039
19	30164.	0.6940
20	31218.	0.7142
21	32273.	0.7644
22	33328.	0.8194
23	34155.	0.8789

R3NR45-4

Point	Hours	Length
1	12656.	0.0390
2	13500.	0.0580
3	14554.	0.0680
4	15609.	0.0930
5	16664.	0.1280
6	17719.	0.1810
7	18773.	0.2400
8	19828.	0.3030
9	20883.	0.3820
10	21937.	0.4620
11	22992.	0.5400
12	24047.	0.6670
13	25101.	0.8040
14	26156.	0.8630
15	26190.	0.8950

R3NR45-5

Point	Hours	Length
1	7383.	0.0172
2	8436.	0.0296
3	9492.	0.0421
4	10547.	0.0564
5	11601.	0.0771
6	12656.	0.1045
7	13500.	0.1443
8	14554.	0.2014
9	15609.	0.2612
10	16664.	0.3240
11	17719.	0.3875
12	18773.	0.4590
13	19828.	0.5390
14	20883.	0.6400
15	21937.	0.8440
16	22950.	0.9150

R3NR45-8

Point	Hours	Length
1	5273.	0.0166
2	6328.	0.0266
3	7383.	0.0420
4	8436.	0.0687
5	9492.	0.1135
6	10547.	0.1883
7	11601.	0.2824
8	12656.	0.3894
9	13500.	0.5015
10	14554.	0.6460
11	15609.	0.7920
12	15660.	0.8380

R3NR45-6

Point	Hours	Length
1	5273.	0.0183
2	6328.	0.0257
3	7383.	0.0357
4	8436.	0.0519
5	9492.	0.0785
6	10547.	0.1037
7	11601.	0.1460
8	12656.	0.1908
9	13500.	0.2400
10	14554.	0.3106
11	15609.	0.3963
12	16664.	0.5011
13	17719.	0.6000
14	18773.	0.6946
15	19826.	0.8939

R3NR45-9

Point	Hours	Length
1	6328.	0.0110
2	7383.	0.0151
3	8436.	0.0194
4	9492.	0.0261
5	10547.	0.0367
6	11601.	0.0507
7	12656.	0.0764
8	13500.	0.1200
9	14554.	0.1727
10	15609.	0.2621
11	16664.	0.3635
12	17719.	0.4818
13	18773.	0.6123
14	19828.	0.7340
15	20250.	0.7845

R3NR45-7

Point	Hours	Length
1	7383.	0.0295
2	8436.	0.0421
3	9492.	0.0682
4	10547.	0.1070
5	11601.	0.1515
6	12656.	0.2086
7	13500.	0.2634
8	14554.	0.3377
9	15609.	0.4538
10	16664.	0.5964
11	17719.	0.7412
12	18495.	0.9075

R3NR45-10

Point	Hours	Length
1	5273.	0.0112
2	6328.	0.0210
3	7383.	0.0472
4	8436.	0.1055
5	9492.	0.1857
6	10547.	0.2832
7	11601.	0.3728

APPENDIX B

Fractographic Analysis Program Parameters

The basic parameters obtained from the initial fatigue quality (IFQ) model are given in this section. These parameters include individual Q, b, TTCI, and EIFS values for each test coupon. Also, included are pooled Q, b, TTCI, and EIFS values for each data set. Data set notations used are listed in Table A-1. Pooled b, α , and Q_β values for each alloy are listed in Table 9.

Fractography Analysis Program

Summary for data set C1HD35

Item	Least Square	Arithmetic Average	Variance of Average
Q	0.16384E-03	0.40038E-03	0.18929E-03
b	0.77743	1.08650	0.35728
R2	0.64490		
Qhat	0.16384E-03	0.25580E-03	0.15879E-03
Qhat*beta(mv)	1.71502	2.67775	1.66224
Qhat*beta(mle)	1.90044	2.96724	1.84195
TTCI		9809.	4599.
EIFS		0.31780E-02	0.53501E-02

Here are the crack growth parameters for C1HD35
Data type.

Specimen	Q	b	R2	qhat	TTCI
1	0.3532E-03	0.67632	0.8128	0.4984E-03	4033.
2	0.5587E-03	0.73460	0.9319	0.6728E-03	4529.
3	0.3334E-03	0.79328	0.9494	0.3494E-03	5147.
4	0.2175E-03	0.71952	0.8439	0.2629E-03	5892.
5	0.4796E-03	1.07995	0.8882	0.2833E-03	7951.
6	0.7393E-03	1.34747	0.9568	0.2917E-03	8819.
7	0.4804E-03	1.08743	0.9117	0.2753E-03	11362.
8	0.2068E-03	0.87093	0.9344	0.1869E-03	9636.
9	0.6206E-03	1.46171	0.8473	0.1899E-03	12559.
10	0.2611E-03	1.03925	0.7883	0.1594E-03	12658.
11	0.3996E-03	1.09899	0.9280	0.2212E-03	12862.
12	0.5991E-03	1.53414	0.9087	0.1513E-03	14610.
13	0.1319E-03	1.40434	0.8587	0.5641E-04	3979.
14	0.1167E-03	0.64298	0.8986	0.1447E-03	13234.
15	0.5077E-03	1.80656	0.9674	0.9336E-04	19665.

Specimen	Qhat * beta(mle)	Qhat * beta(mv)	EIFS
1	5.781370	5.217326	0.1411E-01
2	7.804647	7.043208	0.9710E-02
3	4.053202	3.657762	0.5866E-02
4	3.049329	2.751829	0.2985E-02
5	3.286667	2.966012	0.2571E-03
6	3.384031	3.053877	0.5868E-04
7	3.192903	2.881396	0.2935E-09
8	2.168270	1.956729	0.5080E-05
9	2.202825	1.987912	-0.7782E-07
10	1.849256	1.668838	-0.1419E-06
11	2.566116	2.315759	-0.4104E-06
12	1.754636	1.583450	-0.6595E-04
13	0.654283	0.590450	0.1468E-01
14	1.678060	1.514344	-0.1900E-05
15	1.082966	0.977310	-0.1787E-01

Summary for data set C1HD40

Item	Least Square	Arithmetic Average	Variance of Average
q	0.46090E-03	0.59284E-03	0.34424E-03
b	0.78999	0.83042	0.27294
R2	0.89327		
Qhat	0.46090E-03	0.51899E-03	0.93577E 04
Qhat*beta(mv)	2.34428	2.63973	0.47596
Qhat*beta(mle)	2.15482	2.42639	0.43749
TTCI		4396.	1160.
EIFS		0.42886E-03	0.104[illegible]5E-0[illegible]

Here are the crack growth parameters for C1HD40
Data type

Specimen	Q	b	R2	qhat	TTCI	Ind.
1	0.8472E-03	0.97022	0.9491	0.6175E-03	2724.	1.0
2	0.2236E-03	0.52948	0.9234	0.4420E-03	3107.	1.0
3	0.2907E-03	0.55969	0.9103	0.6102E-03	4302.	1.0
4	0.7993E-03	1.05564	0.9761	0.5385E-03	2438.	1.1
5	0.4945E-03	0.86094	0.9676	0.4477E-03	3952.	1.0
6	0.6459E-03	0.83777	0.9518	0.6170E-03	4476.	1.0
7	0.4105E-03	0.63102	0.8636	0.6136E-03	4141.	1.0
8	0.9127E-03	1.22123	0.9916	0.4121E-03	4451.	1.0
9	0.8073E-03	0.98267	0.9799	0.5726E-03	4131.	1.0
10	0.1411E-02	1.36117	0.9733	0.5488E-03	4925.	1.0
11	0.7558E-03	0.93573	0.9840	0.5762E-03	5084.	1.0
12	0.6314E-03	0.84006	0.9805	0.6078E-03	4631.	1.0
13	0.2125E-03	0.57882	0.8026	0.3747E-03	4666.	1.0
14	0.1298E-03	0.35343	0.8619	0.4200E-03	7100.	1.1
15	0.3209E-03	0.73845	0.8710	0.3860E-03	5808.	1.0

Here are the crack growth parameters for C1HD40

Specimen	Qhat * beta(mle)	Qhat * beta(mv)	EIFS
1	2.887129	3.140980	0.1943E-02
2	2.066604	2.248310	0.7081E-03
3	2.852626	3.103444	0.3226E-05
4	2.517619	2.738981	0.3728E-02
5	2.093275	2.277326	0.2836E-04
6	2.884685	3.138321	0.7084E-06
7	2.868645	3.120871	0.9740E-05
8	1.926738	2.096146	0.9103E-06
9	2.677131	2.912518	0.1032E-04
10	2.565566	2.791144	0.8622E-10
11	2.694059	2.930934	-0.8107E-12
12	2.841464	3.091300	0.1164E-06
13	1.751997	1.906042	0.6978E-07
14	1.963709	2.136368	-0.1031E-02
15	1.804655	1.963330	-0.4261E-05

Summary for data set C1NR45

Item	Least Square	Arithmetic Average	Variance of Average
Q	0.51434E-03	0.55743E-03	0.30714E-03
b	1.12859	1.06713	0.24606
R2	0.90285		
Qhat	0.51434E-03	0.27413E-03	0.10563E-03
Qhat*beta(mv)	7.23407	3.85554	1.48561
Qhat*beta(mle)	7.17883	3.82610	1.47427
TTCI		12643.	4538.
EIFS		0.14896E-02	0.35249E-02

Here are the crack growth parameters for C1NR45
Data type

Specimen	Q	b	R2	qhat	TTCI
1	0.6860E-03	0.94271	0.9753	0.5287E-03	5537.
2	0.3267E-03	0.79611	0.9708	0.3492E-03	7932.
3	0.3073E-03	0.91388	0.9582	0.2352E-03	9391.
4	0.1078E-02	1.41497	0.9824	0.2311E-03	9156.
5	0.9608E-03	1.26005	0.9418	0.2748E-03	14511.
6	0.3258E-03	0.91778	0.9353	0.2479E-03	14540.
7	0.8147E-03	1.35870	0.8611	0.2735E-03	11802.
8	0.5065E-03	1.21410	0.9417	0.1782E-03	17699.
9	0.3568E-03	1.15650	0.9363	0.1450E-03	17403.
10	0.2112E-03	0.69648	0.9586	0.2777E-03	18463.

Specimen	Qhat * beta(mle)	Qhat * beta(mv)	EIFS
1	7.379910	7.436697	0.1133E-01
2	4.873246	4.910745	0.2195E-02
3	3.282090	3.307345	0.5973E-03
4	3.226236	3.251061	0.7528E-03
5	3.836109	3.865627	0.3918E-09
6	3.459988	3.486613	0.2669E-09
7	3.816987	3.846358	0.2485E-04
8	2.486647	2.505782	-0.1192E-04
9	2.023756	2.039328	-0.6317E-05
10	3.876023	3.905848	-0.4669E-04

Summary for data set C2NR45

Item	Least Square	Arithmetic Average	Variance of Average
Q	0.15314E-03	0.36890E-03	0.64975E-03
b	0.83433	1.05968	0.64503
R2	0.91519		
Qhat	0.15314E-03	0.15636E-03	0.30159E-04
Qhat*beta(mv)	3.17757	3.24430	0.62576
Qhat*beta(mle)	3.15260	3.21881	0.62085
TTCI		18657.	5257.
EIFS		0.14404E-02	0.24576E-02

Here are the crack growth parameters for C2NR45
Data type

Specimen	Q	b	R2	qhat	TTCI
1	0.2183E-03	0.87964	0.9759	0.1968E-03	10914.
2	0.1502E-03	0.83695	0.9666	0.1492E-03	16379.
3	0.1439E-03	0.78469	0.9586	0.1580E-03	14077.
4	0.1731E-03	0.90544	0.9785	0.1474E-03	15460.
5	0.1591E-03	0.84334	0.9640	0.1555E-03	17075.
6	0.2321E-02	2.96115	0.9551	0.1281E-03	15728.
7	0.1349E-03	0.80379	0.9635	0.1454E-03	18068.
8	0.1697E-03	0.77558	0.9902	0.1925E-03	22798.
9	0.9642E-04	0.67399	0.7499	0.1312E-03	20167.
10	0.3024E-03	0.99781	0.9606	0.2052E-03	27770.
11	0.1884E-03	1.19416	0.9688	0.1108E-03	26788.

Specimen	Qhat * beta(mle)	Qhat * beta(mv)	EIFS
1	4.051627	4.083716	0.8444E-02
2	3.071751	3.096079	0.9325E-03
3	3.251788	3.277542	0.2605E-02
4	3.033389	3.057413	0.1436E-02
5	3.200510	3.225857	0.6579E-03
6	2.636104	2.656982	0.1270E-02
7	2.992907	3.016610	0.3855E-03
8	3.963755	3.995147	0.1147E-04
9	2.700763	2.722152	0.1034E-03
10	4.223589	4.257040	0.2545E-09
11	2.280711	2.298774	0.1516E-07

Summary for data set R1HD40

Item	Least Square	Arithmetic Average	Variance of Average
Q	0.79538E-04	0.10603E-03	0.67070E-04
b	0.52518	0.49458	0.32274
R2	0.64111		
Qhat	0.79538E-04	0.11576E-03	0.62915E-04
Qhat*beta(mv)	0.73165	1.06480	0.57873
Qhat*beta(mle)	0.83266	1.21182	0.65864
TTCI		8756.	4919.
EIFS		0.12481E-01	0.17708E-01

Here are the crack growth parameters for R1HD40
Data type

Specimen	Q	b	R2	qhat	TTCI
1	0.2144E-03	0.52915	0.8733	0.2426E-03	3125.
2	0.2116E-03	0.60660	0.7882	0.2129E-03	4997.
3	0.1605E-03	0.51260	0.7976	0.1851E-03	3206.
4	0.1154E-03	0.30647	0.8984	0.1789E-03	3888.
5	0.1483E-03	0.75643	0.8459	0.1111E-03	8631.
6	0.9900E-04	0.59103	0.8667	0.1014E-03	6007.
7	0.1550E-04	0.00000	-0.1212	0.7059E-04	15389.
8	0.7401E-04	0.32288	0.6598	0.1046E-03	4557.
9	0.6161E-04	0.36462	0.8042	0.8967E-04	6965.
10	0.1126E-04	0.00000	-0.5485	0.4633E-04	16928.
11	0.2971E-04	0.16152	0.7694	0.7205E-04	13428.
12	0.1318E-03	0.97734	0.9832	0.8189E-04	13320.
13	0.6073E-04	0.79241	0.9520	0.4874E-04	7778.
14	0.1506E-03	1.00299	0.9835	0.7469E-04	14359.

Specimen	Qhat * beta(mle)	Qhat * beta(mv)	EIFS
1	2.540196	2.232023	0.4764E-01
2	2.228729	1.958343	0.1654E-01
3	1.937784	1.702694	0.4587E-01
4	1.872702	1.645508	0.3259E-01
5	1.162576	1.021534	0.6204E-07
6	1.061862	0.933038	0.7238E-02
7	0.738993	0.649339	-0.7863E-01
8	1.095155	0.962292	0.2212E-01
9	0.938760	0.824871	0.2297E-02
10	0.485017	0.426175	-0.1333
11	0.754229	0.662727	-0.3255E-01
12	0.857249	0.753249	-0.3070E-01
13	0.510241	0.448339	0.4299E-03
14	0.781948	0.687083	-0.5140E-01

Summary for data set R1HD45

Item	Least Square	Arithmetic Average	Variance of Average
Q	0.22222E-03	0.39332E-03	0.32580E-03
b	0.52658	0.57324	0.19791
R2	0.75040		
Qhat	0.22222E-03	0.36212E-03	0.24773E-03
Qhat*beta(mv)	0.81914	1.33484	0.91320
Qhat*beta(mle)	0.77725	1.26658	0.86650
TTCI		3227.	1165.
EIFS		0.67746E-02	0.14543E-01

Here are the crack growth parameters for R1HD45
Data type .

Specimen	Q	b	R2	qhat	TTCI
1	0.1272E-02	0.67184	0.9868	0.1156E-02	1064.
2	0.4284E-03	0.55328	0.9499	0.4732E-03	1920.
3	0.8489E-03	0.85908	0.9939	0.4773E-03	3150.
4	0.3830E-03	0.55180	0.9539	0.4271E-03	2024.
5	0.3861E-03	0.58542	0.7851	0.4000E-03	1641.
6	0.7477E-03	0.85652	0.9341	0.4548E-03	4115.
7	0.3431E-03	0.68612	0.9810	0.3044E-03	3271.
8	0.2422E-03	0.54077	0.9703	0.2752E-03	3322.
9	0.2152E-03	0.47049	0.9674	0.2775E-03	3216.
10	0.2279E-03	0.53446	0.9432	0.2647E-03	4486.
11	0.1670E-03	0.39104	0.8402	0.2324E-03	3724.
12	0.1339E-03	0.31238	0.7601	0.2022E-03	2881.
13	0.2915E-03	0.91295	0.9692	0.1680E-03	5100.
14	0.8820E-04	0.23419	0.6809	0.1593E-03	3858.
15	0.1243E-03	0.43824	0.8484	0.1601E-03	4638.

Specimen	Qhat * beta(mle)	Qhat * beta(mv)	EIFS
1	4.042309	4.260170	0.5276E-01
2	1.655019	1.744217	0.1398E-01
3	1.669385	1.759357	0.8090E-06
4	1.493913	1.574428	0.1120E-01
5	1.398990	1.474389	0.2334E-01
6	1.590809	1.676546	-0.6574E-02
7	1.064533	1.121907	-0.1761E-04
8	0.962546	1.014423	-0.5369E-04
9	0.970528	1.022835	-0.1790E-05
10	0.925820	0.975717	-0.1544E-01
11	0.812815	0.856622	-0.1648E-02
12	0.707378	0.745502	0.3464E-03
13	0.587670	0.619343	-0.4135E-01
14	0.557124	0.587150	-0.2890E-02
15	0.559880	0.590055	-0.2043E-01

Summary for data set R1NR45

Item	Least Square	Arithmetic Average	Variance of Average
Q	0.10598E-03	0.13550E-03	0.50550E-04
b	0.68351	0.70868	0.13442
R2	0.87226		
Qhat	0.10598E-03	0.11354E-03	0.52126E-04
Qhat*beta(mv)	2.13091	2.28292	1.04809
Qhat*beta(mle)	2.30370	2.46805	1.13308
TTCI		18636.	9672.
EIFS		0.10099E-01	0.14643E-01

Here are the crack growth parameters for R1NR45
Data type

Specimen	Q	b	R2	qhat	TTCI
1	0.1808E-03	0.64119	0.9778	0.1689E-03	7492.
2	0.2144E-03	0.62458	0.9849	0.2072E-03	9734.
3	0.1188E-03	0.47410	0.9369	0.1697E-03	8995.
4	0.1349E-03	0.67504	0.9735	0.1190E-03	11648.
5	0.1960E-03	0.88058	0.9691	0.1053E-03	21595.
6	0.1255E-03	0.76026	0.9774	0.9554E-04	17608.
7	0.1051E-03	0.73312	0.9879	0.8099E-04	18300.
8	0.6748E-04	0.74721	0.9175	0.5040E-04	23977.
9	0.1473E-03	0.93605	0.9870	0.7443E-04	30662.
10	0.6489E-04	0.61467	0.9190	0.6387E-04	36349.

Specimen	Qhat * beta(mle)	Qhat * beta(mv)	EIFS
1	3.672502	3.397033	0.3970E-01
2	4.503451	4.165654	0.2216E-01
3	3.688482	3.411815	0.2726E-01
4	2.587268	2.393201	0.1180E-01
5	2.289636	2.117894	-0.1528E-02
6	2.076695	1.920925	0.6463E-04
7	1.760410	1.628364	0.1498E-05
8	1.095607	1.013427	-0.6610E-02
9	1.617972	1.496610	-0.5110E-01
10	1.388446	1.284301	-0.1366

Summary for data set R1NR50

Item	Least Square	Arithmetic Average	Variance of Average
Q	0.17273E-03	0.23089E-03	0.17823E-03
b	0.65543	0.69492	0.27676
R2	0.88742		
Qhat	0.17273E-03	0.16235E-03	0.25818E-04
Qhat*beta(mv)	1.88470	1.77141	0.28170
Qhat*beta(mle)	1.69990	1.59771	0.25408
TTCI		9245.	2850.
EIFS		0.13356E-02	0.26249E-02

Here are the crack growth parameters for R1NR50
Data type

Specimen	Q	b	R2	qhat	TTCI
1	0.4087E-03	0.97399	0.9893	0.2061E-03	8101.
2	0.1650E-03	0.54429	0.9875	0.1867E-03	6090.
3	0.1692E-03	0.51749	0.8349	0.1979E-03	6579.
4	0.2566E-03	0.83704	0.9520	0.1573E-03	9015.
5	0.1373E-03	0.55644	0.9702	0.1541E-03	8374.
6	0.1122E-03	0.51902	0.9571	0.1312E-03	7723.
7	0.1337E-03	0.56390	0.9294	0.1457E-03	8712.
8	0.1514E-03	0.66748	0.9559	0.1350E-03	10454.
9	0.1065E-03	0.43925	0.9228	0.1509E-03	11447.
10	0.6684E-03	1.33031	0.9685	0.1587E-03	15952.

Specimen	Qhat * beta(mle)	Qhat * beta(mv)	EIFS
1	2.028134	2.248624	0.2720E-03
2	1.837334	2.037081	0.7606E-02
3	1.947120	2.158802	0.4617E-02
4	1.547552	1.715795	-0.5188E-05
5	1.516578	1.681454	0.8601E-04
6	1.291330	1.431718	0.7711E-03
7	1.433652	1.589512	0.3812E-05
8	1.328654	1.473099	-0.1874E-02
9	1.485240	1.646709	-0.6456E-02
10	1.561550	1.731315	-0.8514E-01

Summary for data set R2HD40

Item	Least Square	Arithmetic Average	Variance of Average
Q	0.17073E-03	0.20292E-03	0.78807E-04
b	0.54408	0.52727	0.15592
R2	0.79959		
Qhat	0.17073E-03	0.20085E-03	0.57183E-04
Qhat*beta(mv)	1.15349	1.35703	0.38635
Qhat*beta(mle)	1.15425	1.35793	0.38661
TTCI		6015.	2360.
EIFS		0.53909E-02	0.73571E-02

Here are the crack growth parameters for R2HD40
Data type

Specimen	Q	b	R2	qhat	TTCI
1	0.2273E-03	0.56699	0.8199	0.2254E-03	3670.
2	0.2111E-03	0.53133	0.9295	0.2197E-03	3746.
3	0.1601E-03	0.45454	0.9370	0.1893E-03	3415.
4	0.2267E-03	0.53221	0.9676	0.2377E-03	5486.
5	0.2475E-03	0.79132	0.9452	0.1468E-03	7168.
6	0.1185E-03	0.32263	0.8800	0.1724E-03	4517.
7	0.2550E-03	0.60881	0.9510	0.2314E-03	7829.
8	0.3213E-03	0.64554	0.9039	0.2898E-03	9573.
9	0.5873E-04	0.29203	0.7926	0.9534E-04	8727.

Specimen	Qhat * beta(mle)	Qhat * beta(mv)	EIFS
1	1.523647	1.522637	--0.1380E-01
2	1.485452	1.484467	0.1261E-01
3	1.279507	1.278659	0.1817E-01
4	1.607232	1.606167	0.5334E-04
5	0.992269	0.991612	-0.7293E-02
6	1.165365	1.164593	0.3889E-02
7	1.564250	1.563213	-0.1674E-01
8	1.959133	1.957834	-0.6445E-01
9	0.644550	0.644123	-0.3695E-01

Summary for data set R2HD45

Item	Least Square	Arithmetic Average	Variance of Average
Q	0.38774E-03	0.42791E-03	0.17778E-03
b	0.62759	0.59750	0.21295
R2	0.85807		
Qhat	0.38774E-03	0.36135E-03	0.67544E-04
Qhat*beta(mv)	1.20522	1.12318	0.20995
Qhat*beta(mle)	1.21399	1.13135	0.21148
TTCI		2786.	1095.
EIFS		0.69617E-02	0.14059E-01

Here are the crack growth parameters for R2HD45
Data type

Specimen	Q	b	R2	qhat	TTCI
1	0.2999E-03	0.29381	0.8996	0.4385E-03	1201.
2	0.3009E-03	0.30270	0.6866	0.4373E-03	1444.
3	0.5738E-03	0.77569	0.9415	0.3781E-03	2666.
4	0.7702E-03	0.92192	0.9743	0.3523E-03	2937.
5	0.4731E-03	0.68793	0.8565	0.3716E-03	2431.
6	0.5445E-03	0.69190	0.9191	0.4177E-03	2917.
7	0.2012E-03	0.43751	0.8645	0.2496E-03	2761.
8	0.3246E-03	0.65974	0.9222	0.2724E-03	4090.
9	0.3629E-03	0.60627	0.9060	0.3347E-03	4631.

Specimen	Qhat * beta(mle)	Qhat * beta(mv)	EIFS
1	1.373058	1.363141	0.3756E-01
2	1.369226	1.359337	0.2463E-01
3	1.183766	1.175216	-0.3334E-05
4	1.103048	1.095081	-0.1002E-02
5	1.163350	1.154948	0.4677E-03
6	1.307781	1.298336	-0.8560E-03
7	0.781382	0.775738	-0.1255E-03
8	0.852766	0.846606	-0.3801E-01
9	1.047794	1.040226	-0.7843E-01

Summary for data set R3HD40

Item	Least Square	Arithmetic Average	Variar of Aver.
Q	0.21369E-03	0.26464E-03	0.20911E-03
b	0.72536	0.63953	0.27097
R2	0.58613		
Qhat	0.21369E-03	0.24871E-03	0.10819E-03
Qhat*beta(mv)	1.36456	1.58820	0.69084
Qhat*beta(mle)	1.74167	2.02712	0.88176
TTCI		6358.	4772.
EIFS		0.16348E-01	0.16960E-01

ography Analysis Program

Here are the crack growth parameters for R3HD40

Data type

Specimen	Q	b	R2	qhat	TTCI
1	0.1567E-03	0.67826	0.5897	0.1643E-03	6773.
2	0.3254E-03	0.89106	0.6065	0.2539E-03	6000.
3	0.7768E-03	1.05246	0.6574	0.4855E-03	4078.
4	0.2034E-03	0.57502	0.5546	0.2411E-03	3610.
5	0.3485E-03	0.84746	0.6291	0.2909E-03	4097.
6	0.1834E-03	0.55095	0.6504	0.2267E-03	5062.
7	0.3524E-03	0.75201	0.5599	0.3362E-03	2441.
8	0.1718E-03	0.34727	0.2314	0.2440E-03	3224.
9	0.3522E-04	0.12122	0.2136	0.1323E-03	18537.
10	0.9277E-04	0.57957	0.7682	0.1124E-03	976

cimen	Qhat * beta(mle)	Qhat * beta(mv)	EIFS
1	1.338916	1.049005	0.1368E-02
2	2.069772	1.621612	0.3678E-02
3	3.956650	3.099931	0.1937E-01
4	1.964786	1.539358	0.2633E-01
5	2.371250	1.857812	0.1912E-01
6	1.847327	1.447332	0.9143E-02
7	2.739768	2.146536	0.5120E-01
8	1.988585	1.558004	0.3327E-01
9	1.077971	0.844562	-0.1705
	0.916214	0.717830	-0.1839E-04

Fractography Analysis Program

Summary for data set R3HD45

Item	Least Square	Arithmetic Average	Variance of Average
Q	0.20410E-03	0.27488E-03	0.14805E-03
b	0.55954	0.59487	0.22595
R2	0.50806		
Qhat	0.20410E-03	0.29702E-03	0.10783E-03
Qhat*beta(mu)	0.80424	1.17035	0.42488
Qhat*beta(mle)	0.70851	1.03105	0.37431
TTCI		3373.	798.
EIFS		0.44522E-02	0.54096E-

Here are the crack growth parameters for R3HD45
Data type

Specimen	Q	b	R2	qhat	T. I
1	0.1132E-03	0.55438	0.4374	0.1346E-03	4271.
2	0.1625E-03	0.22483	0.7659	0.3926E-03	2364.
3	0.3872E-03	0.61948	0.6423	0.4298E-03	2618.
4	0.3106E-03	0.80560	0.5712	0.2734E-03	4091.
5	0.2051E-03	0.41590	0.9300	0.3097E-03	3456.
6	0.1058E-03	0.37881	0.8576	0.1655E-03	4266.
7	0.4769E-03	0.79661	0.6377	0.4287E-03	25[illegible]
	0.4376E-03	0.90336	0.5857	0.3418E-03	

Specimen	Qhat * beta(mle)	Qhat * beta(mu)	EI
1	0.467149	0.530264	0.2349E-04
2	1.015652	1.152875	0.1315E-01
3	1.491930	1.693502	0.9785E-02
4	0.949125	1.077360	0.1088E-03
5	1.075223	1.220494	0.1431E-02
6	0.574663	0.652305	0.3083E-04
7	1.488284	1.689364	0.1042E-
8	1.186347	1.346633	0.1666E-.

actography Analysis Program

Summary for data set R3NR45

Item	Least Square	Arithmetic Average	Varis of Av. age
Q	0.16420E-03	0.21366E-03	0.13878E-03
b	0.71707	0.74215	0.19543
R2	0.88939		
Qhat	0.16420E-03	0.18086E-03	0.57636E-04
Qhat*beta(mv)	2.58311	2.84524	0.90672
Qhat*beta(mle)	2.29264	2.52530	0.80476
TTCI		13467.	3514
EIFS		0.46448E-02	0.5125[illegible]

Here are the crack growth parameters for R3NR45
Data type

Specimen	Q	b	R2	qhat	TTC.
1	0.1328E-03	0.70549	0.9940	0.1337E-03	17246.
2	0.7131E-04	0.45998	0.9639	0.1090E-03	19536.
3	0.1323E-03	0.47997	0.9638	0.1814E-03	10538.
4	0.2532E-03	0.93220	0.8678	0.1860E-03	17181.
5	0.1285E-03	0.64003	0.9572	0.1448E-03	13614.
6	0.1845E-03	0.80427	0.9937	0.1550E-03	11698.
7	0.2182E-03	0.79167	0.9959	0.1913E-03	11568.
8	0.5744E-03	1.07910	0.9128	0.2999E-03	10117.
	[illegible]	.87986	0.9764	0.1528E-03	14095.
		64896	0.9655	0.2547E-03	907[illegible]

Specimen	Qhat * beta(mle)	Qhat * beta(mv)	EI
1	1.866909	2.103435	0.1799E-0[illegible]
2	1.521865	1.714677	-0.5213E-05
3	2.533206	2.854149	0.8436E-02
4	2.596993	2.926018	0.2114E-04
5	2.022134	2.278327	0.1613E-02
6	2.164225	2.438420	0.4942E-02
7	2.670831	3.009210	0.5269E-02
8	4.187189	4.717682	0.1005E-[illegible]
	2.133332	2.403613	0.1136E
	3.556328	4.006894	0.1496E